The Role and Mechanism of Action of BRK in Tamoxifen-resistant Breast Cancer

A Thesis Submitted to the College of Graduate and Postdoctoral Studies

In Partial Fulfillment of the Requirements for

The Degree of Doctor of Philosophy in the

Department of Biochemistry, Microbiology, and Immunology

University of Saskatchewan, Saskatoon

By

Aditya Mandapati

PERMISSION TO USE

In presenting this thesis in partial fulfillment of the requirements for the Doctoral degree in Biochemistry from the University of Saskatchewan, I agree that the Libraries of this University may make it freely available for inspection. I further agree that permission for copying of this thesis in any manner, in whole or in part, for scholarly purposes may be granted by the professor or professors who supervised my thesis work or, in their absence, by the Head of the Department or the Dean of the College in which my thesis work was completed. It is understood that any copying or publication or use of this thesis or parts thereof for financial gain shall not be allowed without my written permission. It is also understood that due recognition shall be given to me and to the University of Saskatchewan for any scholarly use of the findings described in my thesis.

Requests for permission to copy or to make other use of any material in this thesis, in whole or part, should be addressed to:

Head of the Department of Biochemistry, Microbiology and Immunology

University of Saskatchewan

Saskatoon, Saskatchewan S7N 5E5

Dean

College of Graduate and Postdoctoral Studies

University of Saskatchewan

116 Thorvaldson Building, 110 Science Place

Saskatoon, Saskatchewan. SK- S7N 5C9

Canada

ABSTRACT

The anti-Estrogen Receptor (ER) therapy Tamoxifen has historically been used as a first-line treatment against ER-positive breast cancer. However, 30% of Tamoxifen-treated tumours develop resistance against the drug (TamR). Breast Tumour Kinase (BRK), a tyrosine kinase, presents itself as a possible target to combat TamR resistance as it drives tumourigenesis in breast cancer cells. Previous research has shown that BRK knockdown re-sensitizes TamR cells to the drug, though the mechanisms behind BRK's functioning in TamR have yet to be elucidated. To address this, I used a global phosphoproteomics approach to compare MCF7 cell lines, that differed in their sensitivity to Tamoxifen, and TamR T47D cells, that differed in BRK expression, and found a total of 1048 differentially expressed phosphopeptides. Pathway analysis revealed overrepresentation of the IGFR and insulin receptor signaling in both MCF7 and T47D TamR cells as well as when BRK was knocked down in T47D TamR cells. Specifically, BRK knockdown resulted in the inhibition of Insulin Receptor Substrate-1 (IRS1) through the hyperphosphorylation of the S1101 site and the hypophosphorylation of the Y896. Subsequent RT-PCR and ChIP-qPCR analyses revealed that both BRK knockdown and inhibition reduced downstream changes in cyclin D1 gene expression mediated by IRS1. To further identify BRK-specific targets, phosphotyrosine-enriched phosphoproteomics analysis was also conducted, comparing T47D Parental, T47D TamR and T47D TamR BRK knockdown cells. Out of 6492 phosphosites identified, 118 high-confidence phosphotyrosine sites were analyzed for significant changes in phosphorylation levels to identify differentially regulated pathways in TamR versus Parental cells and changes in these pathways when BRK is knocked down in TamR. Total proteomics analysis was then used to calculate the phosphorylation levels of these peptides relative to their total levels. Through this, I identified potential BRK-specific targets involved in TamR such as CDK1, GSK3-beta and catenin delta-1. Of these targets, I was able to validate that both the knockdown and inhibition of BRK in TamR cells resulted in the hypophosphorylation of both CDK1 and catenin delta-1 at the Y15 and Y904 phosphosites respectively. Overall, these findings indicate that BRK helps regulate TamR through its interaction with signaling intermediaries in the IGFR/insulin receptor signaling pathway.

ACKNOWLEDGMENTS

I would like to extend my deepest gratitude to my supervisor and mentor, Dr. Kiven Erique Lukong for seeing my potential as a researcher, for pushing me to fulfill that potential and for always seeing the best in me, despite my own blindness to the same. I'd like to thank my committee members Dr. Terra Arnason, Dr. Scot Leary, Dr. Yuliang Wu, Dr. Andrew Freywald, and Dr. Linda Chelico for their guidance and for everything they have taught me through my journey. I would not be the budding scholar I am today without their fastidious feedback and support. I would also like to extend my gratitude to my collaborators, Dr. Paulos Chumala, Dr. George Katselis and Dr. Laurent Brechenmacher (from UCalgary) for their contributions to this work. I would especially like to thank Dr. Zhibin Ning from the University of Ottawa for guiding me through crucial phases of the project and providing his timely insight.

On a personal note, I would like to thank all my friends and lab members for their support throughout these years, through thick and thin. I would especially like to thank Dr. Raghuveera Goel, Dr. Akanksha Baharani, Josh MacAusland-Berg, Chandrabose Prabaharan, Nayoung Kim and Stefany Cornea.

On a more personal note, I would like to thank my parents, Kiran Mandapati and Neeraja Mandapati, and my sister Sanjana Mandapati for their patience, love, and support over the last five years, through thick and thin. Their strength and belief in me have made this possible.

TABLE OF CONTENTS

LIST OF TABLES

LIST OF FIGURES

LIST OF ABBREVIATIONS

AF1 - Activation function 1

AhR – Aryl hydrocarbon Receptor

AI – Aromatase Inhibitor(s)

AKT/PKB – Protein Kinase B

AP1 – Activator Protein 1

APS – Ammonium persulfate

ATF – Activating Transcription Factor

ATP – Adenosine Triphosphate

BAD - BCL2 Associated Agonist Of Cell Death

BC – Breast Cancer

BCRP - Breast Cancer Resistance Protein

BRK – Breast Tumour Kinase

BSA – Bovine Serum Albumin

CCK8 – Cell Counting Kit 8

DMEM – Dulbecco's Modified Eagle Medium

DTT – Dithiothreitol

EDTA - Ethylenediaminetetraacetic acid

EGF – Epidermal Growth Factor

EGFR – Epidermal Growth Factor Receptor

ER – Estrogen Receptor

ERE – Estrogen Response Elements

ERK – Extracellular signal-Regulated Kinase

FAK – Focal Adhesion Kinase

FBS – Fetal Bovine Serum

FDA – Food and Drug Administration

FOXO3a – Forkhead box O3

FRK – Fyn-related Kinase

GFP – Green fluorescent protein

GPER – G-Protein coupled Estrogen Receptor

HDAC – Histone Deacetylase

HEPES - N-2-hydroxyethylpiperazine-N'-2-ethanesulfonic acid

HER2 – Human Epidermal growth factor Receptor 2

HGF – Hepatocyte Growth Factor

HPLC – High Performance Liquid Chromatography

IAA – Iodoacetamide

IGF – Insulin Growth Factor

IGF1R/IGFR – Insulin Growth Factor 1 Receptor

IGFBP-1 – Insulin Growth Factor Binding Protein -1

IHC – ImmunoHistoChemistry

ILK – Integrin-Linked Protein Kinase

IMAC - Immobilized Metal Affinity Chromatography

IR – Insulin Receptor

IRS1 – Insulin Receptor Substrate 1

JAK – Janus Tyrosine Kinase

KD – Knockdown

LCMS – Liquid Chromatography Mass Spectrometry

LFQ – Label-Free Quantification

MAPK – Mitogen Activated Protein Kinase

MCF7 – Michigan Cancer Foundation cell line 7

MOAC – Metal Oxide Affinity Chromatography

mTOR – Mammalian Target of Rapamycin

NRTK – Non-Receptor Tyrosine Kinase

PAK2 – p21 Activated Kinase 2

PBS – Phosphate-buffered Saline

PEI – Polyethylenimine

PI3K – Phosphoinositide 3-kinase

PMSF - Phenylmethylsulfonyl fluoride

PR/PGR – Progesterone Receptor

PTEN – Phosphatase Tensin Homologue

PTK6 – Protein Tyrosine Kinase 6

QPCR – Quantitative Polymerase Chain Reaction

ROS – Reactive Oxygen Species

RPMI – Roswell Park Memorial Institute 1640 media

RTK – Receptor Tyrosine Kinase

RTPCR – Reverse Transcriptase Polymerase Chain Reaction

SDS PAGE - Sodium Dodecyl Sulfate Polyacrylamide Gel Electrophoresis

SERD – Selective Estrogen Receptor Down-regulator

SERM – Selective Estrogen Receptor Modulator

SLUG – Zinc finger protein SNAI2

SMAD - Suppressor of Mothers against Decapentaplegic

SNAIL – Zinc finger protein SNAI1 which is referred to as SNAIL

SRMS - Src-related kinase lacking C-terminal regulatory tyrosine and N-terminal myristoylation sites

STAT – Signal Transducer and Activator of Transcription

TamR – Tamoxifen resistant/resistance

TEMED – Tetramethylethylenediamine

TFA – Trifluoroacetic acid

TNBC – Triple-Negative Breast Cancer

TR – Tamoxifen resistant

UPLC - Ultra Performance Liquid Chromatography

VEGF – Vasothelial Endothelial Growth Factor (VEGF)

1.0 BACKGROUND

1.1 Breast Cancer

According to global cancer statistics, as of 2021, breast cancer surpassed lung cancer as the most diagnosed malignancy with over 2.3 million new cases (Sung *et al.*, 2021). In women, breast cancer is also the leading cause of cancer death in 110 countries, as it accounts for 1 in 4 cancer cases and for 1 in 6 cancer deaths (Sung *et al.*, 2021). Current efforts in curtailing the disorder have been focussed on primary prevention through programs that encourage weight reduction and physical activity alongside early detection through mammography (Sung *et al.*, 2021). In fact, women that have participated in mammography screenings have been shown to significantly benefit from therapy at the time of early diagnosis and are associated with reduced breast cancer mortality (Coldman *et al.*, 2014; Tabár *et al.*, 2019). While these measures have been effective, current treatment strategies are important to prolong survival and quality of life in patients. Due to the heterogeneity of breast cancer at a molecular level, treatments have been developed to tackle the molecularly diverse nature of these tumours (Harbeck *et al.*, 2019). Recently, therapies have been developed to target specific molecules in order to address the heterogeneity of breast tumours (Harbeck *et al.*, 2019).

1.1.1 Subtypes of Breast Cancer

Breast tumours have been grouped according to the molecular alterations that distinguish them. The classification system, first reported in 2000, divided breast cancers into 4 subtypes, luminal A and luminal B (overexpressing ER), Human Epidermal growth factor Receptor 2-enriched (HER2-enriched but without ER expression), and basal-like or Triple-Negative (Perou *et al.*, 2000). This system helped determine diagnostics and clinical management of breast cancer and allowed for a more biology-based approach to therapy (Sorlie, 2007). Today, breast cancer cases are classified into 5 subtypes instead, with an additional subtype dedicated to luminal B-like cancers that also overexpress HER2 (Vuong *et al.*, 2014). Tumours that express the hormone receptors ER, progesterone receptor (PR) and/or HER2 are considered hormone receptor-positive tumours while those that do not express any of the hormone receptors are called Triple Negative Breast Cancers (TNBCs). The major focus of this thesis will be on Luminal A breast cancer and its therapy Tamoxifen.

1.1.2 Luminal A Breast Cancer

A vast majority of breast tumours are classified as either luminal A-like (60-70%) or luminal B-like (20-25%) with both TNBC (5-10%) and HER2-positive cases (13-15%) representing the remaining minority (Harbeck *et al.*, 2019). The term "luminal" refers to the similarity between the genes expressed by the luminal epithelial cells of the breast and those expressed by the tumour (Johnson *et al.*, 2020). Luminal A subtype tumours generally are well differentiated carcinoma with a low frequency of p53 mutations, higher expression of PR and low Ki-67 expression, an IHC marker for cell proliferation (Johnson *et al.*, 2020). Due to the high expression of ER in these tumours, patients are highly receptive to endocrine therapy (which targets the estrogen receptor) and benefit more from single endocrine therapy than combined chemo-endocrine therapy (Puppe *et al.*, 2020). The preponderance of luminal tumour cases displays the highly important role of the estrogen receptor in the progression of breast cancers. In fact, since 1970, the targeting of ER has been considered complementary to surgery as a treatment of ER+ breast cancer in patients (Lumachi *et al.*, 2015).

1.1.2.1 Role of the estrogen receptor in luminal A breast cancers

Estrogen, otherwise known as 17β-estradiol, a steroid hormone, plays a vital role both in the development of the mammary gland and the progression of breast cancer (Manavathi *et al.*, 2013). The ligand performs its function by binding to the estrogen receptor, a ligand-dependent transcription factor that drives multiple cellular functions, including proliferation and migration (Manavathi *et al.*, 2013). While there are two subtypes of the ER, ERα and Erβ, the predominant presence of ERα in the mammary gland makes it more relevant to the current discussion (Fuentes and Silveyra, 2019). The interaction between estrogen and the ER occurs in the cytosol, where intracellular ERα is located. Once the ligand binds to its receptor, ERα can either regulate signaling cascades in the cytosol, through GPER1 or PI3K signaling, or it can recognize and bind to Estrogen Response Elements (EREs) of genes that drive cell proliferation, differentiation and migration, amongst other functions (Fuentes and Silveyra, 2019; Lee *et al.*, 2005). Thus, ERα has both genomic and non-genomic functions. The genomic effects of ERα are directed by its translocation into the nucleus where it identifies EREs in gene promoter regions (Fuentes and Silveyra, 2019). However, a report in 2004 suggested that more than 30% of genes regulated by ERα do not contain

an ERE (Fuentes and Silveyra, 2019; O'Lone *et al.*, 2004). Non-genomic signaling of ERα includes its regulation of PI3K/AKT signaling downstream of various growth factor signaling pathways (Manavathi *et al.*, 2013).

1.1.2.2 Non-genomic role of ERα in breast cancer

The presence of ERα in the nucleus, plasma membrane, mitochondria and the endoplasmic reticulum suggests the receptor performs extranuclear functions that are important to the development and progression of breast cancer (Levin, 2009). Particularly, the functioning of ERα in the cytosol results in the activation of several signal transduction cascades (Levin, 2009). For example, the methylation of ERα at the arginine 260 residue allows for its interaction with the tyrosine kinases Src and Focal Adhesion Kinase (FAK) (Le Romancer *et al.*, 2008). Additionally, in ER+ breast cancer cells, it has been shown that estrogen dependent ERα activity increases the phosphorylation and activation of the effector protein AKT through its Ser473 residue (Lee *et al.*, 2005). Previous studies have also demonstrated that, through its interaction with the adapter protein Shc, ERα interacts with IGF1R and induces its phosphorylation as well as AKT and MAPK phosphorylation downstream, resulting in the formation of a Shc-ERα-IGF1R complex in breast cancer cells that regulates signaling cascades (Manavathi *et al.*, 2013; Song *et al.*, 2004). This crosstalk between ERα and growth factor receptor signaling appears to be mediated by adapter proteins such as Shc (Manavathi *et al.*, 2013). In fact, when Shc was knocked down in ER+ breast cancer cells, estrogen-induced IGF1R activation was reduced by 87% (Song *et al.*, 2004). Another example of this crosstalk was found when investigators identified the mammalian target of rapamycin (mTOR)/S6 kinase 1 complex as critical to the interaction between IGF1R and ERα as the inhibition of S6K1 kinase activity ablated its association with ERα and thereby prevented ERα from performing its genomic transcription function downstream (Becker *et al.*, 2011). As S6K1 overexpression is associated with poor survival in ER+ breast cancer patients, the interaction between S6K1 and ERα is suggested to be crucial for breast cancer development (Becker *et al.*, 2011).

ERα signaling activity also impacts processes such as drug resistance, migration, and apoptosis prevention (Manavathi *et al.*, 2013). Integrin-linked kinase (ILK) binds to ERα and regulates breast cancer cell migration through the PI3K pathway and the inhibition of PI3K reduces ILK-mediated

cell migration regulation by ERα (Acconcia *et al.*, 2006). Additionally, it was found that Tamoxifen, an ERα antagonist, could act as an agonist in ERα's role in the deacetylation of tubulin, implying the role of ERα in drug resistance (Acconcia *et al.*, 2006). More recently, ERα was found to interact with histone deacetylase 6 (HDAC6) to deacetylate tubulin, resulting in enhanced cell migration and growth in ER+ breast cancer cells (Azuma *et al.*, 2009). Estrogen stimulation and ERα has also been shown to block apoptosis in breast cancer cells through the phosphorylation and inactivation of BAD, a proapoptotic protein, through the Ras/PI3K/AKT pathway (Fernando and Wimalasena, 2004). The study showed that hydrogen peroxide or serum withdrawal induced cell death was abrogated by the action of estrogen and ERα through the PI3K/AKT pathway (Fernando and Wimalasena, 2004).

In addition to its interactions with intermediaries in growth factor signaling cascades, G-protein-coupled ER (GPER1) acts as an alternative estrogen receptor and mediates a rapid non-genomic response (Hsu *et al.*, 2019). GPER1 is a transmembrane receptor with a structure that is different from the nuclear ER receptors (Hsu *et al.*, 2019). GPER, upon stimulation with estrogen, has been shown to mediate activation of the EGFR signaling pathway, resulting in the upregulation of HIF1α (Hypoxia Inducible Factor 1α) (De Francesco *et al.*, 2014). Additionally, estrogen mediated GPER activation resulted in the inactivation of FOXO3a through PI3K and EGFR transactivation (Zekas and Prossnitz, 2015). The overall effect of the action of GPER is an increase in breast cancer cell survival as well as a greater propensity in these cells for drug resistance as traditional therapies such as Tamoxifen act as agonists of GPER rather than antagonists (De Francesco *et al.*, 2014; Zekas and Prossnitz, 2015). However, contrasting results have been found wherein GPER1 expression correlates with increased disease-free survival of ER+ breast cancer patients and activation of GPER1 reduces cell proliferation in ER+ breast cancer cells (Ariazi *et al.*, 2010; Broselid *et al.*, 2013). The contradicting results indicate a context dependent function for GPER in ER+ breast cancer.

Overall, the induction of the ER by estrogen in breast cancer cells results in the increased cell survival, growth, and migration mainly through growth factor signaling mechanisms, either through ER interaction with intermediaries such as PI3K, AKT, Src, ERK1/2 or through direct interaction between GPER and EGFR, resulting in activation of the growth factor receptor itself.

1.1.2.3 Genomic role of ERα in ER+ breast cancer

Known as the classical mechanism of ER signaling, direct genomic signaling involves the action of ERα as a transcription factor induced by its ligand estrogen (Fuentes and Silveyra, 2019). Estrogen binding to the ER causes a conformational change in the receptor, allowing for its dimerization and subsequent translocation to the nucleus where it recognizes and binds to ERE sequences of target genes (Le Dily and Beato, 2018). A landmark genome-wide screening in 2004 identified 70,000 EREs in the human genome, using HeLa cells (Bourdeau *et al.*, 2004). A more recent analysis used gene expression data from the Gene Expression Omnibus database and discovered that, in ER+ breast cancer cells, ERα positively regulated approximately 160 genes and negatively regulated 70 genes (Cheng *et al.*, 2020). Overall, genes regulated positively by ER were associated with reduction in apoptosis and an activation of G-protein coupled receptor signaling pathways (Cheng *et al.*, 2020). These genes include, for example, progesterone receptor (PGR) and Growth receptor estrogen binding-1 (GREB1) (Cheng *et al.*, 2020). PGR is itself overexpressed in luminal A breast cancers and is a key regulator of tumourigenesis as they bind to progesterone response elements and regulate gene expression (Daniel *et al.*, 2011). GREB1 was found to be a crucial regulator of breast cancer cell growth in ER+ breast cancer cell line MCF7 when they were induced with estrogen (Sun *et al.*, 2007).

In addition to directly interacting with ERE sites to induce gene expression, ERα also performs its genomic function indirectly by binding to transcription factors or proteins which themselves have direct interactions with promoter sites (Fuentes and Silveyra, 2019). For example, ERα has functional interactions with AP-1 and Sp-1 in an ERE independent manner by regulating genes such as cyclin D1, leading to cell cycle progression and estrogen-stimulated breast cancer cell proliferation (Yaşar *et al.*, 2016). This interaction between unliganded ERα and these transcription factors is also a crucial mechanism for anti-ER therapy resistance (Fuentes and Silveyra, 2019).

In concordance with its relationship with IGFR, ER was also found to associate with nuclear-localized IRS1 (Insulin Receptor Substrate 1), a docking protein of IGFR, at ERE sites to drive transcription of the gene pS2 (Morelli *et al.*, 2004). In fact, another study has suggested that IRS1 may be a coactivator of unliganded ER, a mechanism that bypasses anti-ER therapies in breast cancer (Sisci *et al.*, 2007).

1.1.2.4 Luminal A breast cancer cell lines: MCF7 and T47D

The MCF7 cell line was isolated in 1970 from the pleural effusion of an ER-positive breast tumour, from the patient Helen Marion, by Soule and colleagues at the Michigan Cancer Foundation after which it is named (Lee et al., 2015). Historically, the MCF7 cell line has been widely used to study the overexpression of ER as it mimics clinical ER-positive breast tumours (Lee *et al.*, 2015). Its successful use in breast cancer research is reflected by over 25,000 publications using the cell line, a figure only eclipsed by the 80,000 reports attributed to the HeLa cell line (Lee *et al.*, 2015).

The T47D cell line is another representative of the ER-positive breast cancer cell line category. The cell line was established in 1979, by Keydar and colleagues, from the pleural effusion of an ER-positive breast cancer patient (Keydar et al., 1979). As T47D cells share molecular and phenotypic characteristics with MCF7 cells, they have also been widely used for breast cancer research (Dai et al., 2015). In fact, the two cell lines are often used interchangeably for *in vitro* research (Dai *et al.*, 2015). While both 2D gel imaging and RTPCR analyses have shown considerable similarities between the two cell lines, proteomics analyses have shown at least 164 differentially expressed proteins between MCF7 and T47D cells (Aka and Lin, 2012). These include interleukin-10, which is more strongly expressed in MCF7 cells and prohibitin, which has a higher expression in T47D cells (Aka and Lin, 2012).

1.1.3 Treatment of luminal A breast tumours

As outlined above, the importance of the estrogen receptor made it a primary target for therapy development. These therapies are often referred to as "endocrine therapy" since they target ER, a hormone receptor. Historically, endocrine therapy has been the most efficient method to treat ER+ breast cancer patients. They can be classified into two main subtypes based on their actions: steroidal and non-steroidal antiestrogen agents (Belachew and Sewasew, 2021). Steroidal anti-estrogen agents are full antagonists of estrogen receptor activity while non-steroidal antiestrogens are partial agonists (Belachew and Sewasew, 2021). To reduce the severity of side effects, it is more desirable to use antiestrogens that also have partial agonist activity, thereby reducing the impact of estrogen receptor inhibition (Belachew and Sewasew, 2021). Tamoxifen, the most widely used antiestrogen agent, is an antagonist of ERα in breast tissue while acting as an agonist elsewhere in the body and is therefore recommended to premenopausal breast cancer patients

(Furman *et al.*, 2019). Fulvestrant is an antagonist of ERα with no partial agonist activity, is associated with more severe side effects as a result and is therefore recommended to postmenopausal breast cancer patients (Boer, 2017). Finally, aromatase inhibitors are a class of drugs that target the synthesis of estrogen itself and, like Fulvestrant, are considered a harsher treatment (Augusto *et al.*, 2018).

1.1.3.1 Aromatase inhibitors

The enzyme aromatase aromatizes the A-ring of androgens, the final step in the biosynthesis of estrogen from its precursor, testosterone (Ghosh *et al.*, 2012). Once the active site of the enzyme was found, it allowed for the design and discovery of aromatase inhibitors (AIs) (Augusto *et al.*, 2018). By reducing the activity of aromatase, AIs reduce the amount of circulating estrogen in a patient, thereby lowering the activity of the estrogen receptor pathway (Augusto *et al.*, 2018). As estrogen production is significantly higher in tumours than in surrounding non-cancerous tissue, AIs were found to be potent and efficacious in treating breast cancer, particularly in post-menopausal women, who produce more estrogen than pre-menopausal women (Bhatnagar, 2007).

Currently there are 3 main AIs that are used to treat estrogen receptor-positive breast tumours (Augusto *et al.*, 2018). These modern, third-generation AIs have been designed to decrease estrogen levels, by inhibiting aromatse, without affecting the synthesis of other steroids (Bhatnagar, 2007). Letrozole inhibits aromatase by mimicking the substrate of the enzyme androstenedione, binding to the active site reversibly and thereby acting as a competitive antagonist and reducing estrogen production downstream (Bhatnagar, 2007). Anastrozole binds to the heme iron domain of the aromatase enzyme reversibly and inhibit the enzyme's catalytic activity (Milani *et al.*, 2009). By contrast, exemestane irreversibly binds to the aromatase active site through covalent bonding (Deeks and Scott, 2009). In a clinical setting, these AIs are being used in post-surgery treatment regimens for postmenopausal breast cancer patients (Augusto *et al.*, 2018). However, more recently, they have been considered for the treatment of premenopausal women (Augusto *et al.*, 2018).

Though AIs are potent and efficacious, clinical trials have shown that they can cause greater side effects when compared to Tamoxifen therapy (Augusto *et al.*, 2018). For example, increased musculoskeletal, cardiovascular and sexual dysfunctions are associated with AI use vs Tamoxifen

therapy (Augusto *et al.*, 2018). Indeed, reduction in bone density and increase in fractures is a major consideration when comparing AIs to Tamoxifen therapy (Augusto *et al.*, 2018). This may be a consequence of the antagonistic effects of AIs vs the partial agonist, partial antagonistic effects of Tamoxifen.

1.1.3.2 Selective Estrogen Receptor Down-regulator (Fulvestrant)

Fulvestrant, first discovered in 1989 as a potent antiestrogen, was approved by the FDA for the treatment of Tamoxifen-resistant breast cancer in 2002 (Boer, 2017). To this day, Fulvestrant is primarily used as a secondary therapy when patients have relapsed after 5 or more years of Tamoxifen treatments (Boer, 2017).

The drug exerts its effect by competitively binding to the ER, preventing estrogen binding and impairing ER activity (Nathan and Schmid, 2017). Once bound to the ER, Fulvestrant impairs ER dimerization, immobilizes the receptor in the nuclear matrix and targets it for proteasomal degradation (Boer, 2017; Long and Nephew, 2006). Interestingly, the Fulvestrant-ER complex interacts with these nuclear matrix proteins (CK8 and CK18) through helix 12 of the receptor, thereby immobilizing the complex and preventing ER from identifying EREs and regulating gene transcription downstream (Long and Nephew, 2006). This interaction was also found to be essential in driving the ubiquitin-mediated targeting of the receptor for proteasomal degradation (Long and Nephew, 2006; Yeh *et al.*, 2013). The depletion of the ER ensures that the receptor is unresponsive to estrogen, reducing the ability of the ligand to stimulate the ER pathway and therefore breast cancer progression overall (Boer, 2017). Importantly, Fulvestrant is a complete ER antagonist in all tissues as it consistently reduces both ER and PR levels in the tumour as well as the whole body (Boer, 2017). Due to its wide ranging effects, Fulvestrant is often only recommended to post-menopausal women with recurring, tamoxifen-resistant breast cancer (Boer, 2017).

Clinical trials have explored the possibility of using Fulvestrant as a single-agent therapy in post-menopausal women who had not been given antiestrogens of any kind previously (Robertson *et al.*, 2016). Fulvestrant showed superior efficacy in this context when compared to anastrozole (Robertson *et al.*, 2016). Therefore, in the future, Fulvestrant may be considered a first-line therapy in postmenopausal women with ER+ breast cancer. Currently, clinical trials are investigating the

possibility of using Fulvestrant in combination with CDK4/6 inhibitors or mTOR inhibitors or growth factor receptor inhibitors (Boer, 2017).

1.1.3.3 Selective Estrogen Receptor Modulator: Tamoxifen

Tamoxifen is currently one of the most widely used and best selling breast cancer drugs (Quirke, 2017). Initially, Tamozifen was synthesized in 1962 as a contraceptive before development of the drug was switched to focus more on its ability to treat breast cancer (Quirke, 2017). Eventually, in 1977, Tamoxifen was approved by the FDA for the treatment of advanced breast cancer (Quirke, 2017). Over time, Tamoxifen also became vital to the prevention of breast cancer recurrence in premenopausal patients after 5 years of treatment (Jordan, 2006). Currently, Tamoxifen is a first-line therapy against ER+ breast cancer before surgery and is used to prevent recurrence of ER+ breast cancer after surgery (Quirke, 2017).

Tamoxifen is a Selective Estrogen Receptor Modulator (SERM). It acts as an agonist in the uterus and bone but, importantly, acts as an antagonist in breast tissue (Chang, 2012). Tamoxifen competes with estrogen for binding to the ER as it has a greater affinity to the receptor than its ligand (Chang, 2012). Once it does bind to the receptor, it forces a conformational change that is similar to that caused by estrogen binding differing only in the repositioning of helix 12, which causes the occlusion of the ER coactivator interaction site (Shiau *et al.*, 1998). This effectively prevents the formation of the AF2-ER complex which traditionally drives gene transcription (Chang, 2012). The conformation induced by Tamoxifen binding to ER also reduces the rate of ER dimerization (Powell and Xu, 2008). Therefore, Tamoxifen not only competitively reduces estrogen binding to ER but also prevents ER from performing its gene expression regulation activity (Chang, 2012).

Functionally, Tamoxifen binding to ER results in a reduction in the proliferation rate of ER+ breast cancer cells as well as a reduction in tumour volume through the inhibition of estrogen-ER dependent growth proliferation regulation (Asghar Butt *et al.*, 2015; Jiagge *et al.*, 2016). In addition, Tamoxifen has been found to increase oxidative stress in these cells (Jiagge *et al.*, 2016). Tamoxifen has been shown to have both cytotoxic and cytostatic effects on breast cancer cells. The cytostatic effects of Tamoxifen have been shown to be associated with its effect on IGF1R

signaling (Guvakova and Surmacz, 1997). As discussed previously, ER signaling is directly associated with that of IGF1R and when ER is inhibited by Tamoxifen, therefore, IGF1R signaling is inhibited (Guvakova and Surmacz, 1997). Additionally, Tamoxifen treatment has been shown to reduce the number of cells that moved to S phase during division, thereby trapping them in G2 phase and perhaps inducing pro-apoptotic signals in these cells (Pérez-Tenorio *et al.*, 2006). Several studies have shown that tamoxifen treatment promotes apoptosis in breast cancer cells through an increase in reactive oxygen species (ROS) and up regulation of proapoptotic pathway genes (Moriai *et al.*, 2009; Rouhimoghadam *et al.*, 2018). One of these investigations revealed as many as 4710 unique genes were altered in terms of their expression when ER+ MCF7 breast cancer cells were treated with Tamoxifen (Rouhimoghadam *et al.*, 2018). These changes included the differential expression of genes in the pro-apoptotic TP53 signaling pathway including intermediaries such as Bak and PUMA (Rouhimoghadam *et al.*, 2018). In fact when the anti-apoptotic protein surviving was overexpressed in MCF7 cells treated with tamoxifen, it abrogated the growth inhibitory effects of the drug, implying that Tamoxifen has a significant role in inducing apoptosis in ER+ breast cancer cells (Moriai *et al.*, 2009). Additionally, treatment with Tamoxifen has been shown to reduce breast cancer cell migration and invasion (Li *et al.*, 2017).

Clinically, treatment with tamoxifen has been shown to reduce tumour volume as well as angiogenesis in patients treated with the drug (Marson *et al.*, 2001). Due to the role of ER in promoting angiogenesis through the regulation of VEGF (Vascular Endothelial Growth Factor, involved in angiogenesis) gene expression, Tamoxifen inhibition of the pathway results in reduced angiogenesis and contributes greatly to reduction in tumour volume (Marson *et al.*, 2001). In addition, Tamoxifen reduces the expression of genes involved in cell cycle and proliferation which are regulated by the estrogen receptor *in vivo* (Davies *et al.*, 2011).

Tamoxifen is prescribed to premenopausal women because, while it is a competitive antagonist in breast tissue, it acts as an agonist in other tissue such as the endometrium where it known to promote endometrial cancer (Rani *et al.*, 2019). After the initial 5-year period of treatment with Tamoxifen, it has been observed that 30% of women relapse within 15 years (Rani *et al.*, 2019). These relapses account for 25% of breast cancer cases overall (Rani *et al.*, 2019). Due to the

incidence of Tamoxifen resistance (TamR), a better understanding of the molecular mechanisms behind the process will lead to more effective strategies that will help tackle resistant cancers as well as prevent their formation in the first place.

1.1.4 Drug resistance in luminal A breast cancer

Despite the development and use of AIs, Fulvestrant and Tamoxifen, as described above, breast tumours do develop resistances and the resultant relapses are major causes for concern. Clinically, endocrine resistance refers to the recurrence of cancer within 2 years after post-surgery endocrine treatment in early breast cancer cases or continued disease progression during the first 6 months of endocrine therapy in advanced breast cancer cases (Hartkopf *et al.*, 2020). A small subset of patients do not respond to initial anti-estrogen drugs despite their tumours expressing ER, a phenomenon called *de novo* resistance (Hartkopf *et al.*, 2020). While resistance against one anti-estrogen agent may be overcome by using another, development of secondary resistances has also been observed (Hartkopf *et al.*, 2020). For example, letrozole or fulvestrant alone have been shown to be effective in treating tamoxifen-resistant patients but these patients do develop resistances against letrozole or fulvestrant eventually (Hartkopf *et al.*, 2020).

1.1.4.1 Mechanisms of Acquired Endocrine Resistance

The status of estrogen receptor expression, mutations in the ER gene ESR1 and growth receptor crosstalk contribute significantly to the development and maintenance of endocrine resistance (Rani *et al.*, 2019). For example, receptor tyrosine kinases (RTKs) such as IGF1R have all been well characterized for their roles in endocrine drug resistance and ongoing clinical trials are investigating the possibility of combining endocrine agents with anti-RTK drugs (Hartkopf *et al.*, 2020). The following section will broadly cover the mechanisms of endocrine resistance with a focus on IGF1R signaling as the pathway was found to be significantly involved in the subject of the project, BRK-driven Tamoxifen resistance.

1.1.4.1.1 Mutation of ER or Loss of Expression of ER

Reduction in ER expression contributes to acquired resistance to endocrine therapies, particularly Tamoxifen (Rani *et al.*, 2019). However, 25% of tumours that become resistant to Tamoxifen are

responsive to either Fulvestrant or an AI and 20% of Tamoxifen resistant tumours do not have a reduction in ER (Gutierrez *et al.*, 2005; Johnston *et al.*, 1995). In the Tamoxifen resistant tumours that lack ER, however, the loss of the primary target of endocrine therapy is the primary driving factor behind the development of resistance.

In the population of breast cancers that display reduced or non-existent ER gene expression, it was found that there was a increase in CpG site methylation which may have contributed to the reduction in ER expression (Ottaviano *et al.*, 1994). An investigation in 2001 suggested that the histone deacetylation at the site of ER transcription may cause the loss of expression of the receptor in breast cancers, as the inhibition of the deacetylase HDAC induced ER transcription in BC cell lines (Yang *et al.*, 2001). Interestingly, it was found that ER-negative breast cancer cells, which would normally be resistant to endocrine therapy, became responsive to Tamoxifen when they were treated with histone deacetylase inhibitor (HDACi) and DNA methylase-1 (DNMT1) inhibitors (Fan *et al.*, 2008). Thus, the loss of ER expression through DNA methylation and histone deacetylation in ER+ breast cancer cells contributes to endocrine resistance and HDAC inhibition might be a viable method to prevent this (Rani *et al.*, 2019). In fact a phase II clinical trial, conducted in 2011 tested the effectiveness of a combination of the HDAC inhibitor vorinostat and tamoxifen in the treatment of tamoxifen resistant breast cancer cases (Munster *et al.*, 2011). They found a clinical benefit rate of 40% with an objective response rate of 19% in 43 patients (Munster *et al.*, 2011).

Mutations in the ESR1 gene, which encodes ER have been observed in at least 1/3rd of breast carcinoma, according to a study by Fuqua and colleagues (Fuqua *et al.*, 2000). In ER+ breast cancer patients treated with tamoxifen, mutations were observed in the ligand binding domain of the receptor and caused the constitutive activation of ER, which itself is a well-known method of acquired resistance (ligand independent activation of ER signaling) (Jeselsohn *et al.*, 2014). Another study found mutations such as Y537S, Y537N and D538G in the ligand binding domain which changed the conformation of the receptor such that the binding of tamoxifen to ER would result in the agonist conformation rather than the antagonist conformation described previously (Toy *et al.*, 2013). Overall, these mutations result in the aberrant activation of ER despite the presence of Tamoxifen or AIs as shown by a study that showed the D538G mutation in ER leads

to enhanced proliferation and resistance to tamoxifen (Merenbakh-Lamin *et al.*, 2013). These studies and others have put a spotlight on monitoring ESR1 mutations and using them as biomarkers for endocrine resistance in ER+ breast cancer patients (Takeshita *et al.*, 2016). These studies demonstrate that ER mutations, while relatively rare, can be used as markers to predict endocrine resistance or response to endocrine therapy (Rani *et al.*, 2019).

1.1.4.1.2 Receptor Tyrosine Kinase Signaling Pathways

Receptor tyrosine kinases (RTKs) are a family of membrane receptors that, upon binding to their respective ligands, induce a signaling cascade that results in the induction of gene transcription, proliferation, migration and invasion (Rani *et al.*, 2019). Of these RTKs, the most prominently characterized in breast cancer have been the Epidermal Growth Factor Receptors (EGFR), which include HER2 and Insulin-like growth factor-1 receptor (IGF1R) (Rani *et al.*, 2019). An overall upregulation of RTKs is a sign of a poor prognosis and is observed widely in breast cancers (Templeton *et al.*, 2014). The major signaling pathways that are utilized by these RTKs to transduce their signal are the Mitogen Activated Protein Kinase (MAPK) pathway, the JAK/STAT pathway and the PI3K/AKT pathway (Rani *et al.*, 2019).

The EGFR family of receptors include HER1, HER2, HER3 and HER4 and are also known as the ErbB family of growth factor receptors. HER2 overexpression occurs in 20-30% of breast cancer cases including ER+ BC cases (Pernas and Tolaney, 2019).

The G-protein coupled Estrogen Receptor (GPER), when stimulated by estrogen, is the primary conduit for the crosstalk between the ER pathway and EGFR signaling (Revankar *et al.*, 2005). Estrogen binding to membrane-bound GPER leads to increased phosphorylation of MAPK in breast cancer cells that express the receptor while MAPK phosphorylation remains unchanged in cells that do not express GPER (Filardo *et al.*, 2000). Additionally, it has been shown that growth factor signaling (primarily HER2 expression) is upregulated not only in ER+ breast cancer cell lines but also in patients treated with tamoxifen (Gutierrez *et al.*, 2005). When MCF7 cells overexpressing HER2 were treated with tamoxifen, it was found that their growth was stimulated rather than inhibited, implying that in HER2-expressing ER+ breast cancer cells Tamoxifen acts as an agonist rather than an antagonist (Shou *et al.*, 2004). More recently, an examination of

tamoxifen resistant tumours revealed that activating HER2 mutations were responsible for the development of therapy resistance in these patients (Nayar *et al.*, 2019).

EGFR (HER1) has also shown to contribute to tamoxifen resistance. A recent article showed that tamoxifen treatment in ER+ breast cancer cells results in the upregulation of EREG, an EGFR activator protein, which subsequently increases EGFR activity in these cells despite tamoxifen treatment (He *et al.*, 2019). Another study showed that both EGFR and HER2 are upregulated in MCF7-xenografts that tamoxifen-resistant but not in those that were sensitive to the drug (Massarweh *et al.*, 2008). They also showed that this increase in EGFR/HER2 was accompanied by heightened MAPK phosphorylation downstream (Massarweh *et al.*, 2008). MCF7 cells expressing EGFR were resistant to the growth inhibitory effects of Tamoxifen and this effect of EGFR was driven primarily by PI3K/Akt signaling (Moerkens *et al.*, 2014).

In tumours that overexpressed HER2 and were tamoxifen resistant, the gene expression of ER-inducible targets was reduced while those representing the targets of HER2 signaling were overexpressed, implying that these tumours switched from traditional ER signaling to HER2 signaling as they developed resistance to Tamoxifen (Creighton *et al.*, 2008). The importance of this switch between ER to HER2/EGFR signaling has been investigated. A dual EGFR/HER2 inhibitor Lapatinib was found to restore Tamoxifen sensitivity in otherwise Tamoxifen-resistant HER2+ breast cancer cell lines (Leary *et al.*, 2010). A recent phase II clinical trial studied the combinatorial treatment of lapatinib and tamoxifen in patients with breast cancer who did not respond to Tamoxifen previously (Gartner, 2017). Another phase II trial investigated the use of EGFR inhibitor Gefitinib in combination with Tamoxifen in patients with ER+ metastatic breast cancer, leading to improved progression-free survival vs placebo (Osborne *et al.*, 2011).

1.1.4.1.3 IGF1R and Insulin Receptor Signaling in Tamoxifen resistance

Both insulin and insulin-like growth factor (IGF) act through their respective receptors to regulate biological processes such as apoptosis, cell growth and differentiation (Rani *et al.*, 2019). The Insulin Receptor (IR) and the Insulin-like Growth Factor-1 Receptor (IGF1R) have a high degree of homology and therefore share a vast majority of downstream signaling, particularly through PI3K/AKT and Ras/MAPK signaling (Nagao *et al.*, 2021). While both insulin and IGF can bind

act as ligands to IGF1R and IR respectively, this ligand-receptor interaction has lower affinity (Nagao *et al.*, 2021). When phosphorylated, hence activated, IGF1R and IR is associated with poor survival outcomes in patients with ER+ breast cancer (Law *et al.*, 2008). Both receptors are also frequently overexpressed in all breast cancers, including ER+ breast tumours (Rostoker *et al.*, 2015).

There are several pieces of evidence showing that IGF1R pathway dysregulation is involved in tamoxifen resistance and endocrine resistance overall (Rani *et al.*, 2019). A recent siRNA screen identified key regulators associated with IGF1R-mediated tamoxifen resistance, including proteins involved in MAPK signaling including the p21-activated kinase 2 (PAK2) which was identified as the strongest inducer of Tamoxifen resistance (Zhang *et al.*, 2018). IGFBP-1, an IGF1 binding protein which regulates the availability of the factor, was found to promote Tamoxifen resistance in ER+ breast cancer cells through IGF1R and ERK pathway activation (Zheng *et al.*, 2020).

Interestingly, however, the inhibition of IGF1R in Tamoxifen resistant MCF7 and T47D cells did not restore sensitivity to the drug in these cell lines (Fagan *et al.*, 2012). Fagan and colleagues found that while IGF1R inhibition did affect AKT phosphorylation in Tamoxifen sensitive cells, it had no affect on AKT phosphorylation in Tamoxifen resistant cells (Fagan *et al.*, 2012). However, a dual IR/IGF1R inhibitor reduced AKT phosphorylation in both Tamoxifen sensitive and resistant cell lines, implying that crosstalk between the two receptors may be responsible for ineffectiveness of the IGF1R inhibitor alone (Fagan *et al.*, 2012). Additionally, IGF1R inhibition was found to reduce the sensitivity of ER+ breast cancer cells to tamoxifen by reducing FoxO1 expression (FoxO1 being a previously characterized inducer of Tamoxifen resistance) (Vaziri-Gohar *et al.*, 2017). Therefore, it appears that the loss of IGF1R rather than its overexpression is associated with reduced tamoxifen efficacy (Vaziri-Gohar *et al.*, 2017). This may be due to the dependence of IGF1R expression on ER functioning, as described previously (Rani *et al.*, 2019). Reduction in IGF1R levels were observed in Tamoxifen resistant breast cancer cells though a similar reduction in IR levels was not observed (Fagan *et al.*, 2012). In fact, patients with Tamoxifen-resistant tumours and high levels of IGF1 and ER expression took a longer time to develop resistance, further bolstering the theory that IGF1/IGF1R enhance tamoxifen sensitivity rather than resistance (Rani *et al.*, 2019). Taken together, these studies indicate that a crosstalk

between both IGF1R and IR is responsible for driving tamoxifen resistance and inhibition of IR may be necessary to tackle Tamoxifen resistance, especially given the lack of effectiveness of IGF1R inhibition in clinical trials investigating Tamoxifen resistance (Fagan *et al.*, 2012; Rani *et al.*, 2019). However, concerns over severe metabolic side effects associated with IR inhibition have slowed development of anti-IR inhibitors (Rostoker *et al.*, 2015).

In addition to dysregulation of RTKs such as EGFR, IGFR and IR, it is important to note the roles of signaling molecules downstream of these receptors in the development and maintenance of Tamoxifen resistance. In Tamoxifen resistant MCF7 cells, it was found that AKT and protein kinase B (PKB) phosphorylation was significantly higher than in their Tamoxifen sensitive counterparts, which may contribute to the relatively higher aggressiveness of Tamoxifen resistant tumours (Jordan *et al.*, 2004). This phenomenon was reversed when these cells were treated with a PI3K inhibitor which reduced AKT phosphorylation (Jordan *et al.*, 2004). By extension the PI3K/AKT/mTOR signaling pathway was implicated in the development of Tamoxifen resistance (Kirkegaard *et al.*, 2005). In patient carcinoma that were previously treated with Tamoxifen, high pAKT expression was observed and predicted reduced overall survival outcomes in these cases (Kirkegaard *et al.*, 2005). The data implied that these markers were indicative of poor therapeutic response, high relapse possibility and increased risk of death (Kirkegaard *et al.*, 2005).

1.2 Breast Tumour Kinase (BRK)

Breast Tumour Kinase or BRK (also known as PTK6) is a non-receptor tyrosine kinase that is highly expressed in breast cancer tissue while being lowly expressed or non-existent in normal mammary gland (Aubele *et al.*, 2008). BRK is a member of a family of non-receptor tyrosine kinases referred to as BRK family kinases (BFKs), along with FRK (Fyn-related Kinase) and SRMS (src-related kinase lacking C-terminal regulatory tyrosine and N-terminal myristylation sites). As non-receptor tyrosine kinases, BFKs show similarities with the Src family kinases in terms of their domain structure (Goel and Lukong, 2015).

As implied by its high expression in breast carcinoma, BRK has an important role in breast cancer progression, and it represents a valid target of investigation. Additionally, BRK has been shown to be an oncogene, as it activates other oncoproteins, resulting in an increase in cell proliferation,

migration, invasion, and metastasis (Ang *et al.*, 2021). As previous clinical trials targeting RTKs and other non-receptor tyrosine kinases have not yielded significant benefits in combating Tamoxifen resistance, BRK presents itself as a target of therapeutic significance (Ang *et al.*, 2021).

1.2.1 Discovery, structure, and biochemical activity

In 1994, the cDNA coding for BRK was cloned from a sample of metastatic breast tumour tissue and from T47D and MCF7 cell lines (Mitchell *et al.*, 1994). At the time Mitchell and colleagues discovered that BRK was capable of autophosphorylation on its tyrosine residues and that it was not expressed in normal breast tissue (Mitchell *et al.*, 1994). Later, PTK6, the gene that encodes for BRK, was located on chromosome 20q13.3 in humans and shares conserved sequences with Src between exons 1/2 and exons 7/8 (Haeyul *et al.*, 1998; Park *et al.*, 1997).

The protein product of the PTK6 gene, BRK, is a 451-amino acid kinase containing 3 important domains: a Src homology 3 (SH3) domain, a SH2 domain and a tyrosine kinase (SH1) domain (Ang *et al.*, 2021). The SH3 domain recognizes and binds to proline-rich peptides on target substrates, for example, peptides with a canonical PXXP-type motif have been recognized by the kinase (Zheng *et al.*, 2010). The SH2 domain regulates substrate binding and phosphorylation as mutations in this domain have been shown to affect BRK binding to and phosphorylation of its target STAP2 (Mitchell *et al.*, 2000). The kinase domain is the region of BRK that catalyzes the phosphorylation of BRK substrates on specific tyrosine residues (Goel and Lukong, 2015).

Studies have shown that autophosphorylation of BRK at its Y342 residue (located in the kinase domain) increased its phosphorylation activity while the phosphorylation of the Y447 residue (located in the C-terminal tail) caused the inhibition of the kinase (Qiu and Miller, 2002). This implied that the activation and inhibition of BRK functioned in a manner similar to c-Src (Goel and Lukong, 2015). Phosphorylation of BRK at Y447 results in the BRK-SH2 domain binding to the site, thereby favouring a close conformation and inhibiting activity (Goel and Lukong, 2015). Dephosphorylation at the Y447 site, by protein tyrosine phosphatases, releases SH2 binding, allowing for an open conformation and the subsequent autophosphorylation of Y342 and the activation of BRK (Goel and Lukong, 2015). Mutation of the site from Y to F results in a 2.5 fold increase in BRK activity while a mutation at the Y342 site abrogated kinase activity (Qiu and

Miller, 2002). Other amino acid sites important to BRK functioning include K219 and W184. K219, located in the ATP-binding pocket of the kinase domain, is a residue required for ATP binding to BRK and is therefore vital to its enzymatic activity (Goel and Lukong, 2015). The W184 residue, located in the linker region between the SH2 and kinase domains, stabilizes the active conformation of BRK as a W184A mutation reduces BRK autophosphorylation significantly (Kim and Lee, 2005). The activity of BRK, particularly the phosphorylation of Y342, appears to be regulated by Protein Tyrosine Phosphatase 1B (PTP1B) (Fan *et al.*, 2013). PTP1B inactivates BRK by directly interacting with and dephosphorylating the Y342 activation site (Fan *et al.*, 2015).

1.2.2 BRK Substrates and Binding Partners

BRK binds to and phosphorylates a variety of proteins by localizing to the nucleus, cytoplasm and cell membrane (Goel and Lukong, 2015). Lukong and colleagues showed that BRK phosphorylates Sam68, an RNA-binding protein, at the Y440 residue resulting in the nuclear localization of Sam68 and inhibiting its RNA-binding activity and tumour suppressor function (Lukong *et al.*, 2005). BRK also phosphorylates paxillin phosphorylation at Y31 and Y118, resulting in cell migration in an EGF-dependent mechanism involving Rac1 activation (Chen *et al.*, 2004). BRK was found to interact with both STAP2 (signal transducing adaptor protein-2) and STAT3 (signal transducer and activator of transcription-3) to drive cell proliferation (Ikeda *et al.*, 2010). Interestingly, BRK also interacts with all 4 members of the ErbB receptor tyrosine kinase family and thereby plays a role in breast cancer progression through stimulation with growth factors (Goel and Lukong, 2015; Kamalati *et al.*, 2000a; Kamalati *et al.*, 1996). Additionally, BRK interacts with IGF-1R, another receptor tyrosine kinase, driving survival, and suppressing apoptosis (Irie *et al.*, 2010). Downstream of IGF-1R and IR, BRK interacts with IRS4 (Insulin Receptor Substrate-4) as its binding with the adaptor protein is increased upon IGF1 stimulation in ER+ breast cancer cells (Qiu *et al.*, 2005). In keeping with the theme of BRK and its role in growth factor receptor signaling, an association between BRK and AKT was found to suppress kinase activity of AKT through the phosphorylation of uncharacterized tyrosine residues (Zhang *et al.*, 2005). By contrast, BRK can enhance AKT activity by phosphorylating Y315 and Y326 residues, therein highlighting the cell-line and context specificity of BRK interaction with its substrates (Zheng *et al.*, 2010). β-catenin, an important intermediary in the Wnt signaling pathway,

was characterized as a BRK substrate and its phosphorylation results in reduced β-catenin transcription (Palka-Hamblin *et al.*, 2010). Presently, there are 35 known interactors of BRK with diverse biological effects including cell proliferation, migration, metastasis and differentiation in cancers in general but breast cancer in particular (Goel and Lukong, 2015).

1.2.3 Cellular roles of BRK in Breast Cancer

The increase in expression of BRK in breast carcinoma and its contrasting low expression in normal breast tissue has been well characterized by previous studies (Goel and Lukong, 2015). A recent publication showed that not only was BRK expression increased by up to 5-fold in breast cancer tissue vs normal mammary tissue, its activity (phosphorylated Y342 levels) was significantly increased in tumour samples obtained from patients (Peng *et al.*, 2014). Half of the patients presented with active BRK while 40% of patients exhibited the membrane-bound form of active BRK which is often associated with higher grade tumours and increased oncogenic activity (Peng *et al.*, 2014). The cause for this overexpression has not been well characterized currently. A study by Aubele and colleagues attempted to find if BRK overexpression was a result of increased copy number (Aubele *et al.*, 2009). In a dataset of 426 invasive breast tumours, BRK gene copy number was only increased in 45% of the same, therefore a clear link between BRK gene amplification and its protein overexpression was not found (Aubele *et al.*, 2009). Therefore, it is reasonable to theorize that the increase in BRK levels may be a result of regulation at the mRNA and post-translational level (Goel and Lukong, 2015). However, recently, it was shown that BRK expression can be induced by Hypoxia-Inducible Factor 1α (HIF1α) in TNBC cell lines because of increased physiological cell stress (hypoxia) (Regan Anderson *et al.*, 2016).

This finding lends credence to theories that BRK is a stress response protein and can be induced during cancer development to combat the various stressors (including hypoxia) that cancer cells must withstand to proliferate. When activated in breast cancer cells, BRK regulates important cellular functions such as proliferation, evasion of cell death, invasion, migration, metastasis and cancer metabolism (Ang *et al.*, 2021).

1.2.3.1 Cancer cell growth and avoidance of cell death

The relationship between BRK and EGFR has been well characterized previously and was one of the first examples of the growth-promoting effects of BRK activity in breast cancer cells (Kamalati *et al.*, 1996). When these cells were stimulated with EGF, BRK active site phosphorylation was increased and BRK, in turn, directly phosphorylated the Y845 site on EGFR's kinase domain (Chen *et al.*, 2004). This residue, when phosphorylated, prevents the ubiquitination and turnover of EGFR, allowing for continual stimulation of the pathway (Li *et al.*, 2012). Overall, the effect of this interaction is the increased proliferation of luminal A breast cancer cells (Kamalati *et al.*, 2000b). It is possible that the BRK-EGFR interaction is an important factor in the low success rate of anti-EGFR therapies in breast cancer (Ang *et al.*, 2021).

BRK interacts with HER2, another member of the EGFR family, resulting in a HER2 induced activation of Ras/MAPK signaling and cyclin E activity downstream which results in increased cell proliferation in breast cancer cells overexpressing HER2 (Xiang *et al.*, 2008). The simultaneous knockdown of BRK and HER2 in HER2+ breast cancer cells not only decreased the phosphorylation of MAPK1/3, but it also reduced the growth of HER2+ tumours *in vivo* (Ludyga *et al.*, 2013). Heregulin, a HER3 and HER4 ligand was also found to activate BRK which then activates ERK5 (Extracelluar signal Regulated Kinase 5) and p38 MAPK in ER+ breast cancer cells (Ostrander *et al.*, 2007). Additionally, overexpression of BRK sustained ERK1/2 activation, increased Ras/MAPK signaling and induced cell growth downstream (Xiang *et al.*, 2008). *In vivo* studies highlighted that BRK expression in tumours increased cell survival and delayed mammary gland involution (Lofgren *et al.*, 2011).

IGF-1, the ligand of the IGF1R receptor, can induce the phosphorylation of BRK at its tyrosine residues (Qiu *et al.*, 2005). This event appears to occur through the direct interaction between IGF1R and BRK wherein BRK modulates IGF1R phosphorylation and vice versa, in breast cancer cells (Irie *et al.*, 2010). This interaction between the two kinases promoted anchorage independent cell survival as well (Irie *et al.*, 2010). This function of BRK, through IGF1R, is mediated by the phosphorylation of ERK and AKT downstream of IGF1R and was found to trigger anti-apoptotic signals (such as Bim) and prevent cell death in anchorage independent conditions (Irie *et al.*, 2010).

A recent study by Lange and colleagues found that the ectopic expression of BRK alone was able to promote cell survival in TNBC cells (Regan Anderson *et al.*, 2016). In their study, it was found that BRK was a regulatory target of a complex between GR (glucocorticoid receptor) and HIF1α when these breast cancer cells were under cellular stress (Regan Anderson *et al.*, 2016). Interestingly BRK expression was not only sufficient to promote cell survival in these cells, but it was also carrying out this function independently of the GR-HIF1α complex, possibly through the activity of p38 MAPK as described previously (Regan Anderson *et al.*, 2016). This study effectively showed that BRK was capable of regulating cell survival on its own.

Another well characterized BRK function in breast cancer has been its interaction with members of the STAT family. Namely, BRK interacts with STAT3 through the adaptor protein STAP2 thereby phosphorylating STAT3 on its Y705 residue in ER+ breast cancer cells (Ikeda *et al.*, 2010; Liu *et al.*, 2006). BRK knockdown in these cells resulted in a reduction of cell proliferation by reducing STAT3 phosphorylation and transcription activity downstream (Liu *et al.*, 2006). STAT5b was also found to interact with BRK in HER2+ breast cancer cells as it phosphorylates STAT5b at Y699 and activates the transcription factor (Weaver and Silva, 2007). Knocking down BRK or STAT5b reduced DNA synthesis and growth in these cells (Weaver and Silva, 2007).

Phosphorylation and inactivation of tumour suppressor protein Rb (retinoblastoma protein) results cells entering the S phase of the cell cycle (Ang *et al.*, 2021). BRK overexpression was found to promote cell proliferation through the activation of the cyclin E-CDK2 complex which phosphorylates and inactivates Rb, allowing for cell cycle progression (Xiang *et al.*, 2008). When BRK is knocked down, therefore, there is a reduction in both cyclin E and cyclin D levels, implying BRK affects the cell cycle (Ludyga *et al.*, 2011).

1.2.3.2 Invasion, Metastasis and Angiogenesis

An important hallmark of cancer malignancy as the disease progresses is the ability of tumour cells to detach and invade surrounding tissue, referred to as metastasis (Hanahan and Weinberg, 2011). As these tumours develop, they require blood supply and thus the formation of blood vessels becomes paramount to providing nutrients and oxygen (Hanahan and Weinberg, 2011). BRK has been implicated in both processes.

In the study by Chen and colleagues, EGF-induction of breast cancer cells resulted in increased cell migration through BRK-mediated activation of paxillin and Rac1 (Chen *et al.*, 2004). Paxillin is a focal adhesion protein that controls interactions between actin and the extracellular matrix (López-Colomé *et al.*, 2017). BRK phosphorylates paxillin at Y31 and Y118, activating the protein to promote migratory and invasive characteristics in breast cancer cells (Ang *et al.*, 2021). A follow up study showed that BRK phosphorylated p190RhoGAP at its Y1105 site, leading to RhoA inhibition and activation of the oncogene Ras which promotes migration and invasion in both ER+ and triple-negative breast cancer cell lines (Shen *et al.*, 2008).

Focal adhesion kinase (FAK) is a tyrosine kinase that plays a vital role in cell-cell communication and is frequently associated with increased cancer metastasis and invasion when its high expression is detected in breast tumours (Zhou *et al.*, 2019). BRK has been characterized as a regulator of FAK as it phosphorylates the latter at its Y576/577 residues and BRK knockdown was found to reduce both the phosphorylation at the site and results in fewer metastases by inactivation of FAK (Peng *et al.*, 2015). The same study identified breast cancer anti-estrogen resistance protein 1 (BCAR) as another BRK target as BRK knockdown disrupted BCAR1 phosphorylation at its Y165 site, inhibiting it (Peng *et al.*, 2015). Functionally, BRK knockdown resulted in reduced metastases *in vivo* in mice that were injected with HER2-positive breast cancer cells (Peng *et al.*, 2015). In a recent study, Miah and colleagues found that BRK phosphorylates SMAD4 and targets it for degradation, resulting in the inhibition of the tumour suppressor FRK downstream (Miah *et al.*, 2019). As FRK is involved in suppressing epithelial to mesenchymal transitions (EMT), this resulted in an increase in EMT-specific transcription factors SNAIL and SLUG in breast cancer cells (Miah *et al.*, 2019). Interestingly, in keeping with the theme of BRK's role in stress response signaling, independent studies by Pires *et al.* and Regan Anderson and colleagues found that hypoxia induced BRK induction resulted in increased tumour metastasis *in vivo* (Pires *et al.*, 2014; Regan Anderson *et al.*, 2013). These results reiterate the point that BRK is a major factor in the induction of hypoxia-induced cancer processes.

Osteopontin is a factor that induces vascular endothelial growth factor (VEGF)-dependent tumour progression and angiogenesis by activating BRK, nuclear factor-kappaB (NFkB) and activating transcription-4 (ATF-4) (Chakraborty *et al.*, 2008). Analysis of clinical specimen revealed an

increase in angiogenesis when osteopontin triggered VEGF-directed pathways (Chakraborty *et al.*, 2008). HIF1α, a regulator of BRK expression and a regulatory partner, is also a well characterized regulator of VEGF-directed angiogenesis (Semenza, 2012).

Overall, BRK plays multiple roles in signaling pathways involved in breast tumour progression. It appears to act as a linker between growth factor receptors and downstream effector proteins by activating the relevant proteins. Additionally, its relationship with HIF1α implies a stress response element to BRK functioning which positions it as a gene that is activated when cells are exposed to stressors such as drug treatments. Therefore, the kinase presents itself as a possible therapeutic target for inhibition.

1.2.3.3 BRK Activity in Breast Cancer and its Inhibition

BRK displays increased activation in breast cancers compared to normal breast tissue, as characterized previously (Chakraborty *et al.*, 2008; Liu *et al.*, 2006; Qiu *et al.*, 2005). In a couple of these reports, BRK was found to be more active in MCF10A and MCF7 breast cancer cells that were stimulated by EGF and IGF respectively (Kamalati *et al.*, 1996; Qiu *et al.*, 2005). The Hepatocyte Growth Factor (HGF) activates the Met receptor which in turn was found to increase BRK kinase activity in triple-negative and ER+ breast cancer cell lines (Castro and Lange, 2010). Osteopontin, as discussed previously, also induced BRK activation and angiogenesis of breast carcinoma (Chakraborty *et al.*, 2008).

It is well established that BRK activation is driven primarily by growth factor receptor activity in breast tumours, however the mechanisms driving the inactivation of BRK are not well known (Goel and Lukong, 2015). Gao and colleagues showed that suppressor of cytokine signaling 3 (SOCS3) associated with the SH2 domain of BRK and targeting it for degradation through its inherent kinase inhibitory activity (Gao *et al.*, 2012). In ovarian cancer models, PTP1B dephosphorylation of BRK at the Y342 active site but currently the same mechanism has not been identified in breast cancer cells (Fan *et al.*, 2013).

A couple of reports have attempted to investigate small molecule BRK inhibitors and their effects on BRK activity and its functioning as a promoter of cell growth (Jiang *et al.*, 2017; Mahmoud *et al.*, 2014). Mahmoud *et al.* determined that 4-anilino substituted α-carboline compounds were

potent inhibitors of BRK and that, of these compounds, a variant with a hydroxyl substitution was the most potent inhibitor of BRK (Mahmoud *et al.*, 2014). The compound, named 4f in the report, was able to inhibit proliferation significantly in MCF7 breast cancer cells and was shown to be highly specific for BRK with no significant inhibition of similar non-receptor kinases such as AKT, JAK3 and Src (Mahmoud *et al.*, 2014). In a follow up study, this inhibitor was found to induce cell death in non-adherent breast cancer cells, an effect similar to BRK knockdown and therefore implying the inhibition was effective (Oelze *et al.*, 2015). The compound 4f is now available commercially as Tilfrinib (Tocris Cat. No. 5579). Another group, Jiang and colleagues, developed small molecule inhibitors against BRK activity (Jiang *et al.*, 2017). Using a compound-centric approach, they identified XMU-MP-2 as an effective BRK specific inhibitor (Jiang *et al.*, 2017). In both T47D and MCF7 cells, XMU-MP-2 inhibition of BRK reduced cell proliferation and tumour growth *in vitro* and *in vivo* respectively (Jiang *et al.*, 2017). Overall, these findings display the possible therapeutic benefits of targeting BRK in breast cancer cells.

1.2.4 BRK and Drug Resistance

Recent studies have investigated the role of BRK in resistance against cancer therapies. In fact the overexpression of BRK was found to confer resistance towards radiotherapy in triple-negative breast cancer cells (Bourton *et al.*, 2015). It was found that BRK performed this function by making these cells resistant to DNA damage, though the role of BRK in the DNA damage response pathway is still being explored currently (Ang *et al.*, 2021). In mammary epithelial cells, BRK expression induced doxorubicin (chemotherapeutic) resistance (Lofgren *et al.*, 2011). In a previous study that identified the co-amplification of BRK and HER2, it was found that BRK expression conferred resistance to the anti-HER2 therapy Lapatinib in HER2+ breast cancer cells (Xiang *et al.*, 2008). A recent article reported that BRK was induced in TNBC cells that were exposed to Taxol or 5-fluorouracil (both chemotherapeutic agents) and the higher expression remained stable in Taxol-resistant MCF7 cells (Anderson *et al.*, 2018). In fact, it was found that stress response factors such as the glucocorticoid receptor and the aryl hydrocarbon receptor (AhR) were found to form a complex with HIF1α and aid the induction of BRK (Anderson *et al.*, 2018). A follow up to these results revealed that BRK in turn mediated AhR by associating with it through its SH2-domain and activating the receptor (Dwyer *et al.*, 2020). By inhibiting AhR, Taxol-resistant cells

were resensitized to the drug (Dwyer *et al.*, 2020). Cetuximab is an anti-EGFR antibody used to treat breast tumours overexpressing the receptor (Li *et al.*, 2012). BRK knockdown in cetuximab resistant breast cancer cells was found to resensitize these cells to the drug by increasing the levels of EGFR that were being degraded (Li *et al.*, 2012).

In both Tamoxifen and Fulvestrant-resistant breast cancer cells, BRK inhibition induced p38-directed induction in apoptosis (Ito *et al.*, 2017). Indeed, tumour growth was abrogated in drug resistant MCF7 xenografts when BRK was knocked down (Ito *et al.*, 2017). Jiang *et al.* also showed that the inhibition of BRK in Tamoxifen resistant MCF7 cells was successful in reducing their proliferation in the presence of Tamoxifen (Jiang *et al.*, 2017).

Taken together, these studies not only implicate BRK in breast cancer disease progression but also in drug resistance against breast cancer therapies including chemotherapeutics and targeted therapies.

1.3 Phosphorylation and its Importance in Cancer

Post-translational modifications of proteins are vital for driving various cellular functions such as gene expression, enzymatic activity, protein stability and degradation as well as protein-protein interactions (Singh *et al.*, 2017). While there are more than 200 types of modifications, both reversible and irreversible, phosphorylation is perhaps the most well characterized PTM (Singh *et al.*, 2017).

Protein phosphorylation involves the attachment of a phosphate group (PO_4) to polar side chains on amino acids causing a protein to change conformation due to the hydrophilic polar nature of the phosphate group (Ardito *et al.*, 2017). The phosphate group is often donated by a molecule of adenosine triphosphate (ATP) which turns into adenosine diphosphate (ADP) upon the transfer of its terminal PO_4 group to the amino acid side chain (Ardito *et al.*, 2017). Conversely, a phosphate group can be removed from an amino acid residue by transferring the PO_4 molecule to an ADP molecule, turning it into ATP (Ardito *et al.*, 2017). Approximately 40% of phosphorylations occur on either serine (S), threonine (T) or tyrosine (Y) residues through the transfer of the PO_4 to the hydroxyl group of these amino acids (Vlastaridis *et al.*, 2017). Within this subset, serine, and threonine phosphorylation accounts for 86.4% and 11.8% of phosphosites respectively with

tyrosine phosphorylation being the rarest at 1.8%, though some large scale phosphoproteomics analyses were able to find pY sites represented 3% of their phosphoproteome (Ardito *et al.*, 2017; Batth *et al.*, 2018). Protein phosphorylation/dephosphorylation on STY sites helps regulate processes such as signal transduction, cell growth and development and protein synthesis as enzymes and receptors are activated or deactivated through phosphorylation and removal of phospho groups through the action of kinases and phosphatases respectively (Ardito *et al.*, 2017). In addition to determining whether a protein is active or inactive, phosphorylation and dephosphorylation can also enhance stabilization, mark proteins for degradation, determine localization and determine protein-protein interactions (Turdo *et al.*, 2021).

Various hallmarks of cancer can be driven by errant phosphorylation events and dysregulation of both kinases and phosphatases (Hanahan and Weinberg, 2011). For example, the overexpression and increased enzymatic activity of the receptor tyrosine kinase HER2 is a hallmark of HER2-positive breast cancer cases (Hsu and Hung, 2016). Increase in phosphorylation (hyperphosphorylation) or decrease in phosphorylation (hypophosphorylation) of specific amino acid residues on kinases or their targets affects signal transduction in crucial growth factor receptor pathways which, in turn, increases tumour growth, evasion of cell death and growth suppressors as well as induction of angiogenesis and metastasis (Hanahan and Weinberg, 2011; Radivojac *et al.*, 2008). As a majority of these pathways involve kinases that recognize and phosphorylation S, T and Y sites, it is important to review the role and importance of these kinases in cancer in general.

1.3.1 Role of Kinases in Cancer

Kinases play overlapping and complex roles in various cancer hallmarks such as cell transformation, tumour growth, survival and proliferation (Bhullar *et al.*, 2018). They can, however, be roughly categorized based on their target residues. Firstly, there are S/T kinases that specifically recognize and phosphorylate serine and/or threonine residues on their targets (Bhullar *et al.*, 2018). These include mitogen-activated protein kinases (MAP kinases) such as ERK1/2, JNK and p38 (Bhullar *et al.*, 2018). MAP kinases often act downstream of receptor tyrosine kinases as they help propagate extracellular signals such as growth factors, hormones and cytokines through downstream signaling cascades (Dhillon *et al.*, 2007). At least 125 of the 518 human protein kinases are S/T kinases (Ardito *et al.*, 2017). Secondly, there are protein tyrosine kinases

(PTK) which make up 90 of the kinases characterized in humans (Robinson *et al.*, 2000). PTKs can be further divided into 2 subclasses: receptor tyrosine kinases and non-receptor tyrosine kinases (Robinson *et al.*, 2000). Of the 90 tyrosine kinases, 58 belong to the receptor tyrosine kinases subclass while 32 belong to the non-receptor tyrosine kinase subclass (Robinson *et al.*, 2000).

1.3.1.1 Serine/Threonine Kinases in Cancer

Of the serine/threonine kinases, PKA (protein kinase A), MAPKs, RAF, AKT, GSK3, and cyclin-dependent kinases (CDKs) have been the most well characterized drivers of cancer (Turdo *et al.*, 2021). In breast cancer cells, PKA is activated through the action of G-protein coupled estrogen receptor upon the binding of estrogen to the receptor and through this, it enhances multiple-drug resistance in these cells (Moody *et al.*, 2015). When triple-negative breast cancer cells were stimulated with insulin growth factor (IGF1), it resulted in an increase in the phosphorylation of MAPKs such as ERK1/2 as well as AKT and that this activation was vital to driving metastasis in these cells (Zhu *et al.*, 2011). In ER-positive MCF7 breast cancer cells, overexpression of active RAF1 made these cells more resistant to chemotherapeutics taxol and doxorubicin (Davis *et al.*, 2003). Inhibition of GSK3β phosphorylation reduced the viability of both breast cancer cells *in vitro* as well as patient-derived xenografts *in vivo* and it also overcame chemoresistance in both cases (Ugolkov *et al.*, 2016). Dysregulation of Cyclin-dependent kinases such as CDK1/2 and CDK4/6 is a well known hallmark of irregular growth and cell cycle progression in cancer (Turdo *et al.*, 2021). CDK1/2 inhibition caused cell cycle arrest and apoptosis in both Tamoxifen-sensitive and Tamoxifen-resistant breast cancer cell lines (Johnson *et al.*, 2010).

1.3.1.2 Receptor Tyrosine Kinases in Breast Cancer

While 58 different RTKs have been found in humans, they can be classified into 20 different subfamilies based on similarities in structural features (Butti *et al.*, 2018). A key feature of RTKs is that they are capable of not only phosphorylating tyrosine residues on target molecules but they are also capable of trans-autophosphorylation of tyrosine sites within the same RTK molecule (Butti *et al.*, 2018). As receptors, RTKs are activated by ligands such as growth factors (EGF, IGF, for example) cytokines or, in some cases, collagen fibres form the extracellular matrix (Butti *et*

al., 2018). When ligands are not present, RTKs are inhibited by the physical contact between phosphorylated inhibition site in the activation loop and the kinase domain (Butti *et al.*, 2018). Ligand binding changes RTK conformation in such a way that dephosphorylates the autoinhibitory phosphosite, resulting in an open, active conformation which itself allows for the ligand-induced dimerization of these kinases (Butti *et al.*, 2018). RTKs then recruit, phosphorylate and activate downstream effector molecules such as Insulin Receptor Substrate (IRS) and Grb2-associated binder 1 (GAB1) which are recruited to IGFR/InsR and EGFR respectively (Du and Lovly, 2018). These effector proteins then participate in downstream signaling cascades, generally through the phosphorylation and activation of MAP kinases (ERK1/2, for example) and PI3K/AKT signaling (Du and Lovly, 2018). Therefore, upon ligand binding and activation, RTKs drive the phosphorylation of key downstream targets that propagate the growth stimulatory signal of their ligands. One key example of this is the activation of the non-receptor tyrosine kinase Src by RTKs upstream (Gocek *et al.*, 2014). Src is phosphorylated on its Y213 residue by the RTKs EGFR and HER2 (Gocek *et al.*, 2014). Upon phosphorylation at this site, Src is activated and can subsequently phosphorylate targets such as STAT3, Akt and MAPKs downstream (Gocek *et al.*, 2014). Key RTKs involved in breast cancer include EGFR (Epidermal Growth Factor Receptor), IGFR (Insulin Growth Factor Receptor), InsR (Insulin receptor) and have been discussed in previous sections with respect to their role in both breast cancer progression and drug resistance (Butti *et al.*, 2018).

1.3.1.3 Non-receptor Tyrosine Kinases in Breast Cancer

The 32 human non-receptor tyrosine kinases (NRTKs) are classified into 10 subfamilies based on similarities in their domain structure (Gocek *et al.*, 2014). Of these NRTKs, perhaps the best characterized and well studied are the Src family kinases, which also include BRK family kinases (Gocek *et al.*, 2014). The prototypical member of this family, Src, plays a role in the regulation of multiple signaling pathways implicated in breast cancer such as PI3K/AKT signaling, MAP kinase signaling and STAT3 activation (Gocek *et al.*, 2014). Previous studies have shown that Src-mediated activation of STAT3 through the phosphorylation of its Y705 activation site regulates cell proliferation of breast cancer cells (Garcia *et al.*, 2001). Src-mediated STAT3 regulation in this manner was found to be mediated by the activation of EGFR upstream (Garcia *et al.*, 2001).

In addition, Src regulates the tyrosine phosphorylation of PTEN, a tumour suppressor that acts upstream of AKT (Lu *et al.*, 2003). The phosphorylation of PTEN at these tyrosine sites inhibits it and prevents PTEN from inhibiting AKT downstream (Lu *et al.*, 2003). This causes increased AKT phosphorylation and activity and therefore increased growth proliferation in breast cancer cells (Lu *et al.*, 2003). Overall, in its role as an NRTK, Src helps to propagate the signal induced by RTKs upstream by affecting secondary signaling pathways such as Akt and MAPK signaling (Gocek *et al.*, 2014). Interestingly, in breast cancer cells, Src also phosphorylates EGFR on Y727, Y764 and Y896, all of which are in the activation loop of the RTK (Irwin *et al.*, 2011). This activity of Src effectively demonstrates the complex and inter-dependent nature of RTK and NRTK signaling in cancer progression.

In many ways, the diverse cellular roles and functions performed by BRK (prototypical member of the BRK family of kinases) exemplifies the properties of NRTKs (Gocek *et al.*, 2014). As described in detail in section 1.2, BRK phosphorylation of its targets such as STAT3, Akt, paxillin and EGFR drive cell proliferation, migration, metastasis, and angiogenesis, amongst other functions (Ang *et al.*, 2021). Another member of the BRK family of kinases is FRK (Fynn-related kinase). In contrast to BRK's oncogenic activity, FRK is a tumour suppressor as its expression is lost in breast tumours while normally expressed in mammary tissue (Brauer and Tyner, 2009). In normal mammary epithelial cells, FRK was found to physically interact with PTEN, another tumour suppressor, to prevent its degradation by phosphorylating it at its Y336 residue (Goel and Lukong, 2016; Yim *et al.*, 2009). In doing so, FRK prevents the activation of AKT downstream of PTEN and thereby prevents pro-oncogenic signaling in mammary epithelial cells (Yim *et al.*, 2009).

Overall, several hallmarks of cancer are driven by phosphorylation of proteins that drive signaling pathways which then result in changes in gene expression that results in cancer progression (Turdo *et al.*, 2021). As a result, many of the kinases discussed are the subject of anti-cancer treatment development. The Src inhibitor dasatinib is currently being tested for the treatment of ER-positive breast cancer in patients who had already been treated with aromatase inhibitors (Martellucci *et al.*, 2020). However, targeting Src has not yielded significantly beneficial results yet as progression free survival rates under dasatinib treatment remain similar to those without dasatinib (Martellucci

et al., 2020). By contrast, the antibody against HER2, called Trastuzumab is effective in the treatment of HER2-positive breast cancers when combined with chemotherapeutic agents (Maennling *et al.*, 2019). Due to the diversity of its roles and actions in breast cancer cells, it is possible that targeting BRK would provide significant benefits in a clinical setting, hence the importance of elucidating the mechanisms by which BRK functions in Tamoxifen-resistant breast cancer.

1.4 Phosphoproteomics

Kinase signaling and its subsequent dysregulation in cancer has been the target of investigation and drug development for decades (Savage and Zhang, 2020). A detailed analysis of kinase signaling, therefore, is necessary to build an understanding of the intricate set of events that drive phosphorylation/dephosphorylation of kinases, phosphatases and their targets (Urban, 2022). Proteomics refers to the large-scale study of proteins contained in a cell line, tissue or organism and it allows for the elucidation of the expression of multiple proteins at once (Graves and Haystead, 2002). Phosphoproteomics is the large-scale study of phosphorylation of these proteins (Savage and Zhang, 2020). Therefore, the advent of mass spectrometry-based phosphoproteomics analysis allows for a more in-depth exploration of these kinase-driven phosphorylation events (Savage and Zhang, 2020).

1.4.1 Mass spectrometry and its role in phosphosite identification

Mass spectrometers are capable of detecting both the presence and the relative abundance of peptides as well as deriving their sequences by using fundamental molecular properties such as mass and charge (Sinha and Mann, 2020). These highly sensitive analytical instruments consist of 3 parts: an ion source, a mass analyser and a detector (Sinha and Mann, 2020). Samples prepared for mass spectrometry are first separated using high performance liquid chromatography (HPLC) before being pumped through a micrometre-sized spray charged at a voltage of between 2-4 kV which results in the disintegration of the liquid sample into highly charged peptide ions in the gas phase (Sinha and Mann, 2020). The mass analyser then separates these ions by their mass-to-charge ratios (m/z) by using a oscillating electrical fields and measuring the velocity of the ions (Time-of Flight analysers) or by measuring the oscillation frequencies of the ions (Orbitrap

analyser) (Sinha and Mann, 2020). Once these ions are separated, they pass through a detector which produces mass spectra which represent the quantitative output of the process (Sinha and Mann, 2020).

Peptides are sequenced through a process called fragmentation which occurs just prior to the detection stage (Sinha and Mann, 2020). Ions from the mass analyser are fragmented through collision with inert gasses, resulting in the breakage of some peptide bonds between amino acid residues in the peptides (Sinha and Mann, 2020). The resultant mass spectra contain information on the amino acid masses in these fragments and can therefore be used to identify the peptide sequence (Sinha and Mann, 2020). Any modifications present on these amino acids can then be detected by looking for shifts in mass at the specific site (Urban, 2022). For example, detecting a mass shift of 80 Da in the spectra at a specific site indicates serine, threonine or tyrosine phosphorylation (Urban, 2022). MS and proteomics analysis software assist in this process by deconvoluting mass spectra to identify peptides by comparing them to a peptide library containing known peptide sequences and their respective spectra (Sinha and Mann, 2020). The software can then use the sequences to identify the protein of which the peptide fragment is a part and can subsequently identify the location of the phosphosite that has been modified on the protein (Savage and Zhang, 2020).

Peptide abundances can then be quantified using either label free or labeled approaches (Sinha and Mann, 2020). In label free quantification (LFQ), either the number of spectra (spectral counting) or the intensity of the MS signal (area under the curve method) are extracted, normalized and used for measuring peptide abundance (Sinha and Mann, 2020). LFQ is experimentally easier to execute and is economical but has greater variance in quantification (Sinha and Mann, 2020). Labelled approaches use stable isotopes to label the peptides such that their mass shift can be detected and quantified during MS spectra analysis (Sinha and Mann, 2020). For example, cells can be grown in a medium containing tyrosine labeled with ^{13}C atoms, hence incorporating the isotope into peptides which will be detected in the MS later (Urban, 2022).

The final output of this process is a data matrix containing a list of the proteins whose peptides were identified, their corresponding abundances, sites of phosphorylation, peptide sequences as well as the respective p-values associated with the quantifications of abundance (Savage and

Zhang, 2020). This data matrix can then be statistically filtered for significantly altered phosphosite or protein expression between given conditions (Savage and Zhang, 2020).

1.4.2 Mass Spectrometry Sample Preparation

To pass a sample through the mass spectrometer for proteomics and phosphoproteomics analysis, it must be appropriately processed. The effective and high-yield extraction of proteins from biological samples (cell lines, in this case) and the subsequent efficient digestion of these proteins into peptides is paramount to ensuring consistent, comparable datasets are obtained across all the cell lines or conditions being tested (Gerritsen and White, 2021).

Sample preparation begins with cell lysis and protein extraction. Currently, urea-based, lysis buffers containing the buffering agent HEPES (4-(2-hydroxyethyl)-1-piperazineethanesulfonic acid) are preferred due to ease of protein denaturation and ease of removal through desalting (Gerritsen and White, 2021). Other buffer systems such as guanidine hydrochloride can be used for their heat resistant properties however they can reduce efficiency of protein digestion downstream (Gerritsen and White, 2021). While sodium dodecyl sulfate (SDS) is a widely used protein denaturing agent in western blotting, it cannot be easily removed in later stages of sample preparation and may interfere with the mass spectrometer (Gerritsen and White, 2021). Typically, the lysis buffers also contain protease and phosphatase inhibitors to preserve the phosphorylation status as well as the integrity of the proteins (Kanshin *et al.*, 2012). These include aprotinin (serine protease inhibitor), phenylmethylsulfonyl fluoride (PMSF) (serine and cysteine protease inhibitor) and leupeptin (serine and cysteine protease inhibitor) (Kanshin *et al.*, 2012). Phosphatase inhibitors include sodium orthovanadate (tyrosine phosphatases), sodium pyrophosphate (Ser/Thr phosphatases) and β-glycerophosphate ((Kanshin *et al.*, 2012).

The reduction and alkylation of denatured proteins takes place immediately after cell lysis and prior to trypsin digestion (Rush *et al.*, 2005). Proteins are reduced using dithiothreitol (DTT) to break disulphide bonds and the resultant cysteine SH-groups are then alkylated using iodoacetamide (IAA) to prevent the formation of new disulphide bonds (Müller and Winter, 2017). These proteins are then digested into peptides, most commonly using the protease trypsin, which cuts peptide chains at the carboxyl side of the amino acids lysine and arginine (Gerritsen and

White, 2021). Due to the frequency of arginine and lysine residues in the proteome, trypsin digestion yields peptide sizes that are compatible with MS detection (Gerritsen and White, 2021). Lys-C is also used as either an alternative to trypsin or in combination with trypsin in double-digestion protocols, a process which minimizes missed cleavages by either enzyme (Gerritsen and White, 2021). Following digestion, samples are desalted to remove salts that would otherwise significantly influence the efficiency of MS ionization and therefore sensitivity (Jehmlich *et al.*, 2014). The samples are then lyophilized in order to remove solvents and increase reproducibility between samples (Jehmlich *et al.*, 2014). Lyophilized peptides can then be dissolved in a mixture of acetonitrile and trifluoroacetic acid (TFA) which is a commonly used solvent for HPLC in MS (Sinha and Mann, 2020). For total proteomics analysis, this peptide mixture can be injected into the mass spectrometer.

1.4.3 Global vs Phosphotyrosine-enrichment phosphoproteomics

After trypsin digestion, desalting and lyophilization, the phosphoproteomics workflow can diverge based on the intended application or the question being investigated (Gerritsen and White, 2021). For labeled quantification approaches, peptides can be labeled at this stage before enrichment but for label-free quantification, phosphopeptide enrichment is conducted (Gerritsen and White, 2021).

Enrichment of phosphoserine, phosphothreonine and phosphotyrosine (denoted as pSTY from here on) can be performed using immobilized metal affinity chromatography (IMAC) or metal-oxid affinity chromatography (MOAC) (Gerritsen and White, 2021). IMAC depends on the affinity of the negatively charged phosphate group for the positively charged Fe^{3+} ion while MOAC depends on its affinity to Ti^{4+} in the form of titanium dioxide (Gerritsen and White, 2021). While this process should yield equivalent enrichment of pSTY sites, the relative abundances of pS vs pT vs pY phosphosites confound efforts to enrich phosphotyrosine sites especially (due to their low abundance of 0.1-1%) (Gerritsen and White, 2021). Thus, while a global phosphopeptide enrichment approach will yield sufficient pST sites, pY phosphopeptides may be inadequately enriched due to their relative rarity in the phosphoproteome (Gerritsen and White, 2021).

The most common method of extracting pY containing proteins and peptides involves the use of anti-phosphotyrosine specific antibodies to immunoprecipitate pY-containing peptides after trypsin digestion and desalting (Stokes *et al.*, 2012). There are several commercially available, pan-specific anti-phosphotyrosine antibodies that can be used for this purpose (Gerritsen and White, 2021). However, due to the low abundance of pY sites, a large quantity of starting material is required during MS sample preparation (Gerritsen and White, 2021). For comparison, while as little as 100-200 μg of starting material is more than sufficient for proteomics analysis and 1 mg of material is enough for TiO_2-directed pSTY enrichment, phosphotyrosine enrichment requires at least 10-30mg of starting material for a significant yield of pY-containing peptides for phosphoproteomics analysis (Gerritsen and White, 2021; Stokes *et al.*, 2012).

Phosphopeptide identification and quantification is vital to build an in-depth understanding of cancer cell signaling (Gerritsen and White, 2021). In this case, phosphoproteomics is critical to propose a mechanism of action for BRK in Tamoxifen resistant breast cancer. While the many targets and roles of BRK have been characterized in breast cancer overall, a high-throughput method like phosphoproteomics allows for the identification of BRK-specific signaling pathways that are affected in Tamoxifen resistant breast cancer cells and how these pathways are affected when BRK is depleted from these cell lines.

2.0 HYPOTHESIS AND OBJECTIVES

Overall, the studies above have shown that, in mammary cell lines, BRK drives the initiation, maintenance and promotion of cancer phenotypes. The protein can be a contributing factor to endocrine resistance due to its differential expression in breast cancer versus normal breast tissue, its interaction with several vital growth factor signaling pathways and its mediation of proliferation and migration. In taxol resistant breast cancer cells, BRK induction has been shown to be vital to the resistant phenotype (Anderson *et al.*, 2018). There is also evidence to show that BRK has a role in conferring cetuximab resistance (Li *et al.*, 2012). By extension, I rationalized that BRK may have a similar role in conferring Tamoxifen resistance. A previous study has shown that BRK is induced in Tamoxifen resistant breast cancer cells (Jiang *et al.*, 2017). Both the knockdown and the inhibition of BRK has been shown to affect Tamoxifen resistant cells (Ito *et al.*, 2017; Jiang *et al.*, 2017). By extension, a detailed, high throughput analysis of the role of BRK in Tamoxifen resistance will reveal pathways and substrates driven by BRK and which can be targeted by combinatorial therapies in the future. In fact, the proposed role of BRK in stress response signaling would make it a more clinically relevant target against breast tumour drug resistance by preventing tumours from activating pathways that circumvent therapies. Therefore, I will be investigating the role of BRK in Tamoxifen resistant breast cancer.

Hypothesis

I hypothesize that BRK contributes to the establishment of tamoxifen resistance as well as the maintenance of resistance thereafter by regulating BRK-specific pathways.

Objectives:

1. To study the effect of BRK inhibition/knockdown on Tamoxifen resistance.
2. To identify pathways and targets involved in Tamoxifen resistance as well as when BRK is knocked down in TamR cells through phosphoproteomics through:
    a. Global phosphoproteomics of Parental vs TamR vs TamR BRK KD cells.
    b. pTyr-enrichment phosphoproteomics of Parental vs TamR vs TamR BRK KD cells.
    c. Total proteomics of Parental vs TamR vs TamR BRK KD cells
3. Validation of BRK-specific targets in TamR.

3.0 MATERIALS AND METHODS

3.1 Reagents and chemicals

Tables 3.1 lists the reagents and chemicals that were used in the experiments described in the thesis. Table 3.2 details the reagents/chemicals manufacturer locations.

Table 3.1 List of reagents and chemicals. The following table details the reagents and chemicals used in experiments described in the thesis. Catalogue numbers and supplier information is also listed.

Reagents/Chemicals	**Supplier and Cat. No.**
30% Acrylamide/Bis Solution, 37.5:1	Bio-Rad, 1610158
Acetonitrile, LC-MS grade	ThermoFisher Scientific, 51101
Acrylamide	Bio-Rad, 1610101
Agar	Fisher Scientific, BP1425-2
Bovine serum albumin	Cytiva, SH30574.02
Bradford's assay dye reagent concentrate	Bio-Rad, 5000006
Aprotinin	Sigma-Aldrich, A62279
Ampicilin	Sigma-Aldrich, A9393
Ammonium persulfate (APS)	ThermoFisher Scientific, 17874
BCA protein assay kit	ThermoFisher Scientific, 23225
Chloramphenicol	Sigma-Aldrich, C0378
Dimethyl sulfoxide (DMSO)	Fisher Scientific, TS-20684
Dithiothreitol (DTT)	Fisher Scientific, 3483-12-3
Dulbecco's modified Eagle's medium (DMEM)	ThermoFisher Scientific/Gibco, 11971025
Ethyl alcohol (EtOH)	Fisher Scientific, S25310
Ethylenediaminetetraacetic acid (EDTA)	Fisher Scientific, S311-500
Fetal bovine serum (FBS)	ThermoFisher Scientific, A3160402
Formic acid, LC-MS grade	ThermoFisher Scientific, 28905
Glycerol	Fisher Scientific, BP229-1

Glycine	Fisher Scientific, S80028
Hydrochloric acid (HCl)	Fisher Scientific, A508-P500
HEPES (4-(2-hydroxyethyl)- 1-piperazineethanesulfonic acid)	Sigma-Aldrich, H3375
Insulin solution from Bovine Pancrease	Sigma-Aldrich, I0516-5ML
Iodoacetamide, LC-MS-grade	Sigma-Aldrich, I6125
Luna Universal One-Step RT-qPCR kit	New England Biolabs (NEB), E3005L
Methanol	Fisher Scientific, A411-4
Nitrocellulose membrane	Bio-Rad, 1620115
Penicillin-Streptomycin solution	ThermoFisher Scientific/Gibco, 10378016
Phenylmethylsulfonylfluoride (PMSF)	Fisher Scientific, 329-98-6
Phosphatase inhibitor cocktail	ThermoFisher Scientific,78420
Polyethyleneimine (PEI)	Polysciences Inc., 23966-1
Prestained Protein Ladder, Broad Range (10-230 kDa)	New England Biolabs (NEB), P7712
Protease inhibitor cocktail	Millipore Sigma, 04693159001
Protein A/G-agarose beads	Santa Cruz Biotech, sc-2003
PTMScan Phospho-Tyrosine Rabbit mAb (P-Tyr-1000) Kit	Cell Signaling Tech, 8803
Roswell Park Memorial Institute (RPMI) 1640 Medium	ThermoFisher Scientific/Gibco, 11835055
Sodium dodecyl sulfate (SDS)	Fisher Scientific/Fisher BioReagents, BP166500
Sodium orthovanadate (Na_3VO_4)	Sigma-Aldrich, S6508-50G
Sodium pyrophosphate	Sigma-Aldrich, S6422
Sodium azide (NaN_3)	Fisher Scientific, S227-100
N,N,N´,N´-tetramethylethylenediamine (TEMED)	Sigma-Aldrich, T9281
Tamoxifen	Sigma-Aldrich, T5648
Trifluoroacetic acid (TFA), LC-MS-grade	ThermoFisher Scientific, 28904

Tris base	Fisher Scientific, BP152-5
Triton X-100	Fisher Scientific, AC215680000
Trypsin (Cell culture grade)	Fisher Scientific, SV3003101
Trypsin (LC-MS grade)	Worthington, LS-003744
Tween-20	Fisher Scientific, BP337500
Urea	Fisher Scientific, U15-500
Water (LC-MS grade)	Fisher Scientific, W-5

Table 3.2 Supplier locations for reagents and chemicals procured. This table lists the names and addresses of all reagent/chemical suppliers.

Supplier	**Location**
Bio-Rad	Hercules, California, USA
Cell Signaling Technologies	Danvers, Massachusetts, USA
Cytiva	Marlborough, Massachusetts, USA
EMD Millipore	Danvers, Massachusetts, USA
Fisher Scientific	Walton, Massachusetts, USA
Invitrogen Life Technologies	Green Island, New York, USA
LI-COR, Odyssey	Lincoln, Newark, USA
New England Biolabs	Ipswich, Massachusetts, USA
Polysciences Inc.	Warrington, Pennsylvania, USA
Sigma-Aldrich	St. Louis, Missouri, USA
Santa Cruz Biotechnologies	Santa Monica, California, USA
ThermoFisher Scientific	Logan, Utah, USA
Waters corporation	Wilford, Massachusetts, USA
Worthington	Lakewood, New Jersey, USA

3.2 Cell lines and cell culture

Parental, Tamoxifen sensitive MCF7 cells and their Tamoxifen resistant (TamR) counterpart were obtained from Axol Biosciences (Cat. No. ax4010 and ax4011 respectively). These cell lines were maintained in high-glucose, phenol red-free DMEM media supplemented with 10% FBS and 1% penicillin/streptomycin solution. Parental, Tamoxifen sensitive and Tamoxifen resistant T47D

cells were obtained from Ximbio (Cat No. 152111 and 152110 respectively). These T47D cell lines were maintained in high-glucose, phenol red-free RPMI media supplemented with 10% FBS and 1% penicillin/streptomycin solutions. Both MCF7 TamR and T47D TamR cell lines were grown in media containing 1 μM Tamoxifen to maintain the resistance phenotype. Parental T47D cells were stimulated with 8 μg/mL insulin for experiments testing the functioning of IRS1.

3.2.1 Lentiviral-mediated shRNA knockdown of BRK in TamR cell lines

Lentiviruses were generated by co-transfecting Human Embryonic Kidney 293T (HEK293T) cells with the vectors pMD2.G, psPAX2 and the shRNA constructs contained in lentiviral GFP vectors obtained from Origene (Cat. No. TL320500). PEI was used as the transfection agent. Media containing the lentiviruses were collected 48 hours after transfection and filtered using a 0.45-micron syringe filter (Pall Laboratory, CA28143-352). Target cells (Parental MCF7 and T47D cells) were then infected with the lentivirus-containing media for a period of 48 hours before selection with puromycin (2 μg/mL).

3.2.2 Cell proliferation assay using CCK8

Parental, TamR and TamR BRK KD cell lines (both MCF7 and T47D) were grown until approximately 80% confluency. 1000 cells per cell line were seeded into 96-well plates in triplicates (technical replicates). Cells were then grown in phenol red-free DMEM (for MCF7 cells) or RPMI (for T47D cells) media containing 1 μM Tamoxifen. After 24 hours, 10 μL of CCK-8 solution (Dojindo Laboratories, CK04) was added to each well and the plate was incubated at 37 °C, 5% CO_2 for 2 hours. Absorbance measurements (at 450 nm) for cell number determination were then taken using a microplate reader. Readings were taken every 24 hours for 5 days in total to generate the growth curves.

3.3 SDS-PAGE

Cell culture plates were aspirated and gently rinsed with ice-cold 1xPBS prior to harvesting directly in lysis buffer composed of 20 mM Tris (pH 7.4), 150 mM NaCl, 1mM EDTA, 1% Triton X-100, protease inhibitor cocktail, 2.5 mM Sodium pyrophosphate, 1 mM β-glycerophosphate, 1 mM Na3VO4, 1 μg/mL Leupeptin. The lysates were then sonicated (on ice) at 10W for 3 pulses

lasting 10s each and were subsequently cleared through centrifugation at 10,000 g. 2x Laemmli was then added to the total cell lysates in a 1:1 ratio. The samples were then boiled at 100 °C for 3 minutes prior to loading onto the gels (10 wells or 15 wells).

For sodium dodecyl sulphate (SDS) Polyacrylamide gel electrophoresis (PAGE), 1.5 mm thick, 10% polyacrylamide gels were prepared. SDS-PAGE was performed using the Mini-Protein 4 gel electrophoresis system (#165800FC, Bio-Rad, USA). The resolving gel comprised 10% acrylamide, 0.8% bis-acrylamide, 0.4% SDS, 375 mM Tris HCl pH 8.8, 0.16% (w/v) APS, 0.1% TEMED and H2O. The stacking gel comprised 4% acrylamide, 0.8% bis-acrylamide, 0.4% SDS, 125 mM Tris HCL pH 6.8, 0.24% (w/v) APS, 0.1% (w/v) TEMED and H2O. The gels were run in 1xSDS running buffer at a constant voltage of 100 volts for 2-3 hours (depending on the separation required for protein visualization) or until the bromophenol blue dye front passed through the gel.

3.3.1 Western Blotting

Following SDS-PAGE, the gels were removed from the apparatus and the stacking sections of the gels were discarded. Each gel was then placed on thick blot filter paper that was cut to the size of the gel and pre-soaked in western blot transfer buffer. A nitrocellulose membrane, also cut to the size of the gel and soaked in transfer buffer, were then placed on the gel and the assembly was completed with a piece of thick blot filter paper on top of the nitrocellulose membrane. The complete transfer assembly was placed into a cassette as a part of the western blotting apparatus (Bio-Rad). The apparatus was then filled with western blotting transfer buffer and protein transfer proceeded for 2 hours at a constant voltage of 100V at 4 °C.

Once protein transfer was completed, the membranes were blocked by incubation in 5% skim milk or 3% BSA in PBS (for phosphosite-specific primary antibodies) at room temperature for 1 hour on a rocking platform. The membranes were then washed in 1xPBS before the addition of primary antibodies diluted in primary antibody buffer (composed of 1xPBS with 5% BSA). The membranes were then incubated overnight on a rocker at 4 °C. They were then removed, washed once with 1 x PBST for 5 min to reduce non-specific primary antibody binding and incubated with the appropriate mouse or rabbit secondary antibody (obtained from LICOR, 926-68070 and 926-

32211 respectively) which were diluted at 1:10,000 concentration in the solution used during block. Secondary antibody incubation was conducted in the dark, at room temperature, on a rocker for a period of 1 hour. Finally, the membranes were washed 3 times with PBST for 3 min per wash. Membranes were scanned using the LICOR CLx Odyssey Scanner and images were acquired and analyzed using the instrument's Image Studio Lite software (LICOR, USA). Images were exported and saved in .tiff format to reduce information loss. All western blotting experiments were repeated thrice for reproducibility and quantification purposes.

3.3.2 Primary and secondary antibodies

The anti-BRK (sc-166171), anti-β-actin (sc-47778), anti-BCRP (sc-377176), anti-ERα (sc-8005), and anti-pTyr20 (sc-508) primary antibodies were obtained from Santa Cruz Biotechnologies. The anti-phosphoBRK (pTyr342) was procured from EMD Millipore (Cat. No. 09-144). All other antibodies were obtained from Cell Signaling Technologies (CST) including anti-AKT (#9272), anti-phosphoAKT (Ser473) (#4060), anti-IRS1 (#2382), anti-phosphoIRS1 (Ser1101), anti-phosphoIRS1 (Tyr895), anti-CDK1/2 (#9116), anti-phosphoCDK1/2 (Tyr15) (#4539), anti-δ-catenin (#59854) and anti-phosphoδ-catenin (Tyr904) (#2910). All CST antibodies were diluted to a working concentration of 1:1000. Both anti-BRK and anti-pTyr20 antibodies were diluted to a working concentration of 1:250. Anti-BCRP and anti-ERα antibodies were diluted to a working concentration of 1:500. Finally, the anti-β-actin (sc-47778) and anti-BCRP (sc-377176) were diluted to a concentration of 1:1000.

Secondary antibodies used for western blotting were obtained from LI-COR Odyssey, USA. Goat anti-rabbit (IR Dye-680RD IgG, #926-68071) and goat anti-mouse (IR Dye-800CW IgG, #926-32210) secondary antibodies were used where applicable for all western blot analyses. As per manufacturer instructions, the secondary antibodies were diluted in double distilled water to a final concentration of 1 mg/mL and their aliquots were stored at 4°C.

3.4 Immunoprecipitation

Cells were cultured to 85-90% confluency on 10 cm cell culture dishes. Cell culture media was then aspirated, and the cells were rinsed twice with ice-cold PBS. To each plate, 500 µL of lysis buffer (containing was added 20 mM Tris (pH 7.4), 150 mM NaCl, 1mM EDTA, 1% Triton X-

100, 1x protease inhibitor cocktail, 2.5 mM Sodium pyrophosphate, 1 mM β-glycerophosphate, 1 mM Na_3VO_4) was added, the cells were then harvested, and lysates were kept on ice. The samples were then sonicated on ice at 10W power for 3 pulses lasting 10s each. The lysates were cleared through centrifugation at 10,000 g for 10 min at 4°C. The supernatant was then divided into 3 portions: 1) 200 µL was kept aside for total cell lysate analysis, 2) 150 µL was kept aside for immunoprecipitation with mouse or rabbit IgG as a negative control and 3) 150 µL was kept aside for immunoprecipitation with the primary antibody against the protein of interest. The total cell lysate was stored at -20°C while the IgG control portion was incubated with either mouse or rabbit IgG (depending on the species of the primary antibody) and the primary antibody was added to the remaining cell lysate. Both cell lysates (IgG and primary antibody pulldown) were incubated at 4°C with gentle rocking overnight. Next, 20 µL protein A/G bead slurry was added to each sample, and they were incubated with gentle rocking for 4 hours at 4°C. The mixture was centrifuged at 6000 g for 30s at 4°C and the resultant pellet was washed 3 times with 500 µL of the lysis buffer, with a 30s, 6000 g centrifugation being conducted after every wash. After the final wash and centrifugation, the pellet was resuspended in 50 µL of 2x Laemmli sample buffer, vortexed for 10s and centrifuged for 30s at 6000 g. The sample was then heated at 100°C for 3 min and centrifuged at 10,000 g for 1 min. Finally, 12 µL of each sample was loaded per well for SDS-PAGE.

3.4.1 Chromatin Immunoprecipitation (ChIP)

Cells were cultured to a confluency of approximately 85%. DNA cross-linking was performed by the drop-wise addition of formaldehyde to a final concentration of 0.75% and swirled at room temperature for 10 min. Glycine was then added to a final concentration of 125 mM and incubated with shaking for 5 min at room temperature. The cells were then harvested as described above in the immunoprecipitation protocol. Cell pellets were resuspended in ChIP lysis buffer which consisted of 50mM HEPES-KOH (pH 7.5), 140 mM NaCl, 1 mM EDTA (pH 8), 1% Triton X-100, 0.1% SDS, 0.1% Sodium Deoxycholate, protease inhibitors and phosphatase inhibitors. The resuspended cell lysates were then incubated with either anti-IRS1 antibody or normal rabbit IgG (negative control) with rotation for 1 hour. Protein A/G-PLUS-agarose beads (sc-2003, Santa Cruz Biotechnology) were then added to the mixtures and left to incubate at 4°C overnight. The mixtures were then centrifuged and washed prior to elution of the immunoprecipitated protein-DNA

complexes. The DNA from these complexes was then purified using the QIAquick PCR purification kit (Qiagen, #28104). Subsequent quantitative PCR analysis was conducted as described below.

3.5 Quantitative and Reverse Transcriptase PCR

3.5.1 Quantitative PCR

Purified DNA obtained from cell lines was analysed using the Luna Universal qPCR kit protocol (New England Biolabs, #M3003). 100 ng of template DNA was added to a reaction mixture containing 1 x qPCR Master Mix, 10 μM forward (5'-CGGACTACAGGGGAGTTTTGTTG-3') and reverse (5'-TCCAGCATCCAGGTGGCGACGAT-3') primers specific to the cyclin D1 promoter region. qPCR analysis was conducted using the manufacturer recommended thermocycling protocol.

3.5.2 Reverse Transcriptase PCR

Total RNA was obtained from cell lines using the Monarch Total RNA miniprep kit (New England Biolabs, #T2010S). Cells were grown to 90% confluency, harvested and pelleted through centrifugation. Cell pellets were resuspended in the RNA lysis buffer provided in the kit. Genomic DNA (gDNA) was then removed and total RNA was purified using the appropriate columns provided. The RNA was then eluted using nuclease-free water. RT-PCR analysis was then conducted using the Luna Universal One-Step RT-qPCR kit protocol. For each cell line, 1 μg total RNA was used as a template for RT-PCR analysis. For the quantification of cyclin D1 gene expression, the forward primer sequence of 5'-GCGGAGGAGAACAAACAGAT–3' and the reverse primer sequence of 5'-GAGGGCGGATTGGAAATGA-3'. For the quantification of c-myc gene expression, the forward primer sequence of 5'-GCTGTAGTAATTCCAGCGAGAG-3' was used with a reverse primer sequence of 5'-GAGTCGTAGTCGAGGTCATAGT-3'. RT-PCR analysis was conducted using the manufacturer recommended thermocycling protocol.

3.6 Sample preparation for global phosphoproteomics analysis

3.6.1 Protein digestion and purification of peptides

MCF7 Parental, MCF7 TamR, T47D TamR and T47D TamR BRK KD cell lines were cultured to 90% confluency in 10 x 10 cm dishes for each cell line and harvested harvested in 1 mL per plate of urea lysis buffer composed of 10M urea and 20 mM HEPES (pH 8.0). The cell lysates were processed as described previously (Stokes *et al.*, 2012). Briefly, the lysates were pooled and sonicated at 10W output with 3 pulses lasting 10s each. The lysates were cooled for 1 min between each pulse and the sonication was conducted at 4°C. The lysates were cleared by centrifugation at 20,000g for 15 min at room temperature and the resulting supernatants was transferred to new 50 mL tubes. The protein concentration in each lysate was then quantified using Bradford's assay. For each cell line, 1 mg of total protein was set aside for further processing as this is the upper limit of starting material for the TiO_2 phosphopeptide enrichment columns (ThermoFisher Scientific, #88303). The proteins in the lysates were reduced through the addition 1.25M DTT to the samples. They were mixed and incubated at 55°C for 30 min. The solutions were then cooled to room temperature before the addition of iodoacetamide and they were then incubated at room temperature for 15 min. Finally, these samples were diluted 4-fold such that the final concentration of urea is approximately 2M and 1/100 volume of Trypsin was added (to digest the proteins into peptides) at room temperature with mixing for 48 hours. The tryptic digests were purified and desalted using C18 Sep-Pak cartridges (#WAT051910, Waters Corporation, USA) which use reversed phase, solid phase extraction to adsorb and purify peptides. The C18 columns were equilibrated using 0.1% TFA solution before the application of the digested peptides. The bound peptides were then washed using 0.1% TFA and eluted using 0.1% TFA and 40% acetonitrile solution. Desalted and purified peptides were lyophilized overnight and later used for phosphopeptide enrichment.

3.6.2 Enrichment of phosphopeptides (pSer, pThr and pTyr) using TiO_2 columns

The lyophilized peptides were resuspended in 150 µL of the provided binding/equilibration buffer, which acidifies the solution to a pH < 3.0. The TiO_2 columns were then washed, equilibrated and the resuspended peptide samples were applied. The columns were centrifuged at 1000g for 5 min

to pass the sample through. The columns were then washed using the equilibration buffer and then the wash buffer provided, and a final wash was conducted using LC-MS grade water. Finally, the phosphopeptides were eluted using 50 µL of phosphopeptide elution buffer and lyophilized immediately prior to LC-MS analysis.

3.6.3 Reversed-phase chromatography and mass spectrometry

Lyophilized peptides were dissolved in 0.1% formic acid prior to LC-MS analysis. Samples were analyzed by nano UPLC-MS/MS with a Proxeon EASY-nLC 1000 system interfaced to a Thermo-Fisher Q Exactive HF mass spectrometer (analysis performed by Southern Alberta Mass Spectrometry Facility, University of Calgary). Peptides were loaded on a trapping column and eluted over a 75 µm x 25 cm analytical column (Thermo-Fisher Scientific, USA) at 300 nL/min using a 4-hour reversed-phase gradient. Both columns were packed with PepMap C18, 3 µM resin (Thermo-Fisher Scientific, USA). Mobile phases A and B consisted of 0.1% formic acid in water and 0.1% formic acid in 90% acetonitrile, respectively. Peptides were eluted from the column at 300 nL/minute using the following linear gradient: from 2 to 25% B in 100 minutes, from 25 to 50% B in 110 minutes, from 50 to 90% B in 112 minutes, from 90 to 2% B in 113 minutes and held at 2% B for an additional 7 min. The spray voltage was 2.2 kV. The mass spectrometer was operated in the data-dependent acquisition mode with the Orbitrap operating at 60,000 FWHM (Full width at half maximum) and 17,500 FWHM for MS and MS/MS respectively. Full scans were acquired at a resolution of 60,000 FWHM with a maximum injection time of 120 milliseconds in the Orbitrap analyzer. The 15 most abundant ions with charge states ≥ 2 were selected for MS/MS fragmentation by high collision-induced dissociation (HCD) and analyzed at a resolution of 17,500 FWHM with a maximum injection time of 60 milliseconds.

3.6.4 Data processing and analysis

Mass spectra were analyzed, and protein identification was performed by Dr. Laurent Brechenmacher at the Southern Alberta Mass Spectrometry Facility using Mascot search engine 2.4.2 (Matrix Sciences, London, UK) against the human UniProtKB/Swiss-Prot database (13/02/2019 release; 20376 sequences). Trypsin was selected as the proteolytic enzyme, with a maximum of two to four potential missed cleavages, for the samples analysed before and after

acetylated-lysine enrichment, respectively. Peptide and fragment ion tolerance were set to, respectively, 10 ppm and 0.02 Da. Carbamidomethylation of cysteine was specified as fixed modifications. Variable modifications included phosphorylation of serine, threonine, and tyrosine. All Mascot result files were loaded together into Scaffold Q+S 4.3.2 (Proteome Software, Portland, OR, USA). Both peptide and protein false discovery rates were fixed at 1% maximum, with a one-unique-peptide criterion to report protein identification. Benjamini-Hochberg correction was used for multiple hypothesis testing for the calculated peptide fold changes between the cell lines. Scaffold PTM 3.0.0 (Proteome Software) was used to annotate post-translational modifications from Scaffold results. Minimum localization probability was 95%. Relative quantification of phosphosites was conducted using Scaffold Q+S software.

3.6.5 Pathway analysis

Functional gene enrichment and pathway analyses were performed by myself using the online tool InnateDB (https://www.innatedb.com) to determine whether the differences in phosphosite regulation in these cell lines is represented at the level of cognate signaling pathways. InnateDB analyzes differential protein/peptide expression datasets, using information of fold change of peptides between two conditions, the associated p-value and uniport ID to generate cellular pathways that are significantly up or downregulated (Breuer *et al.*, 2012). Thus, after the quantification information was obtained from Scaffold Q+S, an excel file containing the fold change, p-value and uniprot ID of MCF7 Parental vs TamR and T47D TamR vs T47D TamR BRK KD comparisons were uploaded to InnateDB. The tool returned several canonical signaling pathways with their associated p-values which represent the probability that the given pathway is statistically overrepresented by chance. A p value ≤ 0.05 was used as a threshold for the pathway analysis for this experiment and a list of overrepresented pathways was shortlisted accordingly.

3.7 Sample preparation for phosphotyrosine-enrichment phosphoproteomics analysis

3.7.1 Protein digestion and purification of peptides

T47D Parental, T47D TamR and T47D TamR BRK KD cell lines were cultured to 90% confluency in 16 x 10 cm dishes for each cell line and harvested in 1 mL per plate of urea lysis buffer composed of 10M urea and 20 mM HEPES (pH 8.0). The lysates were then pooled, sonicated, and cleared

through centrifugation as described in section 3.6.1. Protein concentration was quantified using the Bradford's assay and 10 mg of protein from each cell line lysate was set aside for further processing as this quantity was the starting quantity recommended for phosphotyrosine enrichment using the PTMScan® Phospho-Tyrosine Rabbit mAb (P-Tyr-1000) Kit, as described by Stokes and colleagues (Stokes *et al.*, 2012). An additional 1 mg of lysate was set aside for total proteomics analysis and therefore did not undergo phosphotyrosine peptide enrichment detailed below in section 3.6.2. Reduction, alkylation, trypsin digestion, desalting and lyophilization of both 10 mg and 1mg peptides were done as detailed in section 3.6.1. The lyophilized peptides set aside for proteomics analysis were resuspended in 0.15% TFA solution and sent to the Proteomics Resource Centre at the University of Ottawa for LC-MS analysis.

3.7.2 Enrichment of phosphotyrosine peptides using immunoaffinity purification

Lyophilized peptides were resuspended in the immunoaffinity purification buffer, as per manufacturer protocol (Stokes *et al.*, 2012). The pTyr1000 antibody-bead conjugates were washed five times with PBS and the resuspended peptides were applied to the 40 µL antibody-beads slurry. The mixture was then incubated on a rotator at 4°C for 4 hours. The beads were then washed five times with immunoaffinity purification buffer and 3 times with LC-MS grade water sequentially. Immunoaffinity-purified phosphotyrosine peptides were then eluted through the addition of 120 µL of 0.15% TFA solution to the beads. The eluted peptides were then purified and desalted using C18 tips (ThermoFisher Scientific, SP201) using the same procedure and solutions described in section 3.6.1. Concentrated and desalted peptides were then sent to the Proteomics Resource Center at the University of Ottawa for LC-MS analysis.

3.7.3 Reversed-phase chromatography and mass spectrometry

Reversed-phase chromatography and mass spectrometry were performed by Dr. Zhibin Ning at the University of Ottawa's mass spectrometry facility. The Exploris 480 mass spectrometer was connected to Dionex ultimate RS3000 HPLC system (ThermoFisher Scientific, San Jose, CA). For this analysis, the mass spectrometer was utilized with a nano-electrospray interface working in positive ion mode. The solvent system consisted of buffer A, consisting of 0.1% FA in water, and buffer B, consisting of 0.1% FA in 80% acetonitrile. Peptides dissolved in 0.15% TFA (as

discussed in section 3.6.2) were loaded ontp a 75 μm I.D. × 150 mm fused silica analytical column which was packed (in-house) with 3μm ReproSil-Pur C18 beads (100 Å; Dr. Maisch GmbH, Ammerbuch, Germany). Flow rate was set to 300nL/min and the gradient was set as 5–35% buffer B in 105 min, followed by 5min from 35%~80%, 5min of 80%, and 5 min of re-equilibration. The heated capillary temperature was set to 300°C and the spray voltage to 2.2 kV. One full MS scan from 350 to 1200 m/z was followed by a data-dependent MS/MS scan of the 15 most intense ions with a dynamic exclusion repeat count of 1 in 20 seconds. The mass resolution was 60000 for ms1 and 15000 for ms2. A real-time internal calibration by the lock mass of background ion 445.120025 was used. All data was recorded with Xcalibur software (ThermoFisher Scientific, San Jose, CA).

The MS spectral peaks thus obtained were analyzed and processed using the software MaxQuant (version 1.6.17.0 (Cox and Mann, 2008; Cox *et al.*, 2011). The spectra were searched and sequenced using the human fasta downloaded from Uniprot (April, 2021 release) along with the built-in contaminant sequences including commonly observed contaminants. Cysteine carbamidomethylation was selected as a fixed modification. Oxidation of methionine, N-terminal acetylation and ubiquitination were set as variable modifications. For phosphoproteomics analysis, an additional phosphorylation variable modification search term was set. Enzyme specificity was set to trypsin, not allowing for cleavage N-terminal to proline. Other parameters were set to default.

3.7.4 Data processing and analysis

Downstream bioinformatic analysis was done using Perseus, a partner software to MaxQuant, using the guidelines described in a publication by Tyanova and Cox and with the assistance of Dr. Zhibin Ning at the University of Ottawa's Proteomics facility (Tyanova and Cox, 2018). Peptide intensities were log2(x) transformed, where x denotes the intensity (a measure of abundance) of each peptide. The transformed intensities were then filtered such that peptides that were not represented in at least 2 out of 3 biological replicates were removed from further analysis. The dataset was then normalized and differential expression between conditions (otherwise known as fold change) was calculated using ANOVA analysis between T47D Parental vs T47D TamR and T47D TamR vs T47D TamR BRK KD. Multiple hypothesis testing was conducted using permutation-based FDR. Significant fold changes were filtered using the ANOVA p-value cutoff

set at 0.05. For proteomics analyses, the uniprot IDs of the proteins corresponding to the peptides, their corresponding fold changes and p-values were exported to an excel file to be prepared for pathway analysis downstream. For phosphoproteomics analyses, an additional column detailing the phosphosite identified on the phosphopeptide was also exported for further analysis.

3.7.5 Pathway analysis

The online tool InnateDB (https://innatedb.com) was used to identify pathways that were overrepresented in the T47D Parental vs TamR comparison and the T47D TamR vs T47D TamR BRK KD comparison, as described in section 3.6.5. Pathway analysis protocol was kept consistent to afford comparisons between the two datasets obtained in sections 3.6 and 3.6.

3.8 Statistical Analysis

Absorbance values obtained through the CCK8 assay were compared across cell lines at a given time point using the two-sample student's t-test (with $p<0.05$ considered statistically significant). This comparison was conducted using the GraphPad Prism 8.0.0 software for Windows (GraphPad Software, San Diego, California USA). Western blot, RT-PCR and ChIP-qPCR quantifications were also similarly compared using two-sample student's t-tests through GraphPad Prism 8.0.0 with $p<0.05$ considered statistically significant.

Statistical analysis of MS data obtained in section 3.6.3 was conducted using Scaffold Q+S 4.3.2, as described in section 3.6.4, using the ANOVA test function in the software ($p<0.05$ considered significant). Statistical analysis of MS data obtained in section 3.7.3 is described in section 3.7.4. The software Perseus (developed by the Jurgen Cox group, https://maxquant.net/perseus/) was used to conduct ANOVA tests to identify statistically significant changes in peptide quantifications across the cell lines (Tyanova and Cox, 2018).

4.0 RESULTS

4.1 The BRK inhibitor Tilfrinib effectively reduces phosphorylation of the BRK active site Y342

Tilfrinib is a small molecule inhibitor that targets the active site of BRK, the tyrosine 342 site (denote henceforth as Y342), thereby preventing ATP binding to the kinase domain (Mahmoud *et al.*, 2014). To find an optimal concentration for Tilfrinib inhibition, HEK293 cells were made to ectopically express BRK through the transfection of BRK-GFP in these cell lines. These HEK293 BRK^+ cells were then treated with increasing concentrations of Tilfrinib, ranging from 0.5µM to 6 µM, for a period of 24 hours. The cells were then lysed and assayed for pBRK (Y342) expression. The main objective of the analysis was to ascertain the optimal concentration of Tilfrinib that would inhibit BRK activation without adversely affecting cell viability.

As seen in Figure 4.1, I observed a dose-dependent inverse relationship between increasing Tilfrinib concentrations and pBRK levels. In fact, there was a drop of 250% in pBRK levels in the comparison between 0.5 µM and 2.5 µM treatments. The highest inhibition was observed when the cells were treated with 5 µM of Tilfrinib, however, these cells showed a significant decrease in viability as there was a reduction in confluency during cell culture in cells treated with 4 µM Tilfrinib or above. There was no significant difference in the inhibition of BRK when using 2.5 µM and and 3.0 µM concentrations of Tilfrinib, therefore the lower concentration of 2.5 µM Tilfrinib appeared ideal for future experiments to inhibit BRK activity. This concentration is close to the initial anti-proliferative GI_{50} values obtained by Mahmoud and colleagues when they tested it with MCF7 cells. Thus, the 2.5 µM concentration of Tilfrinib was used from hereon to inhibit BRK.

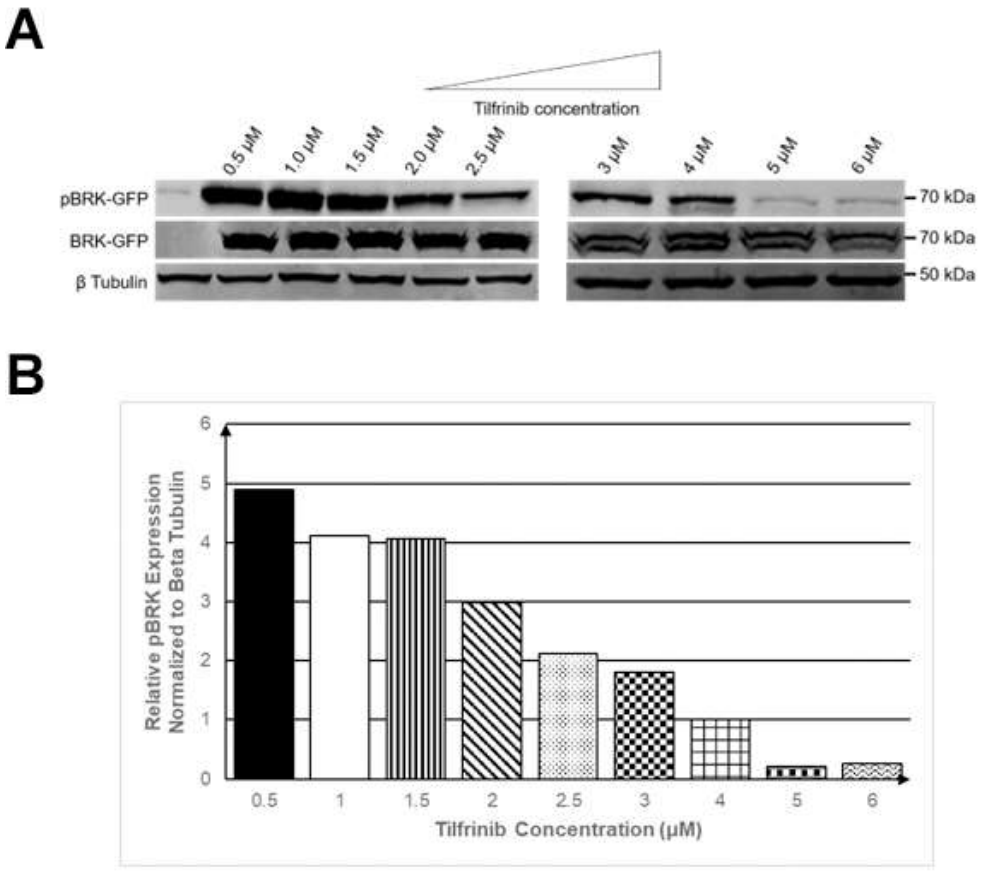

Figure 4.1 western blot analysis of the effect of Tilfrinib on HEK293 cells ectopically expressing BRK-GFP. **A)** HEK293 cells were transfected with BRK-GFP and analyzed for phospho-BRK (Y342), total BRK and beta tubulin (loading control) expression. **B)** Quantification of the immunoblot where phospho-BRK levels were calculated relative to total BRK and loading control levels.

4.2 BRK is more active in TamR cells

Tamoxifen sensitive (denoted as Parental or Par) and Tamoxifen resistant (denoted as TamR) MCF7 and T47D cells were assessed for differences in BRK expression and activity. A previous study by Jiang and colleagues showed that BRK levels increased upon the development of Tamoxifen resistance in MCF7 cells that were passaged in 1 µM Tamoxifen for 6 months (Jiang *et al.*, 2017). For this analysis, parental MCF7 and T47D cells were grown in an equal volume of DMSO, the solvent used to dissolve Tamoxifen, to control for any effects the solvent may have. TamR MCF7 and T47D cells were grown in 1 µM Tamoxifen to maintain resistance.

While there was a slight increase in BRK levels in both MCF7 and T47D TamR cells, it was not statistically significant (Fig. 4.2A & B). The lack of a difference in BRK levels in both MCF7 and T47D TamR cells implied this was not a cell-line specific occurrence. I next questioned if BRK was more active in Tamoxifen resistant cells. This was investigated using an antibody specific to the Y342 active site on BRK. As seen in Fig. 4.2A and B and as quantified in Fig. 4.1C, BRK activity (relative to total protein expression) was significantly higher in Tamoxifen resistant MCF7 and T47D cells versus their Tamoxifen sensitive counterpart. This implies that while BRK expression did not change upon the induction of Tamoxifen resistance, the activity of BRK increased in Tamoxifen-resistant cells.

There was no detectable difference in ER expression between TamR and parental cells, a result that is in corroboration with literature as Tamoxifen does not affect ERα protein levels (Guney Eskiler *et al.*, 2016). Breast Cancer Resistance Protein (BCRP) expression was used to confirm that these cells had indeed become drug resistant (Krisnamurti *et al.*, 2016). As seen Fig. 4.2A and B, BCRP levels were significantly increased in Tamoxifen resistant cells.

Having found that BRK was more active in these ER+, Tamoxifen resistant, breast cancer cell lines, I then queried if the inhibition of BRK, using the inhibitor Tilfrinib, would resensitize these cells to Tamoxifen. MCF7 and T47D parental as well as TamR cells were passaged as before. A thousand MCF7 and T47D parental and TamR cells were seeded into a 96 well plate in technical triplicates. They were all then treated with 1 μM Tamoxifen with one set of TamR cells being treated with both 1 μM Tamoxifen and 2.5 μM Tilfrinib. The cells were grown for 5 days with absorbance at 450nm as an indicator of cell growth. As shown in Fig. 4.2D and E, both MCF7 and T47D TamR cells growth at a higher rate than their Tamoxifen sensitive counterparts in the presence of 1 μM Tamoxifen ($p<0.01$ indicated by *). Interestingly, the inhibition of BRK through the action of Tilfrinib resulted in the resensitization of MCF7 and T47D TamR cells as these cells grow at a rate that was not different from Tamoxifen sensitive parental cells ($p>0.05$) (Fig. 4C and D). The combinatorial treatment of Tilfrinib and Tamoxifen significantly enhanced the growth cytostatic action of the latter drug.

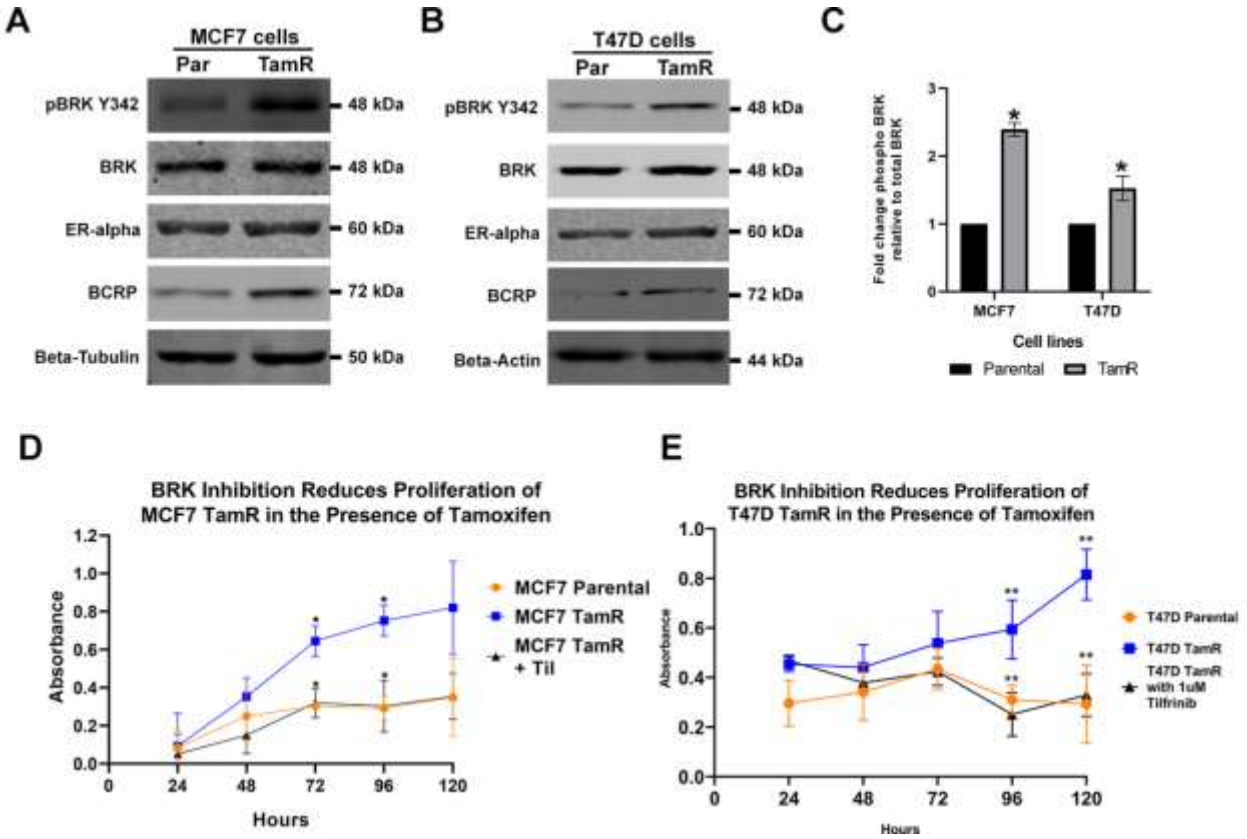

Figure 4.2 BRK and phospho-BRK (Y342) expression in Tamoxifen resistant cells and the effect of Tilfrinib inhibition of BRK on TamR cell proliferation. **A and B)** Both MCF7 and T47D cells were compared for their BRK expression, BRK activity (pBRK levels), ER-alpha and BCRP levels with beta tubulin and beta actin as loading controls. **C)** Quantifications of pBRK bands were first normalized against their respective loading controls. They were then divided with quantification of total BRK levels which were normalized against their loading controls. Relative activity of BRK in TamR vs Parental cells was then calculated and graphed (n=3 replicates). **D and E)** MCF7 and T47D TamR cells were treated with 1 μM Tilfrinib and grown in the presence of Tamoxifen for 5 days. Growth was measured using the CCK8 assay. * denotes significant differences with p value < 0.05, n=3. ** denotes significant differences with p<0.01, n=3.

4.3 TamR breast cancer cells are re-sensitized to the growth inhibitory effects of Tamoxifen upon BRK knockdown

Using the method described in section 3.2.1, Tamoxifen-resistant T47D cells were transduced with scrambled shRNA (a non-specific shRNA control) and BRK shRNA to stably knock down BRK expression in these cells. T47D cells were chosen as the model for knockdown as these cells express more BRK than MCF7 cells. Therefore, I predict greater quantifiable changes, through phosphoproteomics, in these cells when BRK is knocked down. After BRK-shRNA transduction,

lysates collected following puromycin selection for successfully transduced cells were immunoblotted for BRK to confirm successful knockdown. As shown in Fig. 4.3A and C, BRK knockdown was successful. Using BRK shRNA, T47D TamR cells expressing 71% less BRK than scrambled shRNA-expressing T47D TamR cells were generated.

Having determined, in section 4.2, that BRK inhibition resulted in resensitization of TamR cells to the drug, it was reasonable to question whether the knockdown of BRK expression would yield similar results. Hence, a proliferation assay was conducted with T47D parental, TamR and TamR BRK KD cells grown in 1 μM Tamoxifen. As seen in Fig. 4.2D, while TamR cells grew at a high rate in the presence of Tamoxifen, TamR BRK KD cells grew at a rate similar to T47D Parental cells (which are sensitive to Tamoxifen's cytostatic action) ($p>0.05$ across all time points). Furthermore, these cells grew at a significantly slower rate than their TamR counterpart ($p<0.01$). These results are consistent with previous studies in which BRK knockdown has reduced cell proliferation rate in drug resistant breast cancer cells (Li *et al.*, 2012).

4.4 BRK knockdown results in the hyperphosphorylation of p38 Y182 and hypophosphorylation of STAT3 Y702

As a proof of principle, I looked to replicate results that were obtained by Ito and colleagues (2017) by assaying phospho-p38 (Y182) levels in T47D TamR with reduced BRK. They found that p38 was activated after BRK was stably knocked down (Ito et. al, 2017). Indeed, in the TamR BRK KD model in T47D cells generated here, it was found that phospho-p38 levels were elevated after BRK was knocked down in T47D TamR cells (Fig. 4.3B). Additionally, I also assayed the phosphorylation status of STAT3 Y702 as this is a known BRK-regulated phosphorylation site on STAT3 (Ikeda *et al.*, 2010). As this is a known BRK substrate, I would expect the Y702 phosphosite to be hypophosphorylated when BRK is knocked down in T47D TamR cells. As shown in Fig. 4.3B, STAT3 is indeed hypophosphorylated at its Y705 site, which results in reduced activity of the transcription factor. As expected, ER-alpha levels did not change upon BRK knockdown as the kinase is not known to regulate ER-alpha. Interestingly, however, BCRP levels were found to be reduced upon BRK knockdown in T47D TamR cells. This could be an

indication of increased drug sensitivity in these cell lines and may imply a direct relationship between BRK and BCRP.

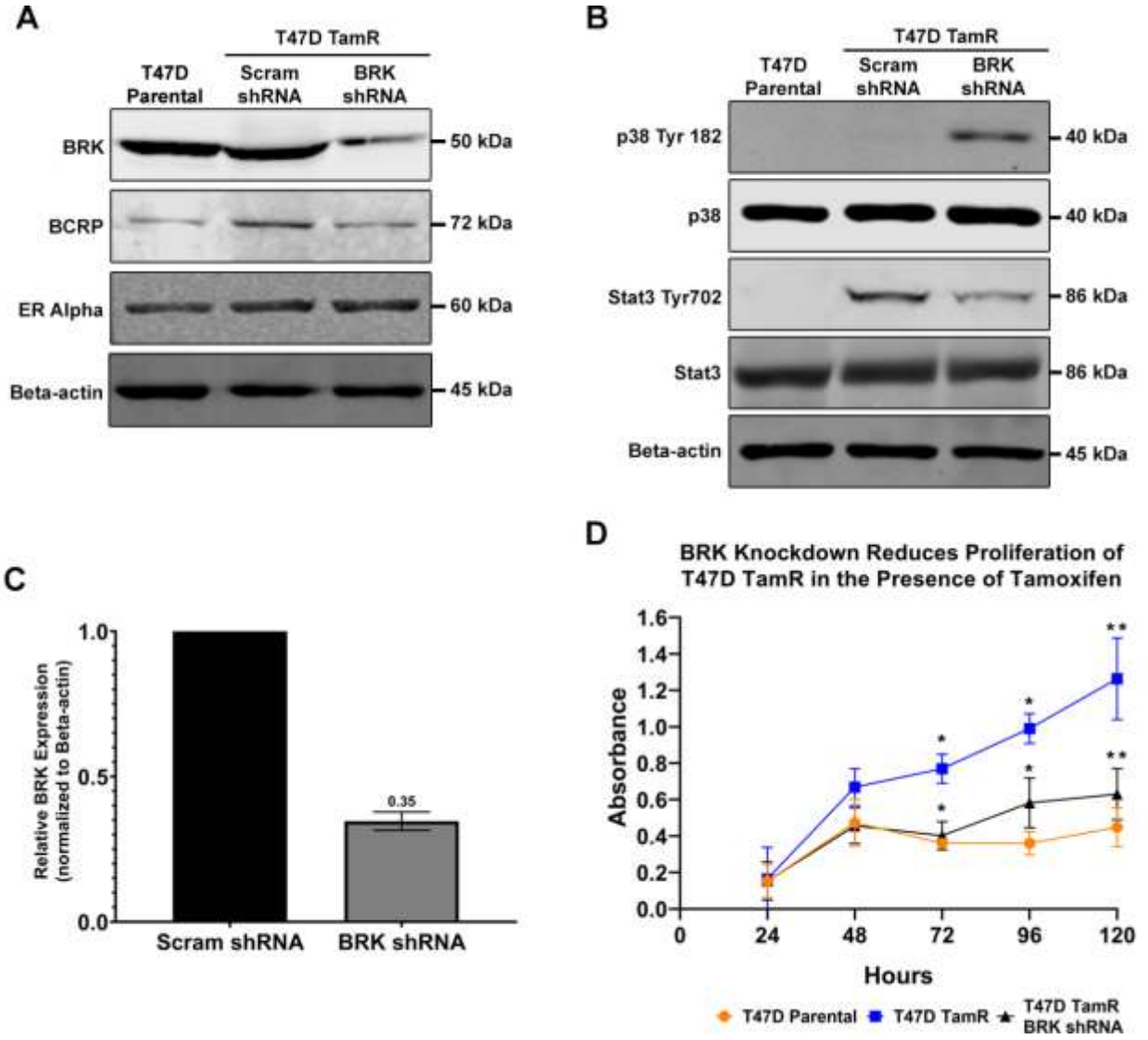

Figure 4.3. Assessment of BRK Expression and Knockdown in T47D TamR cells. A) Western blot analysis of T47D parental, TamR and TamR BRK KD cells for BRK, BCRP and ER-alpha expression. **B)** These cell lines were then assessed for the phosphorylation status of previously characterized phosphosites that have been affected by BRK knockdown in breast cancer cells. These include STAT3 Y702 and phospho-p38 Y182. **C)** Western blots were then quantified for BRK knockdown (n=3). **D)** Parental, TamR and BRK- T47D cells were subjected to a CCK8 cell proliferation assay for 5 days in RPMI + 10% FBS media containing 1μM Tamoxifen. * denotes significant differences with p value < 0.05, n=3. ** denotes significant differences with p<0.01, n=3).

4.5 While BCRP levels were reduced in BRK KD, BCRP induction does not affect BRK

While BCRP levels were reduced in T47D TamR BRK KD cells, it was unclear whether there was a direct relationship between BRK and BCRP that may have caused this reduction in BCRP levels. To investigate if there was a relationship between these proteins, I investigated if BCRP induction would also result in an increase in BRK expression. To this end, I stimulated T47D parental cells with 1 µM Doxorubicin for a period of 24 and 48 hours, as described previously by Davies and colleagues (Davies *et al.*, 2014). As shown in Fig. 4.4A and C, BCRP expression increased significantly after 48 hours. However, this does not cause a concurrent increase in BRK levels, with no significant change in BRK expression after 24 and 48h Doxorubicin treatment ($p>0.05$ across all comparisons).

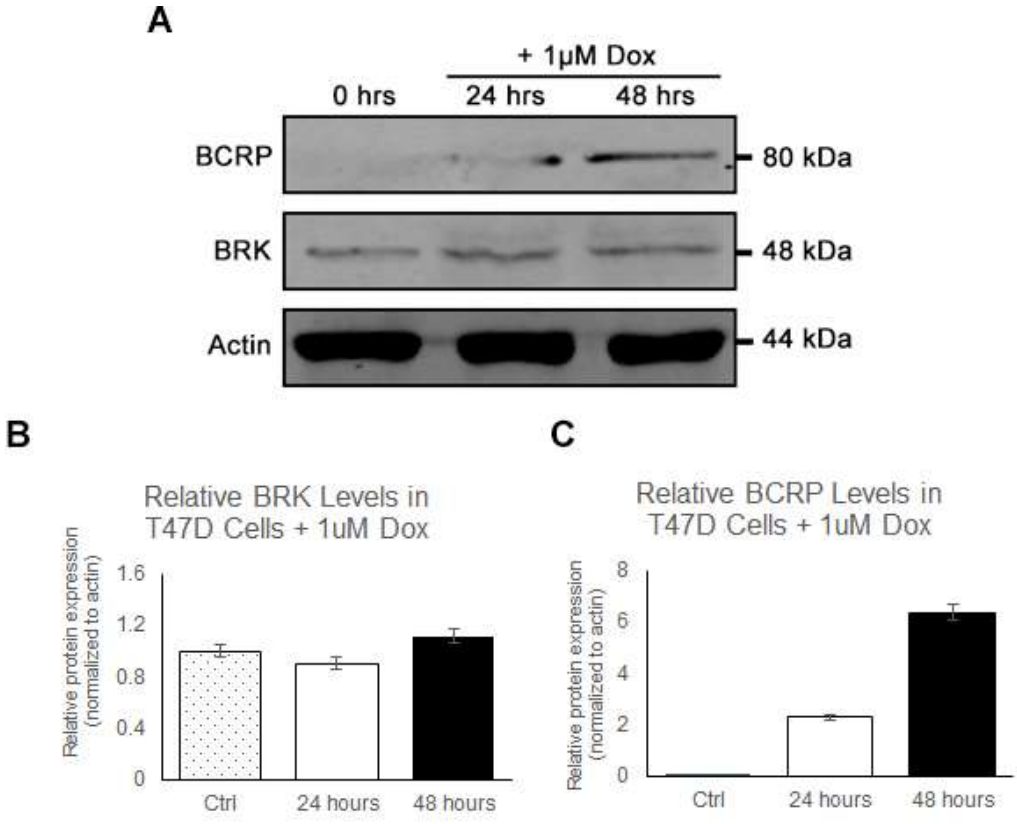

Figure 4.4. BCRP induction using 1 µM Doxorubicin did not cause an increase in BRK levels. **A)** T47D parental cells were treated with 1 µM Doxorubicin for 24 and 48 hours. BRK, BCRP and actin levels were assessed through western blotting. **B)** Blots were repeated thrice and quantified. BRK and BCRP levels were normalized to actin to control for loading. Error bars represent standard error. n=3 replicates for all samples.

4.6 Global phosphoproteomics of MCF7 Parental vs TamR and T47D TamR vs T47D TamR BRK Knockdown cell lines

4.6.1 Phosphoproteomics workflow to enrich pSer/pThr/pTyr peptides using TiO_2 columns

To investigate changes in cellular signaling driven by phosphorylation, phosphoproteomics analysis was conducted. The first comparison was made between MCF7 Parental and TamR cells to determine serine, threonine, and tyrosine phosphosites (denoted as pSTY) and pathways that are altered in TamR cells compared to parental cells. The second comparison was made between T47D TamR and T47D TamR BRK KD cells to determine pSTY phosphosites and pathways that have been affected by BRK reduction in TamR cells. Pathways and phosphosites that are differentially regulated in both comparisons will be assessed. In other words, if a phosphosite or a signaling pathway is affected in TamR vs Parental cells and is also affected when BRK is knocked down in TamR cells, it is an ideal candidate for further validation on the effects of BRK on TamR.

To accomplish this, label-free phosphoproteomics analysis through the enrichment of pSTY phosphopeptides was conducted, as described in the workflow diagram in Fig. 4.5. Briefly, MCF7 Parental, MCF7 TamR, T47D TamR and T47D TamR BRK KD cell lysates containing 1 mg of protein were isolated, reduced and alkylated before being digested by trypsin to yield peptides appropriate for phosphoproteomics analysis. Then, these peptides were purified and used for phosphopeptide enrichment using TiO_2 columns. The pSTY peptides thus obtained were analyzed using LC-MS/MS. Peptides were sequenced and identified from the mass spectra using the search engine Mascot which also identified the proteins the peptides were derived from and the phosphosites modified on these peptides (Helsens *et al.*, 2007). Phosphopeptides were then quantified using the software Scaffold (Searle, 2010).

When comparing MCF7 Parental vs TamR cells, a total of 2036 phosphopeptides, mapping to 1102 phosphorylated proteins were found (Fig. 4.6A). 1048 phosphopeptides mapping to 663 proteins were common between Parental and TamR cells (Fig. 4.6B and C). When comparing T47D TamR vs TamR BRK KD cells, 2209 phosphopeptides, mapping to 1125 unique

phosphoproteoins, were identified (Fig. 4.7A). 827 phosphopeptides, mapped to 547 proteins, were common to both cell lines in this case (Fig. 4.7B and C).

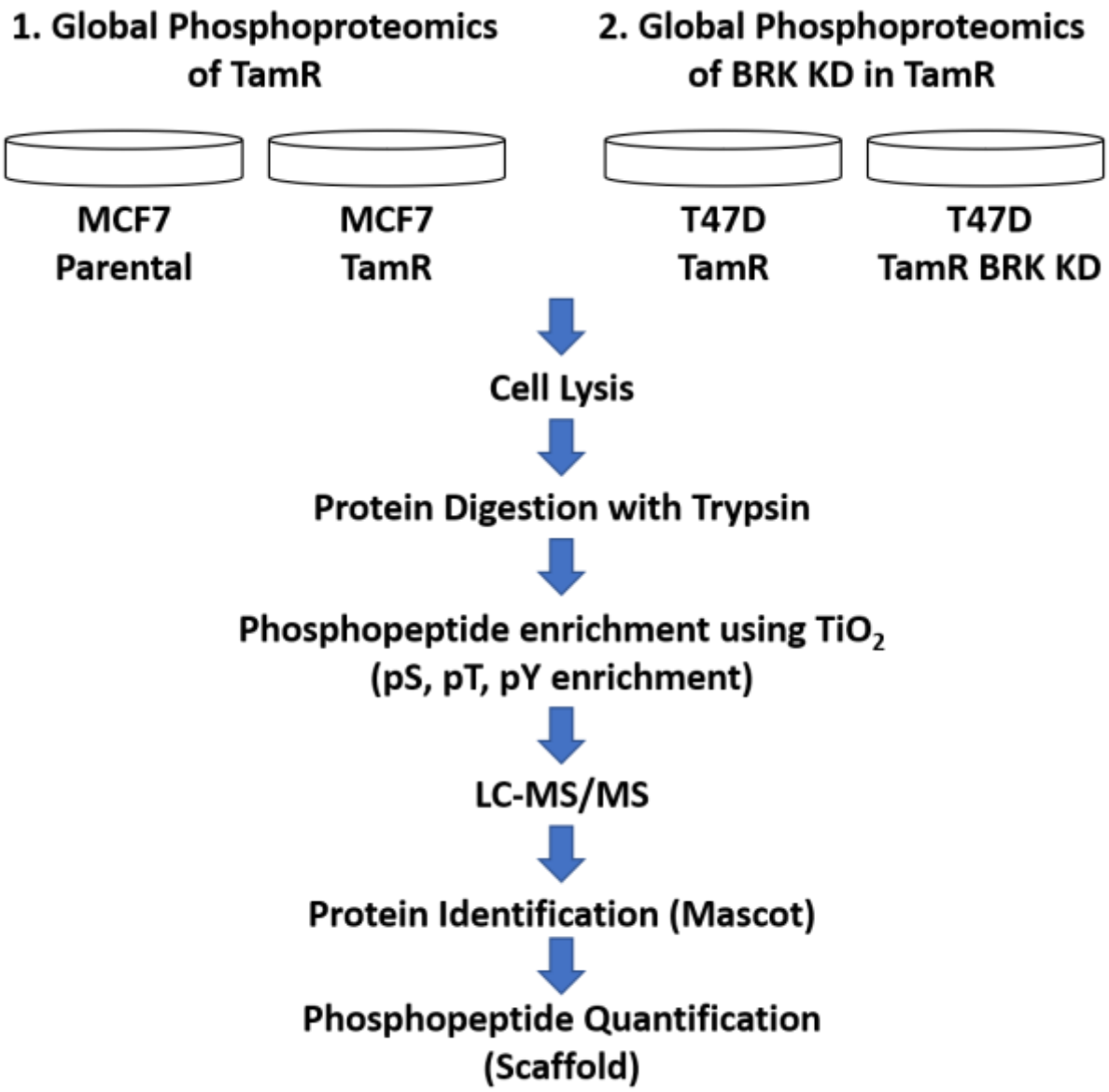

Figure 4.5. Workflow of the label-free, quantitative, global phosphoproteomics experiments conducted.

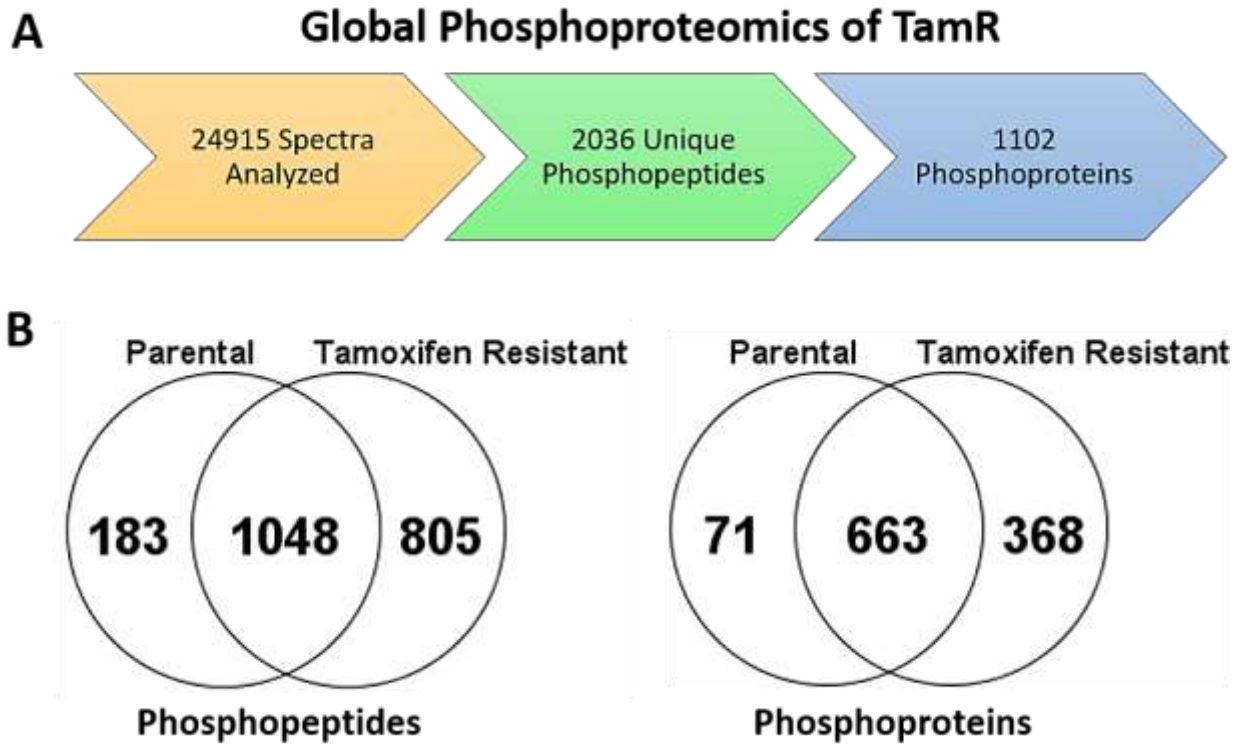

Figure 4.6. Global Phosphoproteomics of MCF7 cell lines that are sensitive (Parental) or resistant to Tamoxifen (Tamoxifen Resistant or TamR). **A)** Schematic describing the number of unique phosphopeptides and proteins identified from the spectra obtained through LC-MS/MS. **B)** Venn diagrams comparing the number of phosphopeptides and phosphoproteins found in Parental vs TamR MCF7 cell lines.

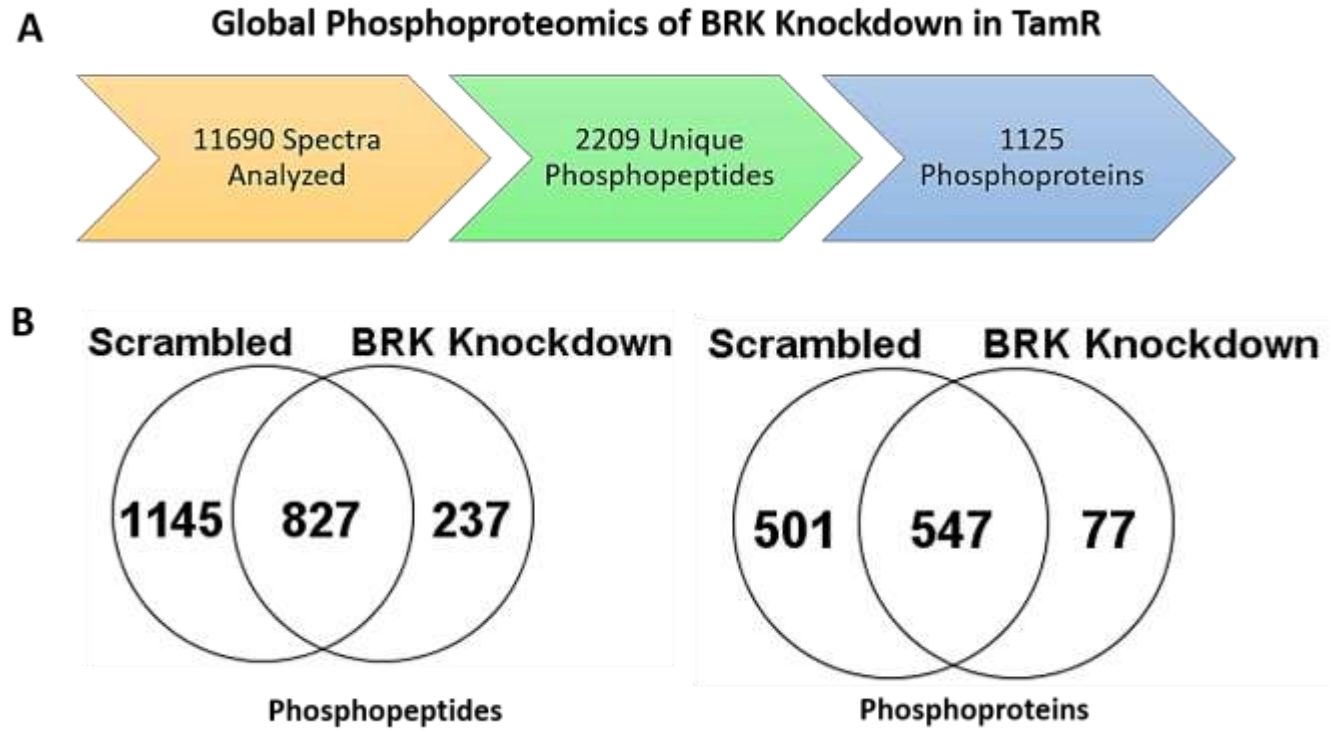

Figure 4.7 Global Phosphoproteomics of BRK Knockdown in T47D TamR cell lines with Scrambled as control. **A)** Schematic describing the number of unique phosphopeptides and proteins identified from the spectra obtained through LC-MS/MS. **B)** Venn diagrams showing similarities and differences in phosphopeptides and phosphoproteins found in T47D TamR (Scrambled control) vs T47D TamR BRK KD cell lines.

4.6.2 Identification of significantly hyper/hypophosphorylated targets in MCF7 TamR vs MCF7 Parental cells

Using the quantification analysis tools in Scaffold, the fold-change in phosphoprotein abundance in MCF7 TamR vs MCF7 Parental cells was calculated, and statistical testing was conducted by performing Welch's t-test. The results were depicted in the form of a volcano plot as shown in (Fig. 4.8A). Significantly up or downregulated phosphoproteins were defined as those that have a greater than ±1 log2 (fold change). Fold changes with a $p>0.05$ were discarded as statistically not significant (Fig. 4.8A). The fold change cut-off has been represented in the volcano plot by the two vertical lines at -1 and +1 FC. The p-value cut-off has been represented by the horizontal line at 1.301 ($-\log_{10}$ of 0.05). Selected hyper and hypo-phosphoproteins have been labeled on the volcano plot and tabled (Fig. 4.8A and Table 4.1).

Of the targets listed in Table 4.1, a particularly notable protein is Insulin Receptor Substrate 1, which was found to be significantly hypophosphorylated at the S1101 residue in Tamoxifen resistant cells (Fold change of -1 with p = 0.047). Since fold change was calculated on a log2 scale, this implies that IRS1 is twice as phosphorylated in MCF7 parental cells than in TamR cells, at the S1101 site. IRS1 is an adaptor protein that plays a role in propagating insulin receptor (IR) and insulin growth factor receptor (IGFR) signaling when these receptors are activated by their respective ligands insulin or IGF (Insulin-like Growth Factor) (Mardilovich *et al.*, 2009). When phosphorylated, the S1101 on IRS1 has been shown to reduce tyrosine phosphorylation and activation of IRS1 as well as downstream AKT pathway activation (Li *et al.*, 2004). With the hypophosphorylation of site in TamR cells, this implies that insulin receptor or IGFR signaling signaling is more active in TamR than in MCF7 parental cells. With previous studies having shown that IR signaling is unchanged in TamR cells while IGFR signaling may be inhibited, it is reasonable to hypothesize that IR signaling, rather than IGFR, is activated in MCF7 TamR cells and contributes to the continued resistance of these cells to Tamoxifen (Fagan *et al.*, 2012).

Table 4.1 Top 10 significantly hyper/hypophosphorylated proteins and peptides found in MCF7 TamR cells when compared to MCF7 parental cells. FC>1 and FC<-1 were considered significant with p<0.05.

Phosphorylation status	Uniprot Name	Protein description	p value	Fold Change	Peptides	Phosphosites
Significantly Hyper-phosphorylated	NPM1	Nucleophosmin isoform 1 [Homo sapiens]	0.0001	2.85	(K)CGSGPVHISGQHLVAVEEDAEsEDEEEEDVK(L)	S125
	ILF3	Interleukin enhancer-binding factor 3 isoform a [Homo sapiens]	0.0075	2.95	(K)QGGYSQSNYNsPGSGQNYSGPPSSYQSSQGGYGR(N)	S860
	ALKB5	RNA demethylase ALKBH5 [Homo sapiens]	0.035	3.00	(K)SYESSEDCSEAAGsPAR(K)	S384
	SF3A1	Splicing factor 3A subunit 1 [Homo sapiens]	0.016	3.32	(K)FGESEEVEMEVEsDEEDDKQEK(A)	S359
	TSC2	Tuberin isoform 4 [Homo sapiens]	0.0031	3.32	(R)SQsGtLDGESAAWSASGEDSR(G)	S1420, T1462
	IPP2	Protein phosphatase inhibitor 2 isoform 2 [Homo sapiens]	0.0001	3.59	(K)IDEPSTPYHSMMGDDEDACsDtEATEAMAPDILAR(K)	S87, T89
Significantly Hypo-phosphorylated	NAB2	NGFI-A-binding protein 2 [Homo sapiens]	0.013	-3.32	(R)APsPTAEQPPGGGDSAR(R)	S6
	NMD3	60S ribosomal export protein NMD3 [Homo sapiens]	0.047	-2.32	(R)DSAIPVEsDtDDEGAPR(I)	S468, T470
	SFR19	Splicing factor, arginine/serine-rich 19 [Homo sapiens]	0.013	-2.32	(R)sPFLKPDER(A)	S874
	IRS1	Insulin receptor substrate 1 [Homo sapiens]	0.047	-1.00	(R)HSsETFSSTPSATR(V)	S1101

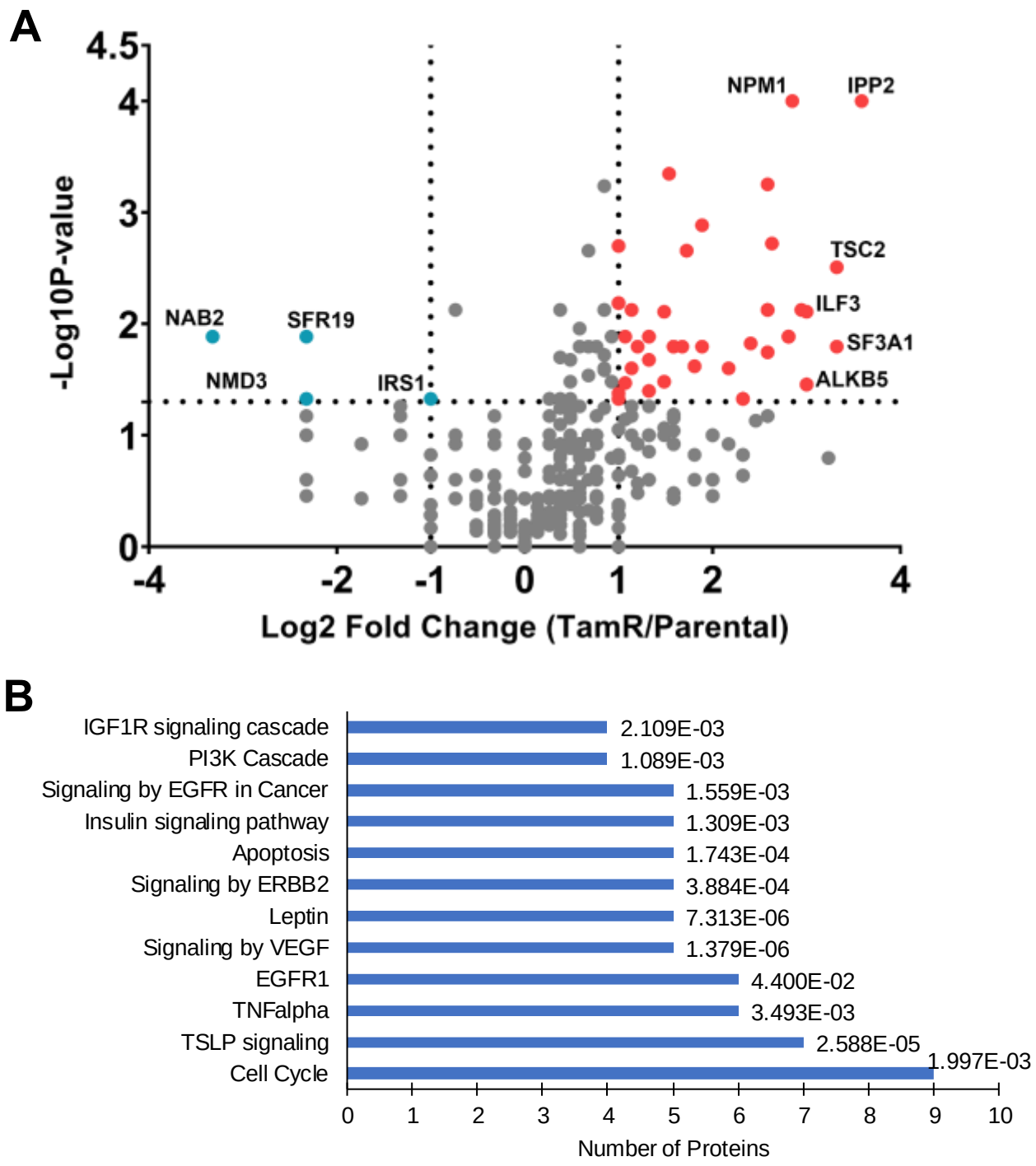

Figure 4.8 Fold-change and pathway analyses of phosphoproteomics data (MCF7 TamR vs Parental). **A)** Volcano plots are depicted with the fold change of each phosphoprotein versus the negative log of p-value which was calculated through t-test (n=3, $p < 0.05$). **B)** Top signaling pathways identified from pathway enrichment analysis of the hyperphosphorylated proteins in the MCF7-TamR cells (figures to the right of the bars are p values).

4.6.3 Identification of significantly hyper/hypophosphorylated targets that are affected by BRK knockdown in TamR

Having identified targets that were differentially phosphorylated in Tamoxifen resistance, I queried if any of these targets were differently phosphorylated when BRK was knocked down. Thus, I used the phosphoprotein quantification analysis of T47D TamR vs T47D TamR BRK KD cells to find if the phosphorylation of targets identified in TamR would change when BRK was knocked down. Statistical analysis and comparison were done using the Welch's t-test, as before in section 4.6.2. The volcano plot shown in Fig. 4.9A and Table 4.2 depict the top hyper and hypophosphorylated hits identified. Fold change and p-value cut-offs for this dataset remained the same as the comparison between MCF7 Parental vs TamR cells. The phosphoprotein IRS1 was also identified in this dataset as its S1101 phosphosite was hyperphosphorylated when BRK was knocked down in T47D TamR cells. There was a 1.722-fold increase in IRS1 S1101 phosphorylation (p value of 0.01). Since fold change was calculated as log2(phosphoprotein abundance), this value implies that IRS1 was 3.7 times more hyperphosphorylated in TamR BRK KD cells than in TamR cells.

Table 4.2 Top 10 Significantly hyper/hypophosphorylated proteins and peptides found in T47D TamR BRK KD cells when compared to T47D TamR cells. FC>1 and FC<-1 were considered significant with $p<0.05$.

Phosphorylation status	Uniprot Name	Protein description	p value	Fold Change	Peptides	Phosphosites
Significantly Hyper-phosphorylated	IRS1	Insulin receptor substrate 1 [Homo sapiens]	0.01	1.72	(R)HSsETFSSTPSATR(V)	S1101
	SCFD1	Sec1 Family Domain Containing 1	0.0001	2.14	(R)VNLEESSGVENsPAGARPK(R)	S303
	KHDR1	KH RNA Binding Domain Containing, Signal Transduction Associated 1	0.00013	2.14	(R)sGsmDPSGAHPSVR(Q)	S18, S20
	HDGF	Heparin Binding Growth Factor	0.00026	2.43	(K)GNAEGssDEEGKLVIDEPAK(E)	S132, S133
	I2BP1	Interferon Regulatory Factor 2 Binding Protein 1	0.0038	2.95	(R)AGGAsPAASSTAQPPTQHR(L)	S453
	ACLY	ATP Citrate Lyase	0.011	3.46	(R)TAsFSESR(A), (K)AKPAMPQDSVPsPR(S)	S455
	FARP1	FERM, ARH/RhoGEF And Pleckstrin Domain Protein 1	0.017	3.46	(K)VSAGEPGSHPsPAPR(R)	S481
Significantly Hypo-phosphorylated	OSBP1	Oxysterol Binding Protein	0.00045	-3.84	(K)MLAEsDEsGDEESVSQTDK(T)	S190, S193
	NACA	Nascent Polypeptide Associated Complex Subunit Alpha	0.00097	-3.64	(K)VQGEAVSNIQENTQTPTVQEEsEEEEVDETGVEVK(D)	S2029
	SF3A1	Splicing Factor 3a Subunit 1	0.00094	-3.32	(K)FGESEEVEMEVEsDEEDDKQEK(A)	S329
	NPM1	Nucleophosmin isoform 1 [Homo sapiens]	0.0001	-3.32	(K)CGSGPVHISGQHLVAVEEDAEsEDEEEEDVK(L)	S125
	RETR3	Reticulophagy Regulator Family Member 3	0.0099	-2.32	(R)AMDNHsDsEEELAAFCPQLDDSTVAR(E)	S258

4.6.4 Pathway analyses reveal significance of IGFR and insulin receptor signaling pathways

As I found that IRS1 S1101 is hypophosphorylated in TamR and hyperphosphorylated when BRK was knocked down in TamR cells, pathway analysis was conducted to ascertain if the datasets indicated changes to either IGFR or IR signaling as well as identifying other functional, pathway-level changes in these datasets. Using the method described in section 3.6.5, Innatedb.com was used to identify overrepresented pathways from the functional phosphoproteomics datasets (Breuer *et al.*, 2012).

The pathway enrichment analysis results show that indeed IRS1-mediated insulin signaling and IGF1R signaling cascades were shown to be enriched in both the TamR vs Par and TamR vs TamR BRK KD datasets (Figs. 4.8b and 4.9b). This was expected, not only due to the presence of IRS1 in the datasets, but also because IGF1R and insulin signaling share similarities in signaling cascades, including AKT pathway activation and IRS1-mediated signaling (Nagao *et al.*, 2021). Amongst these phosphoproteins that were enriched as a part of these pathways, both IRS1 and PDPK1 were found in both TamR vs Par and TamR vs TamR BRK KD datasets. PDPK1 is involved in AKT signaling and is an important mediator of the AKT signaling cascade which follows IRS1 activation (Jiang *et al.*, 2022). It is possible that BRK KD resulted in the inhibition of IRS1 downstream, potentially affecting IGFR signaling in TamR as a result (Fig. 4.9B). Due to these findings, it was reasonable to investigate how the phosphorylation status of IRS1 was affecting Tamoxifen resistant breast cancer cells and how IRS1 S1101 phosphorylation changes when BRK is knocked down.

Pathway enrichment analysis, through InnateDB and Reactome, also revealed over-representation of ERBB2 (HER2) signaling, EGFR1 signaling and cell cycle signaling pathways (Figs. 4.8b and 4.9b). These pathways were expected to be present in the analysis as they have been characterized extensively in their involvement in both the conferral and maintenance of Tamoxifen resistance (Rani *et al.*, 2019).

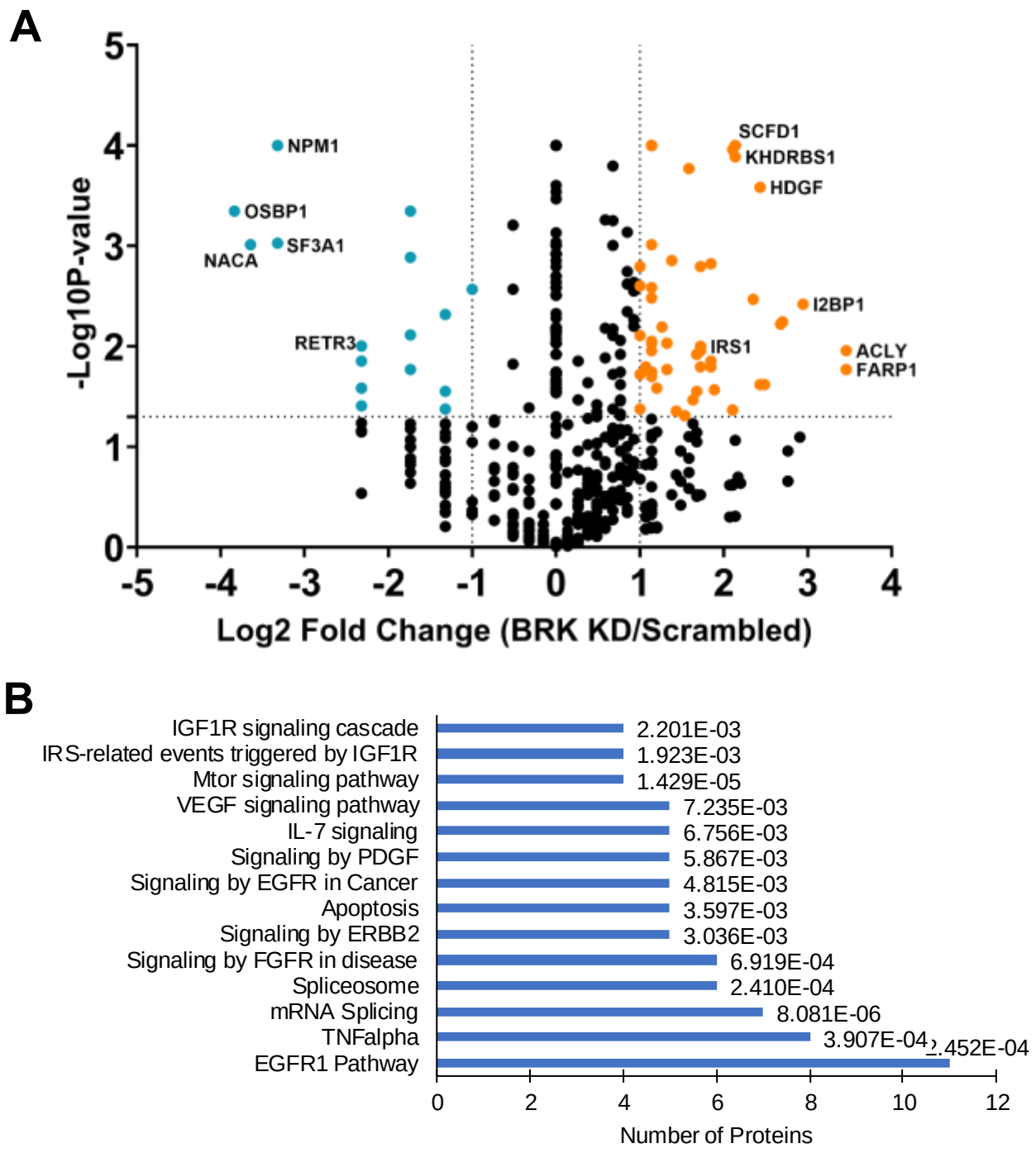

Figure 4.9. Expression and pathway analyses of phosphoproteomics data (T47D TamR BRK KD vs T47D TamR (denoted as Scrambled). **A)** Volcano plot depicting the fold change of each phosphoprotein versus negative log of p value which was calculated through a t-test (n=3, $p < 0.05$). **B)** Top signaling pathways identified from pathway enrichment analysis of the hyperphosphorylated proteins in the T47D TamR BRK KD cells (figures to the right of the bars are p values).

4.6.5 BRK knockdown and inhibition results in hyperphosphorylation of IRS1 S1101

Immunoblotting of cell lysates was conducted to validate the results described above. As shown in Fig. 4.10A, IRS1 was indeed hypophosphorylated in MCF7 TamR compared to Parental. When BRK was knocked down in T47D TamR cells, however, IRS1 was found to be hyperphosphorylated (Fig. 4.10B). To address cell line differences in the phosphoproteomics datasets, T47D parental cells were used to see if the changes seen in MCF7 parental vs TamR cells was represented in T47D cells as well. Comparing T47D parental and TamR cells showed changes in S1101 phosphorylation as discovered through MS analysis in their MCF7 counterparts (Fig. 4.10B). Indeed, when quantified, these changes displayed the same trends of hyperphosphorylation and hypophosphorylation as the MS analyses (Fig. 4.10C). The observation of IRS1 S1101 hypophosphorylation in both MCF7 and T47D TamR cells further validates the phosphosite's importance to Tamoxifen resistance and that this is cell-line independent (Fig. 4.10C).

The knockdown of BRK in TamR cells resulted in a hyperphosphorylation of the site (Fig. 4.10B). The differences in total IRS1 expression across parental, TamR and TamR BRK KD cells appeared to be negligible (Fig. 4.10B). By quantifying and comparing the changes in IRS1 S1101 expression between TamR vs Parental and TamR BRK KD vs TamR cell lines, a comparison can be made between the western blot quantifications and the fold change observations obtained through phosphoproteomics analysis (Fig. 4.10B and C). While the western blot quantifications showed the same overall trends as the MS quantifications (hypophosphorylation in TamR/Parental and hyperphosphorylation in BRK KD/TamR), the magnitude of the changes was significantly different between the MS and western blot quantifications ($p<0.05$, $n=3$) (Fig. 4.10C). The persistence of the trend across cell lines and techniques, however, is a validation of the observations in both MS and western blotting analyses.

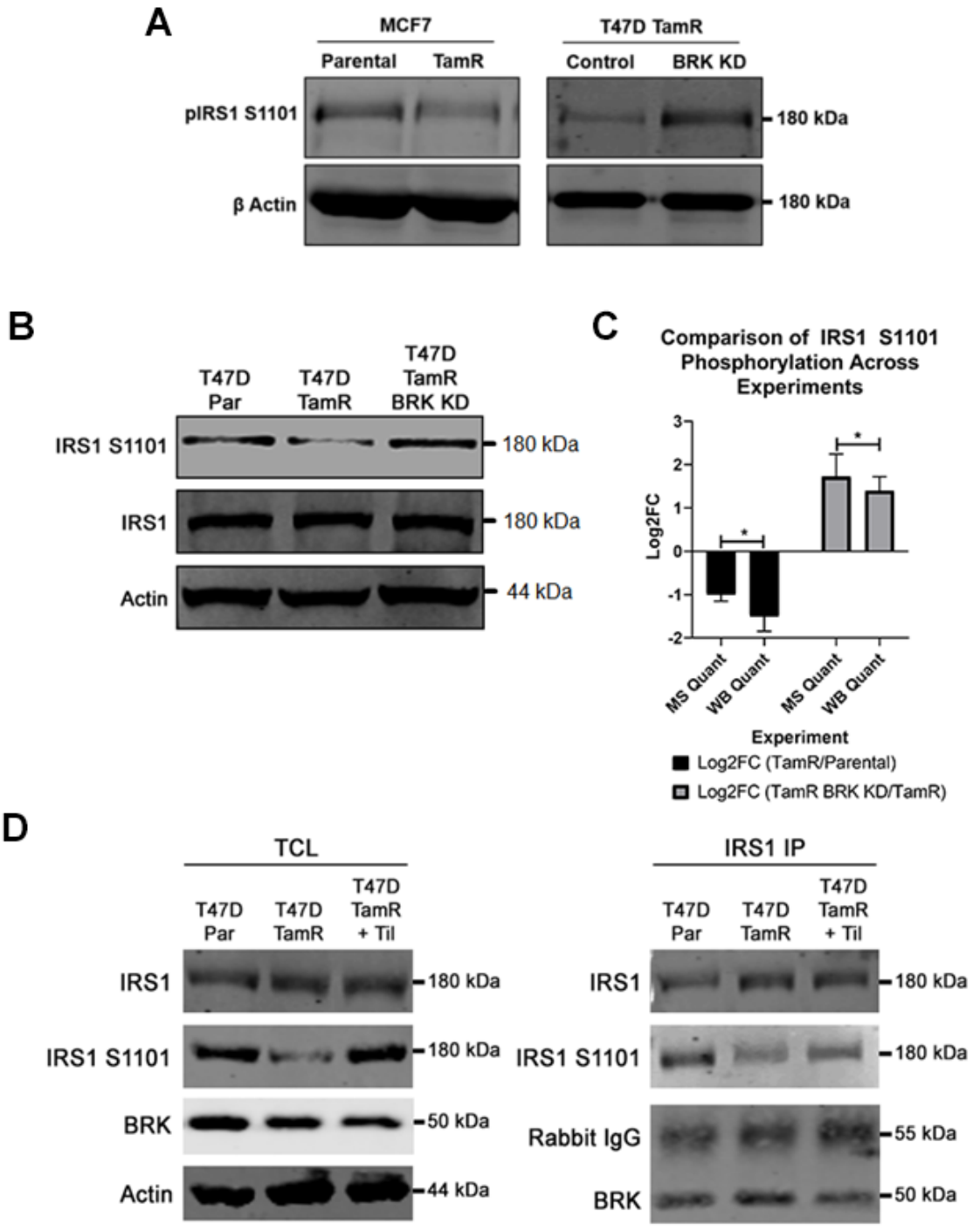

Figure 4.10. **A)** Western blot analysis of IRS1 S1101 phosphorylation with actin as a loading control. **B)** Western blot analysis of IRS1 S1101 phosphorylation and total IRS1 levels in T47D cells. **C)** Graphical representation of the quantification of the immunoblot and comparison of the calculated fold changes with the values obtained from phosphoproteomics analysis. Statistically significant changes represented by * ($p<0.05$, $n=3$). **D)** Western blot analyses of total cell lysates (TCL) and IRS1 immunoprecipitation (IRS1 IP) from T47D Parental, TamR and TamR + Tilfrinib (2.5 μM treatment over 48 hours). Expression of BRK, IRS1 S1101 and total IRS1 were assessed.

4.6.6 BRK interacts directly with IRS1

Having validated that IRS1 S1101 is hyperphosphorylated when BRK is knocked down, the interaction between IRS1 and BRK was further investigated through co-immunoprecipitation. T47D Parental and TamR cells were lysed in a non-denaturing Tris-HCL buffer. Additionally, to study the effect of BRK inactivation on its interaction with IRS1, T47D TamR cells treated with the BRK inhibitor Tilfrinib (2.5 μM treatment for 48 hours) and lysed as described above. While IRS1 pulldowns did yield coimmunoprecipitation of BRK, the reciprocal pulldown was unsuccessful in precipitating IRS1 (Fig. 4.10D). The unsuccessful reciprocal pulldown may have been due to the anti-BRK antibody affecting the binding site between BRK and IRS1, either directly or allosterically.

Immunoblotting of the total cell lysates for total IRS1, IRS1 S1101 and BRK expression show that the inhibition of BRK using Tilfrinib results in the hyperphosphorylation of the IRS1 S1101 phosphosite (Fig. 4.10D). I also found that BRK was pulled down with IRS1 immunoprecipitation from all 3 cell lines. This indicates a clear interaction between BRK and IRS1, apparently independent of BRK activation as BRK was pulled down in T47D TamR cells treated with 2.5 μM Tilfrinib (Fig. 4.10D). Assessment of IRS1 S1101 phosphorylation in the IRS1 pulldowns showed the same trend of hypophosphorylation in TamR vs Parental and hyperphosphorylation in TamR + Tilfrinib vs TamR (Fig. 4.10D). Overall, these results corroborate the western blot validation of the phosphoproteomics results (Fig. 4.10D) and indicate that the inactivation of BRK is sufficient for IRS1 inactivation through the hyperphosphorylation of the S1101 inhibition site.

4.6.7 Stimulation of T47D cells with insulin induces IRS1-mediated cyclin D1 gene expression

Previous studies have indicated that IRS1 has important functions in the nucleus, particularly in response to estrogen treatment and in combination with ER (Morelli *et al.*, 2004; Wu *et al.*, 2008). Indeed, chromatin immunoprecipitation (ChIP) of c-myc and cyclin D1 promoters in mouse fibroblasts has shown that IRS1 localizes to these promoters and activates the gene transcription (Wu *et al.*, 2008). Furthermore, in breast tumours that overexpressed IRS family proteins (including IRS1), increased levels of cyclin D1 and c-myc were observed (Dearth *et al.*, 2006).

I therefore sought to study the effects of BRK knockdown and inhibition on the nuclear, gene regulatory function of IRS1 using the expression of c-myc and cyclin D1 as functional readouts. To this end, RT-PCR analysis of T47D Parental, TamR, TamR BRK KD and TamR + Tilfrinib (2.5 μM for 48 hours) cell lines were collected. Primers against cyclin D1, c-myc, BRK and actin coding regions were designed. RNA conversion to cDNA was followed by RT-PCR quantification of gene expression in one step using the kit protocol provided (New England Biolabs, #E3005L).

As a proof of principle, T47D Parental cells were treated with insulin and cyclin D1 and c-myc expression were analyzed (Fig. 4.11A). By treating these cells with 8 μg/mL insulin, I expect the activation of the insulin receptor signaling pathway which would lead to the activation of IRS1-mediated cyclin D1 and c-myc transcription downstream (Lai *et al.*, 2001; Mawson *et al.*, 2005). Indeed, a significant increase in cyclin D1 and c-myc mRNA levels was observed when these cells were treated with 8 μg/mL of insulin for 48 hours (Fig. 4.11A). It should be noted, however, that c-myc mRNA was not detected in the untreated cells. The lack of c-myc expression in the untreated T47D Parental cell line does not align with RTPCR results from the experiments that followed as c-myc expression was otherwise detected in T47D parental cells (Fig. 4.11A).

Having established that both c-myc and cyclin D1 mRNA increase upon insulin-mediated activation of IRS1 signaling, I analyzed the effects of BRK knockdown (Fig. 4.11A) and BRK inhibition using 2.5 μM Tilfrinib on the expression of these genes, with actin included as a housekeeping gene and BRK included as a control whose transcription levels should not change. When BRK was knocked down in T47D TamR cells, I observed a statistically significant ($p<0.001$, $n=6$) decrease in cyclin D1 mRNA levels (Fig. 4.11B). Additionally, there was a significant increase in cyclin D1 mRNA levels in T47D TamR cells compared to their Parental counterpart ($p<0.05$, $n=6$) (Fig. 4.11B). These results align with the hypothesis that the inhibition of IRS1 due to BRK knockdown affects its ability to regulate cyclin D1 expression. By contrast, c-myc mRNA levels appear to be unaffected by BRK knockdown in TamR cells (Fig. 4.11B**)** with no significant differences observed in mRNA levels across the 3 cell lines. While c-myc was undetected in T47D Parental cells in the insulin-stimulation experiment, c-myc was detected here in all 3 cell lines (Fig. 4.11A and B). As expected, BRK levels were reduced in the BRK KD cell line.

When assessing the effect of BRK inactivation, using the BRK-specific inhibitor Tilfrinib at a concentration of 2.5 μM for a treatment period of 48 hours, on the gene transcription of cyclin D1 and c-myc, a similar trend was observed with cyclin D1 expression (Fig. 4.11C). Cyclin D1 expression was significantly reduced ($p<0.05$, $n=6$) in T47D TamR BRK KD cells vs their TamR counterpart. However, there was no significant difference in cyclin D1 mRNA levels between TamR and Parental cells (Fig. 4.11C). Since this comparison yielded significant differences previously, it is possible that experimental error increased variance in results. Interestingly, the difference in c-myc mRNA levels between TamR and Parental cells was found to be significant, a finding which is not corroborated by results presented in Fig. 4.11B. Again, it is possible that variance between the two experiments was caused by either experimental error or differences in the replicates used in each experiment.

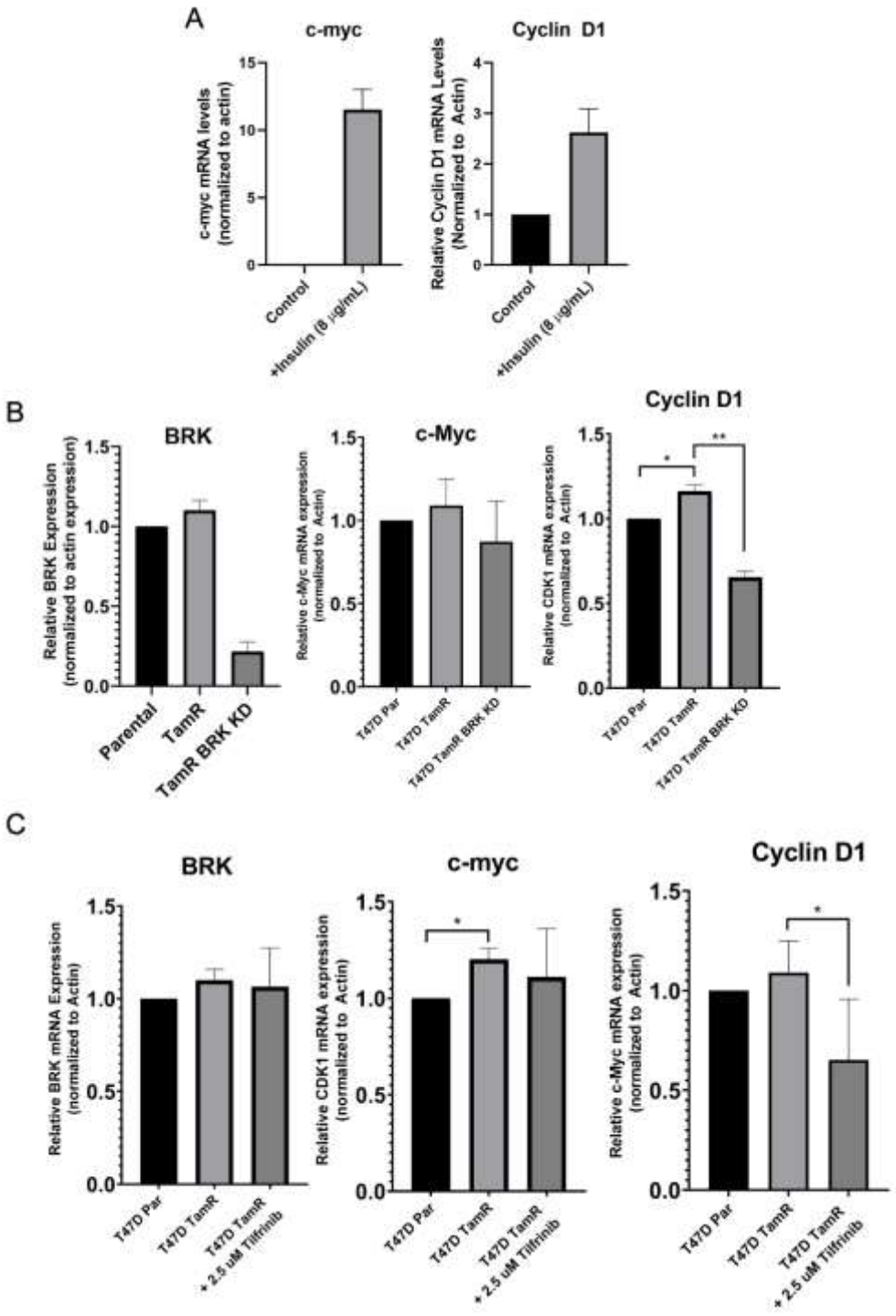

Figure 4.11. Cyclin D1 and c-myc RTPCR analyses of **A)** T47D cells stimulated with insulin (8 μg/mL) and their untreated counterparts. **B)** T47D Parental, TamR and TamR BRK KD cell lines and **C)** T47D Parental, TamR and TamR + Tilfrinib (2.5 μM treatment over 48 hours) cell lines. mRNA levels were quantified by normalizing to the housekeeping gene and calculating expression relative to T47D Parental as the control. * denotes stastically significant differences ($p<0.05$, $n=6$).

4.6.7.1 Serum starvation before insulin stimulation results in a significant response in the insulin receptor signaling pathway

In previous experiments, a treatment of 8 µg/mL insulin for 48 hours was used to stimulate IRS1 activity. As insulin stimulation results in changes within minutes, it was important to establish a more appropriate window for measuring insulin-stimulated, IRS1-mediated gene expression. To this end, T47D Parental cells were treated with 8 µg/mL insulin for the time periods listed in Fig. 4.13A. Phospho-AKT (S473) was used as a readout for the stimulation of the insulin receptor signaling pathway as it is a downstream signaling intermediary that is activated upon insulin stimulation (Fig. 4.13A).

As quantified in Fig. 4.12B, AKT activity increased drastically after 5 min with an approximate 4.75x increase. AKT phosphorylation (relative to total AKT levels) peaked after 1 hour (approximately 12.5x increase) and remained constant until the 12-hour timepoint where there is a significant drop in AKT phosphorylation (Fig. 4.13B). Therefore, it was determined that a 30 min stimulation of 8 µg/mL insulin would be appropriate for future testing of insulin mediated IRS1 functioning.

Stimulation with insulin for these time periods also affected c-myc and cyclin D1 mRNA levels. Both c-myc and cyclin D1 transcription levels peak at 30 min with cyclin D1 mRNA levels remaining similar up to the 2-hour time point (Fig. 4.13A and B). Interestingly, c-myc transcription levels become undetectable beyond 2 hours of insulin stimulation, which is in keeping with c-myc's function as an early response gene (Fig. 4.13A). This result also explains why c-myc detection was unreliable in the previous experiment (Fig. 4.11A and B). Cyclin D1 levels peaked between 30 min to 1 hour, as mRNA levels were not significantly different between these timepoints (Fig. 4.13B). Taking these results into account, stimulation of the T47D parental, TamR and TamR BRK KD cells with 8 µg/mL insulin for 30 min was ideal for future experiments to probe IRS1 mediated gene regulation.

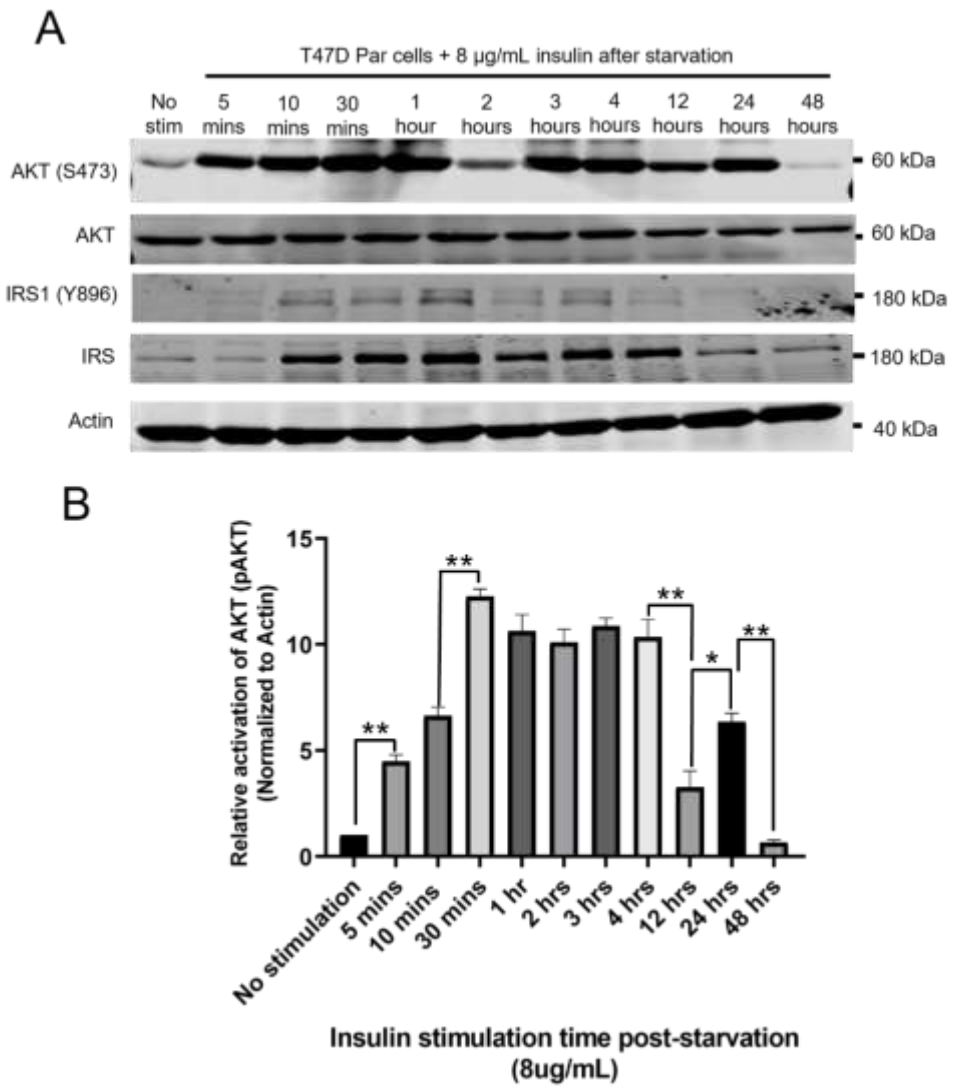

Figure 4.12. A) T47D Parental (T47D Par) cells were serum-starved for 24 hours and treated with 8µg/mL of insulin for the indicated time periods with a no stimulation control. AKT activation (S473), total AKT, active IRS1 (Y896), total IRS1, BRK and actin were assayed with AKT activation as a measure of insulin stimulation. **B)** Western blot quantification, specifically for the phosphorylation of AKT at S473, normalized to actin expression. * denotes significant differences with p value < 0.05, n=3. ** denotes significant differences with p<0.01, n=3.

4.6.7.2 BRK knockdown and inhibition reduce IRS1-mediated cyclin D1 gene expression as well as affecting IRS1 activity.

Having established that a 30 min stimulation of 8 µg/mL insulin would be appropriate for probing IRS1-mediated gene regulation, the experiments described in section 4.6.7 were repeated with this new stimulus condition in mind. When T47D parental, TamR and TamR cells treated with 2.5 µM tilfrinib were assayed for c-myc and cyclin D1 mRNA levels, the results showed that BRK inhibition by Tilfrinib reduced both c-myc and cyclin D1 mRNA levels significantly ($p<0.05$) (Fig. 4.13C and D). When BRK was knocked down in T47D TamR cells, similar trends were observed as both c-myc and cyclin D1 levels were reduced (Fig. 4.13E and F). Overall, these results indicate that BRK inhibition and knockdown affects IRS1-mediated cyclin D1 and c-myc gene regulation.

To investigate this further, two aspects of IRS1 were analyzed, its phosphorylation at the Y896 activation site and its localization to the promoter regions of c-myc and cyclin D1 to initiate its gene regulatory activity (Fig. 4.14). As shown in figure 4.14A, IRS1 Y896 levels were lowered upon BRK knockdown, implying reduced activity. Using ChIP qPCR, the localization of IRS1 to the promoter regions of cyclin D1 and c-myc were assessed using the protocol and primer sequences described previously by Wu and colleagues (Wu *et al.*, 2008). I found that IRS1 bound to the cyclin D1 promoter region (Fig. 4.14B). Furthermore, both the inhibition and the knockdown of BRK reduced IRS1 binding to the cyclin D1 promoter region. These results imply that BRK knockdown reduces IRS1 activity by affecting its Y896 site while also affecting its ability to bind to the promoter of cyclin D1.

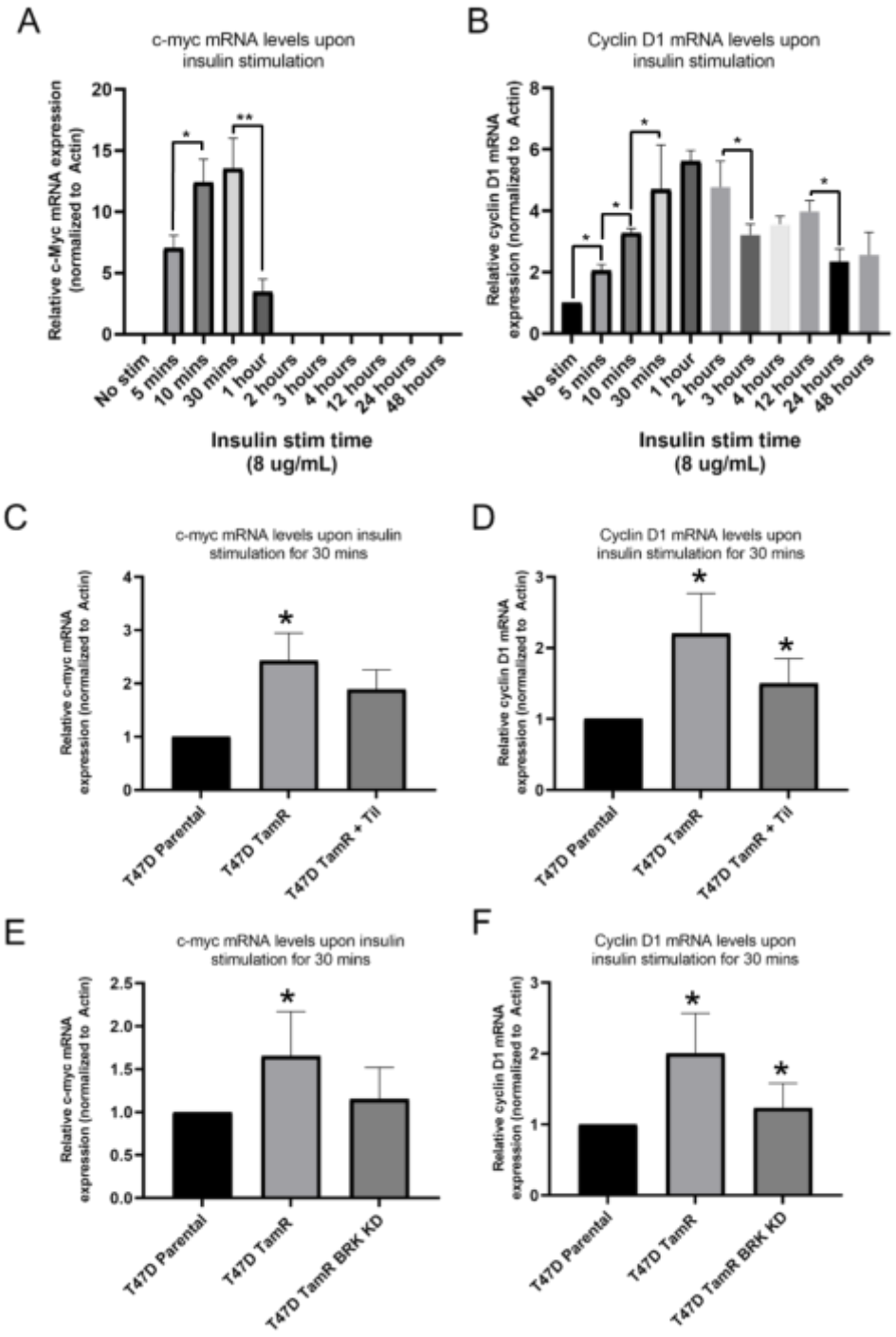

Figure 4.13. A-B) Quantitative PCR analysis of T47D Parental cells serum-starved for 24 hours and treated with 8ug/mL of insulin for the time periods indicated. Cyclin D1 and c-myc mRNA levels were quantified. **C-F)** Quantitative PCR analysis of T47D Parental vs TamR vs TamR BRK KD or TamR + Tilfrinib cells for the mRNA expression of cyclin D1 and c-myc. Significant changes are denoted by * and ** ($p<0.05$ and $p<0.01$ respectively) and n=6 for all samples.

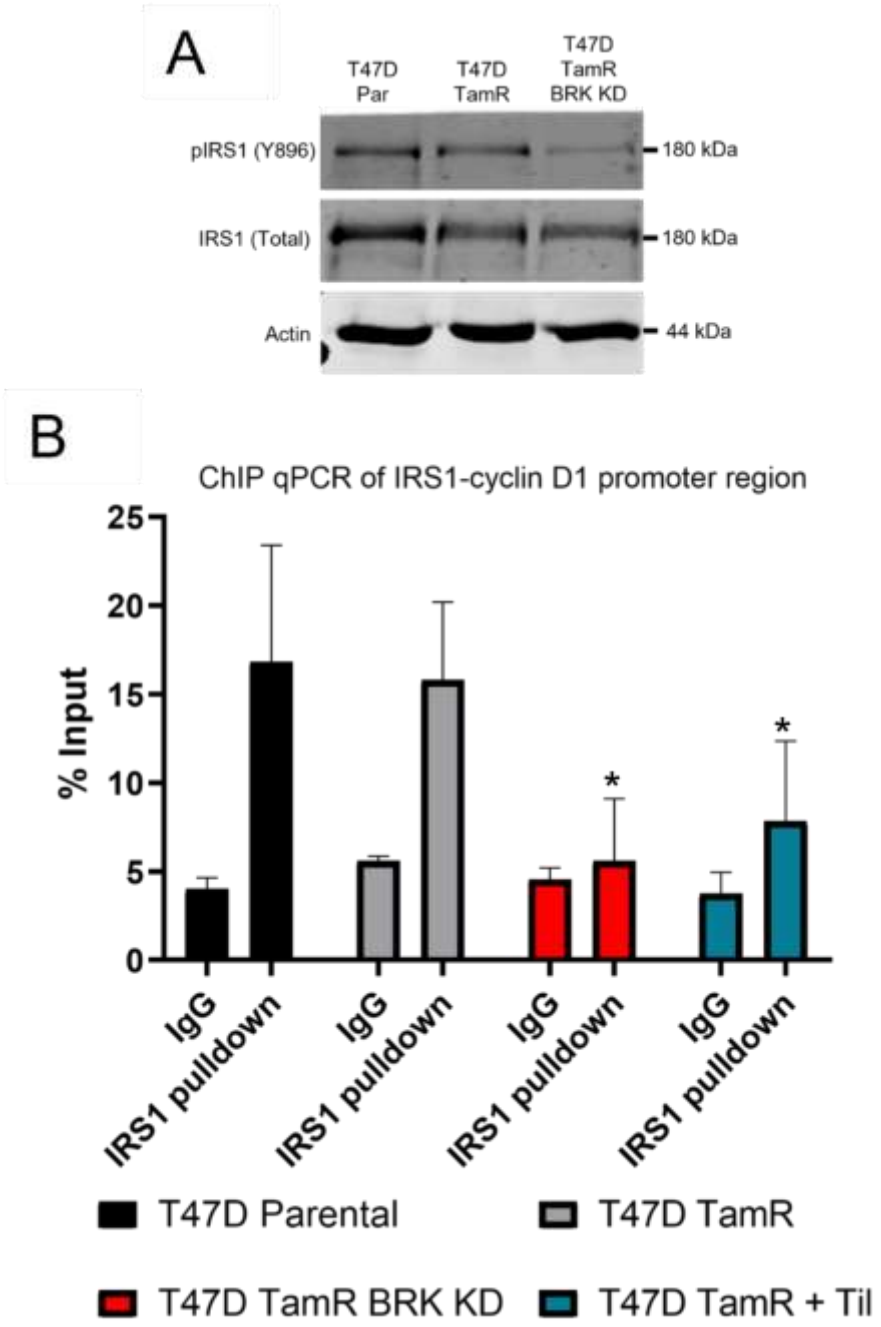

Figure 4.14. A) Western blot analysis of IRS1 and IRS1 Y896 with actin loading control. **B)** ChIP-qPCR analysis of the cyclin D1 promoter site quantified from IRS1-chromatin pulldowns. T47D parental cells were serum-starved for 24 hours, followed by treatment with 8ug/mL insulin for 30 min. Significant changes are denoted by * ($p<0.05$, n=6 for all samples).

4.7 Phosphotyrosine phosphoproteomics of T47D Parental vs T47D TamR vs T47D TamR BRK KD cells

4.7.1 Phosphoproteomics workflow to enrich pTyr peptides using immunoaffinity purification

Having looked at changes in pSTY peptides in MCF7 parental vs TamR cells and T47D TamR vs T47D TamR BRK KD cells, it was prudent to consolidate the phosphoproteomics data by analyzing one cell line instead of comparing across two cell lines. Additionally, because BRK is a tyrosine kinase, the next step in the phosphoproteomics analysis pipeline was to analyze tyrosine phosphorylation changes between T47D parental vs TamR vs TamR BRK KD cells.

T47D TamR cells were transduced with scrambled shRNA and BRK shRNA to generate stable TamR cells and their BRK KD counterparts as before. The extent of BRK knockdown was then verified through western blot. As shown in Fig. 4.15B, BRK expression was reduced by approximately 70% in the knockdown cell line vs control. Furthermore, as a proof of principle, I was able to replicate prior results in these cell lines (Fig. 4.15A). Previously, I observed a reduction in phosphorylation of STAT3 (Y702), a direct BRK substrate, when BRK was knocked down in T47D TamR. I also found that p38 was hyperphosphorylated at the Y182 residue in the BRK knockdown cell line. Both these results were replicated in the newly generated cell lines were able to replicate these results for the newly generated counterparts of these cells. Therefore, I can be reasonably confident that the signaling changes discovered in these cell lines can be compared with the previous phosphoproteomics analysis to yield a cohesive model of BRK's action in Tamoxifen resistance.

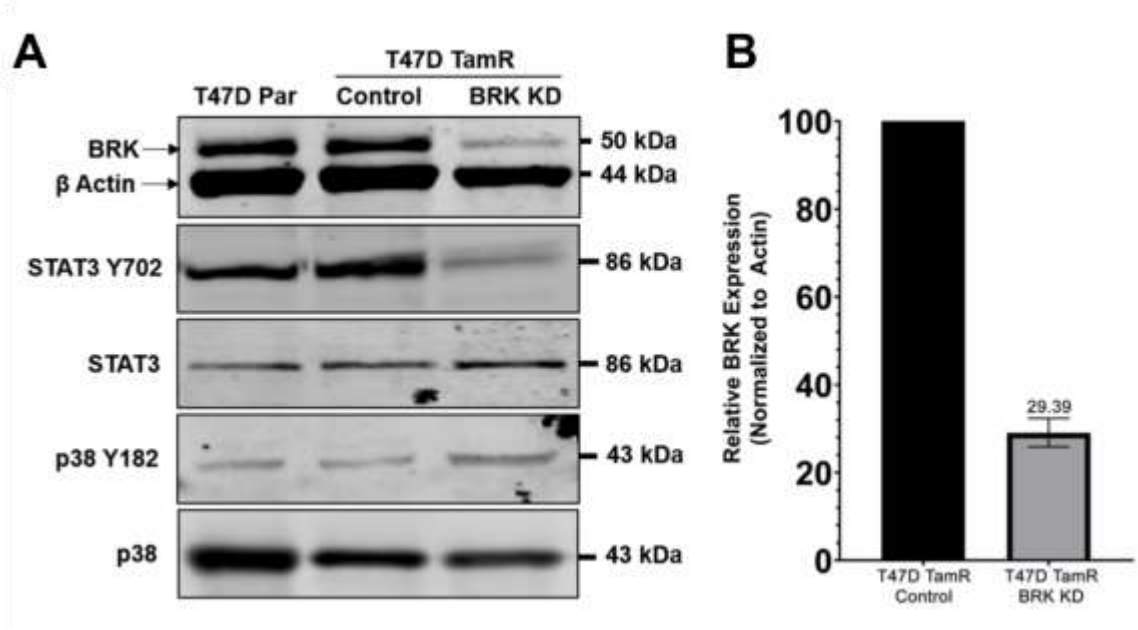

Figure 4.15 Generation of T47D TamR BRK KD cells for phosphotyrosine-enrichment phosphoproteomics. **A)** western blot of BRK, STAT3 Y702, STAT3, p38 Y182 and total p38 in the generated cell lines. **B)** Quantification of immunoblots of BRK knockdown in T47D TamR cells (n=3).

Lysates of these cell lines were harvested from 16 x 10 cm culture plates grown to 90% confluence. They were then prepared for mass spectrometry as shown in Fig. 4.16. Before sample preparation began, each lysate was divided into 10 mg and 1mg fractions (in 3 technical triplicates) for pTyr enrichment and global phosphoenrichment respectively as pTyr enrichment requires more starting material, as per the protocol described by Stokes and colleagues (2012). The lysates were then reduced, alkylated, and digested as stated in section 4.6.1. The resultant peptides were purified and lyophilized prior to enrichment. The 1 mg fractions were subjected to phosphopeptide enrichment using TiO_2 columns as per section 4.6.1. The 10 mg fraction was subjected to phosphotyrosine enrichment using pTyrosine antibody-conjugated beads (Stokes *et al.*, 2012).

Spectra obtained from the MS analysis were sequenced using the Andromeda search engine as part of the MaxQuant software, thereby yielding sequenced phosphopeptides as well as the respective phosphosites found in the respective samples. The search results were subsequently analyzed using the Perseus software as described previously (section 3.6.5) (Batth *et al.*, 2018; Tyanova and Cox,

2018). Phosphosite search results were filtered to remove reverse hits and contaminants before statistical processing, including normalization and log2 transformation were performed. In total, across all replicates and cell lines, the phosphoproteomics analysis identified 6492 phosphosites. Of these sites, 6325 were phosphoserine and phosphothreonine (pST) sites while 167 phosphotyrosine (pY) sites were found. When these sites were filtered for high confidence phosphosites (with localization probability greater than 75%), 3739 pST sites and 118 pY sites were found (Fig. 5A). Localization probability refers to the confidence with which the search engine can assign a phosphosite at that location along the peptide sequence (Cox *et al.*, 2011). Therefore, 3% of the total high confidence phosphoproteome obtained from the analysis contained pY phosphosites (Fig. 4.17A). All the identified pY sites were detected through the pY-specific enrichment approach, indicating that the immunoaffinity purification process was successful. Using a similar pY enrichment method, Batth and colleagues also obtained an approximate 3% pY site enrichment yield (Batth *et al.*, 2018). Approximately 962 phosphosites were shared between T47D TamR and T47D Parental cells with 412 and 216 phosphosites unique to each condition, respectively (Fig. 4.17B). In comparing phosphosites between TamR and TamR BRK KD cells, 516 and 264 phosphosites were found to be unique in TamR and TamR BRK KD respectively (Fig. 4.17C).

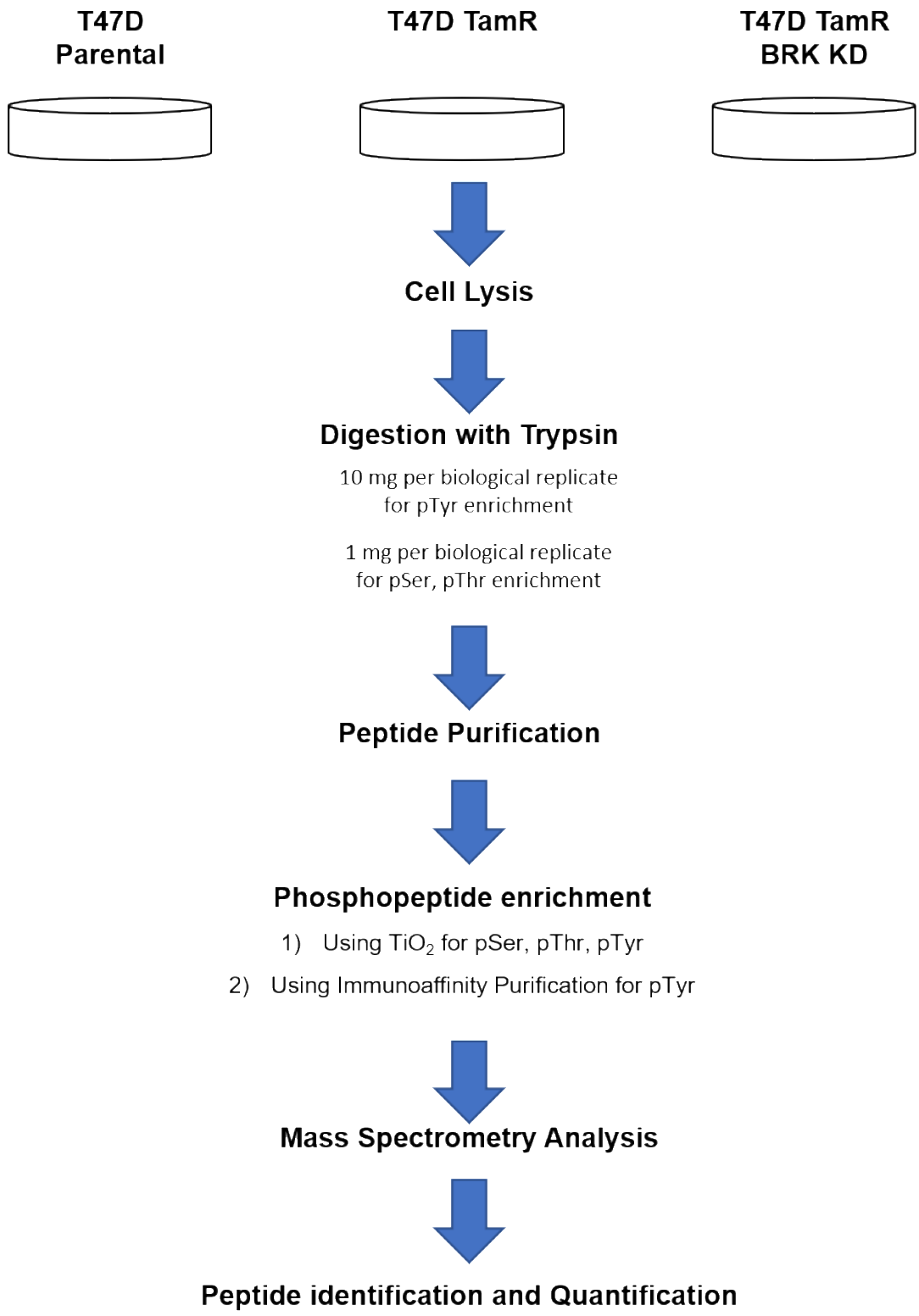

Figure 4.16. Phosphoproteomics workflow for the analysis of T47D Parental vs TamR Vs TamR BRK KD cell lines.

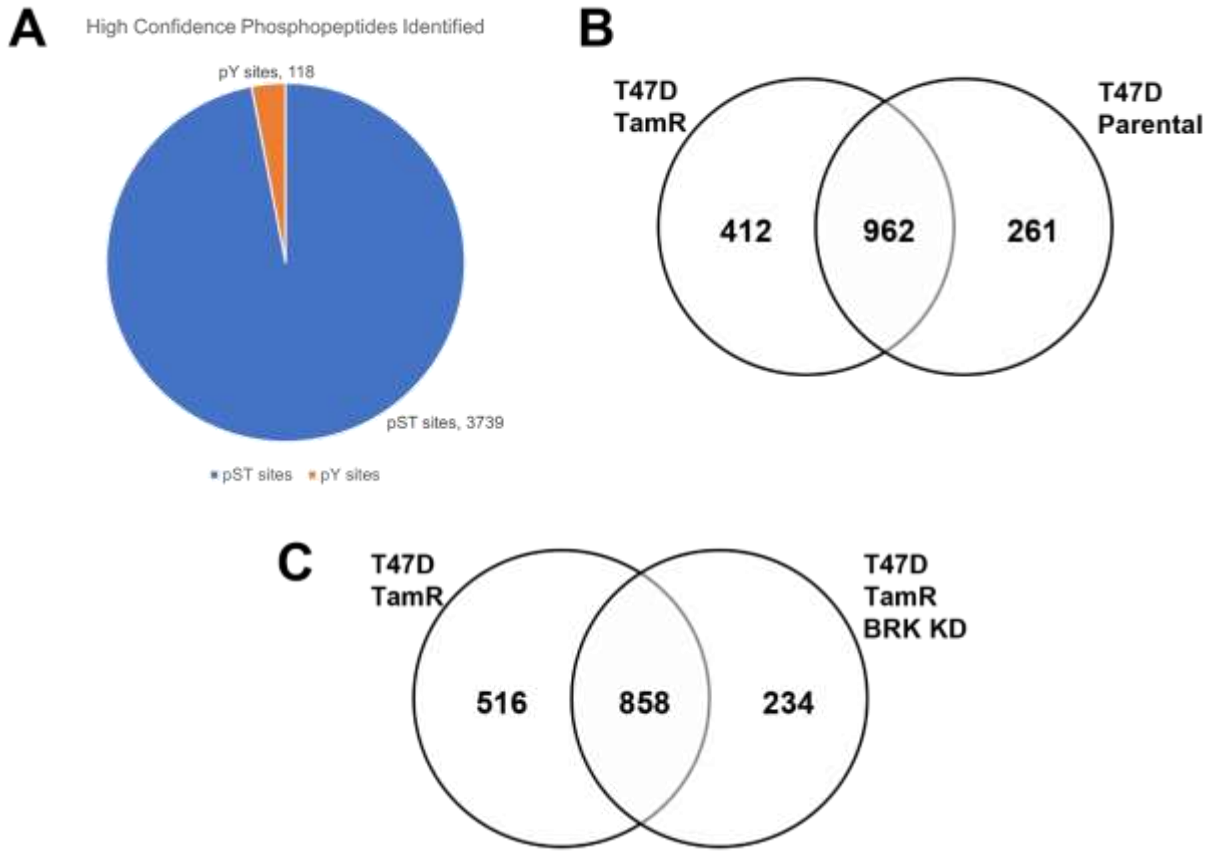

Figure 4.17. Global phosphoproteomics analysis of T47D Parental vs TamR vs TamR BRK KD cell lines. **A)** Pie chart breakdown of the high confidence (probability > 0.75) phosphopeptides identified in the experiment. **B and C)** Venn diagram representations of common and unique phosphopeptides between T47D TamR vs Parental and T47D TamR vs TamR BRK KD.

4.7.2 Identification of phosphosites differentially hypo/hyperphosphorylated in TamR vs Parental T47D Cells

To identify pathways, substrates and kinases involved in TamR and differentially affected by BRK KD in TamR cells, it was important to identify phosphosites that showed significant differences between TamR vs Parental as well as TamR BRK KD vs TamR cell lines. To this end, I defined fold change and statistical significance cutoffs. The cutoff criteria for significant fold change were defined as a 1-fold change in either direction while the cutoff for statistical significance was defined as $p<0.05$. Fold change was calculated by subtracting the log2 (Intensity in TamR) – log2 (Intensity in Parental) for these phosphopeptides, where intensity is the measure of abundance of the phosphopeptides calculated by the MaxQuant software.

After filtering for significantly hypo- and hyper- phosphorylated pTyr peptides, 17 targets were identified and have been listed in Table 4.3. Notably, the MAP kinase MAPK14, also known as p38 was found to be hypophosphorylated in TamR cells, a finding that corroborates not only previous results shown in Figs 4.3 and 4.15 but also work done by Ito and colleagues in 2017 (Ito *et al.*, 2017). Other targets of interest include CDK1 and CDK2 which were found to be hypophosphorylated at the Y15 site. Both these cell cycle proteins have been implicated in controlling the transition between G1 and S phase in mitosis and have been targeted for inhibition in pre-clinical evaluations for Tamoxifen-resistance treatment (Johnson *et al.*, 2010). Interestingly, the increased phosphorylation of CDK1 and CDK2 at the Y15 site has been associated resistance to chemotherapy (Tan *et al.*, 2002). An analysis of CDK1/2 phosphorylation at Y15 relative to total CDK1/2 levels quantified through proteomics (section 4.7.4 and 4.7.5) may shed further light on this observation.

Amongst the pST sites found, CD44 S706 and AKT1 S124 were hyperphosphorylated in Tamoxifen-resistant cells (Fig. 4.18A). Both phosphosites have been found to induce enzymatic activity when phosphorylated (Bellacosa *et al.*, 1998; Peck and Isacke, 1998). The activity of both proteins has also been previously implicated in driving tamoxifen resistance, which further validates the drug resistant phenotype displayed by the T47D TamR cells (Frogne *et al.*, 2005; Hiscox *et al.*, 2012). AKT1 is also a known BRK substrate at the Y315 phosphosite which also induces enzymatic activity (Zheng *et al.*, 2010). However, AKT Y315 was not identified in this experiment across all samples. This finding is also in line with the increased activity of IRS1 observed in Fig. 4.14 as increased IRS1 activity causes activation of AKT signaling downstream (Li *et al.*, 2004).

Analysis of the pathways enriched in this dataset (using Innatedb) revealed the overrepresentation of both IGF-1 signaling (through IGFR) and insulin receptor signaling (Fig. 4.18B). These pathways were also enriched in the phosphoproteomics dataset comparing MCF7 TamR and parental cells (section 4.6), which displays the importance of both pathways to TamR in a cell-line independent manner.

Table 4.3 Significantly hyper/hypophosphorylated pTyr peptides found in the phosphoproteomics comparison of T47D TamR vs T47D parental cells. FC>1 and FC<-1 were considered significant with $p<0.05$.

Phosphorylation status	Uniprot Name	Protein Description	pvalue	Fold Change	Peptide	Phosphosite
Significantly Hyper-phosphorylated	CASKIN2	CASK interacting protein 2	0.001483676	2.083940665	RLLLEGGVDVNIRNTYNQTALDIVNQFTTSQ	Y253
	HIPK2	homeodomain interacting protein kinase 2	0.02061858	1.943695237	DFGSASHVSKAVCSTYLQSRYYRAPEIILGL	Y361
	PARD3	par-3 family cell polarity regulator	0.001650773	1.62862962	AKTREFRERQARERDYAEIQDFHRTFGCDDE	Y1080
	HSPB1	heat shock protein family B (small) member 1	0.011861506	1.238508721	AVAAPAYSRALSRQLSSGVSEIRHTADRWRV	Y82
	MGP	matrix Gla protein	0.029840333	0.608641403	ELNREACDDYRLCERYAMVYGYNAAYNRYFR	Y82
Significantly Hypo-phosphorylated	GAB1	GRB2 associated binding protein 1	0.021280809	-1.113883033	KSSGSGSSVADERVDYVVVDQQKTLALKSTR	Y659
	STAT5A	signal transducer and activator of transcription 5A	0.060431913	-1.158032467	FSKYYTPVLAKAVDGYVKPQIKQVVPEFVNA	Y694
	PLEKHA6	pleckstrin homology domain containing A6	0.05432546	-1.258839081	PSARFERLPPRSEDIYADPAAYVMRRSISSP	Y492
	MAPK3	mitogen-activated protein kinase 3	0.033959757	-1.268397619	RIADPEHDHTGFLTEYVATRWYRAPEIMLNS	Y204
	PTPN11	protein tyrosine phosphatase non-receptor type 11	0.058288227	-1.525312205	RNGAVTHIKIQNTGDYYDLYGGEKFATLAEL	Y62
	CDK1	cyclin dependent kinase 1	0.041140993	-1.775558012	_MEDYTKIEKIGEGTYGVVYKGRHKTTGQVV	Y15
	CDK2	cyclin dependent kinase 2	0.040996557	-1.775558012	_MENFQKVEKIGEGTYGVVYKARNKLTGEVV	Y15
	ATP8B1	ATPase phospholipid transporting 8B1	0.040996557	-1.805742711	VSTRRSAYAFSHQRGYADLISSGRSIRKKRS	Y1217
	MAPK14	mitogen-activated protein kinase 14	0.002341169	-1.852256586	LDFGLARHTDDEMTGYVATRWYRAPEIMLNW	Y182
	CRKL	CRK like proto-oncogene, adaptor protein	0.012280005	-1.891459296	GPVFAKAIQKRVPCAYDKTALALEVGDIVKV	Y251
	SHC1	SHC adaptor protein 1	0.006888675	-1.891511932	PPPPCPGRELFDDPSYVNVQNLDKARQAVGG	Y427
	CRIP1	cysteine rich protein 1	0.001213549	-1.963146418	____MPKCPKCNKEVYFAERVTSLGKDWHRP	Y12

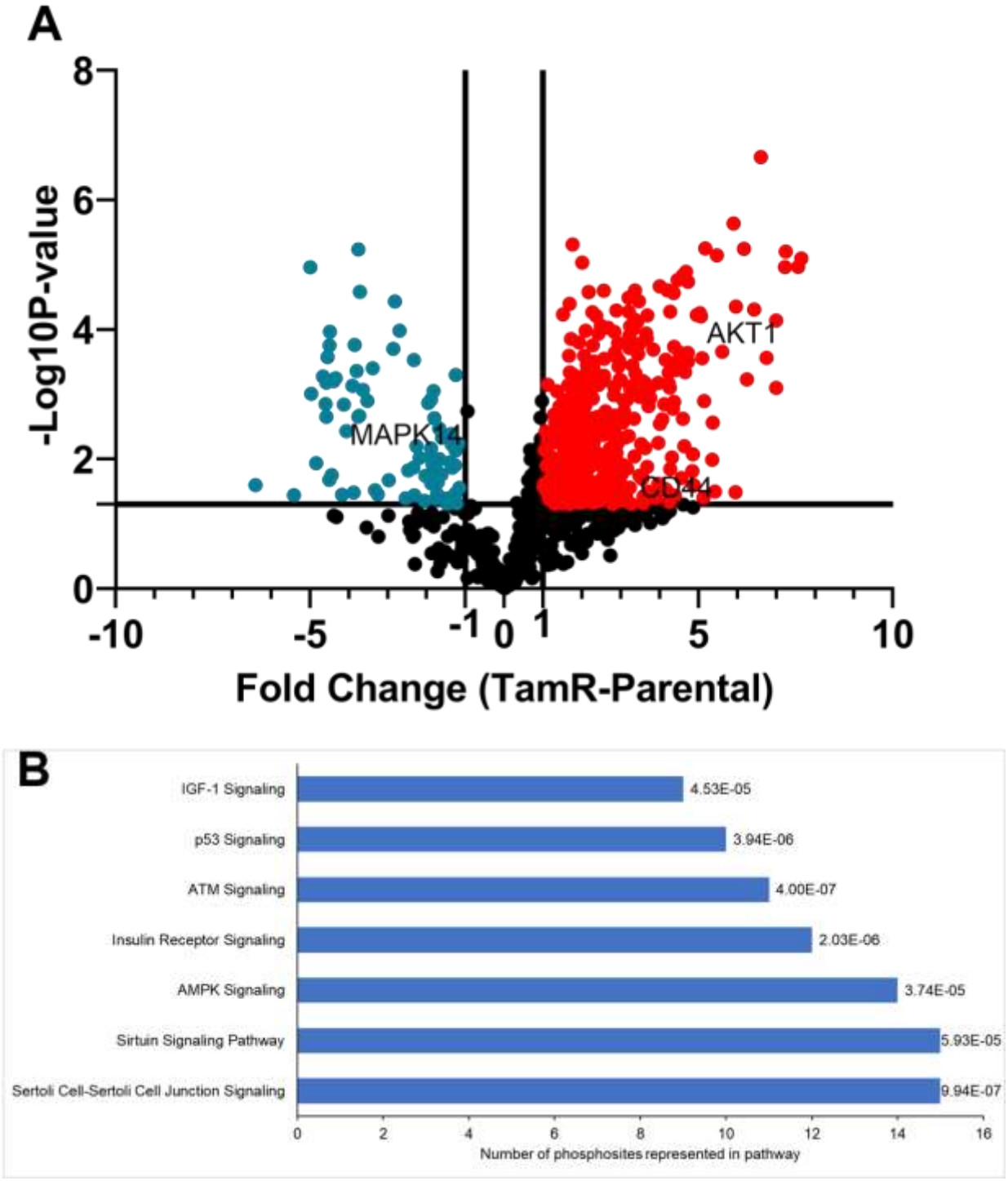

Figure 4.18. Fold-change and pathway analyses of phosphoproteomics data comparing the phosphopeptides quantified in TamR cells vs their Parental counterpart. **A)** Volcano plot depicting hyper and hypophosphorylated peptides in TamR vs Parental. ($p<0.05$, n=3) **B)** Top signaling pathways overrepresented in pathway enrichment analysis of the hyper and hypophosphorylated peptides represented in **A)**.

4.7.3 Identification of pTyr phosphosites differentially hypo/hyperphosphorylated when BRK is knocked down in TamR

Having identified targets involved in TamR, changes in these targets when BRK was knocked down in T47D TamR cells were analyzed. Using the fold change and p value cutoffs defined in section 4.7.2, significantly hyper/hypophosphorylated peptides were filtered, with a focus on targets already identified as being differentially regulated in TamR. Of the 14 pTyr peptides identified after filtering, p38 (MAPK14) was found to be hyperphosphorylated in TamR BRK KD cells, which once again corroborates findings in Figs. 4.3 and 4.15 and a previous study (Ito *et al.*, 2017). In line with the conclusions drawn by Ito *et al.*, it is possible that BRK knockdown in this cell lines induces apoptosis through the hyperphosphorylation of p38 MAPK when treated with Tamoxifen, thereby restoring sensitivity (Ito *et al.*, 2017). Unlike in the comparison between T47D TamR and parental cells, CDK1/2 was not found. AKT1 S124 and CD44 S706 were both hypophosphorylated (implying inhibition of activity) when BRK was knocked down, implying a reduction in AKT pathway activation. This finding reiterates the inhibition of IRS1 when BRK is knocked down in TamR, resulting in the relative inhibition of the AKT pathway.

Pathway analysis of differentially phosphorylated targets in T47D TamR BRK KD revealed the dysregulation of insulin receptor signaling which corroborates our experiments on IRS1 activity and functioning (section 4.6). Furthermore, the enrichment of this pathway in both T47D TamR cells and T47D TamR BRK KD cells indicates the importance of the pathway and its disruption to TamR and restoring sensitivity to TamR upon BRK KD.

Table 4.4 Significantly hyper/hypophosphorylated pTyr peptides found in the phosphoproteomics comparison of T47D TamR BRK KD vs T47D TamR cells. FC>1 and FC<-1 were considered significant with $p<0.05$.

Phosphorylation status	Uniprot Name	Protein Description	pvalue	Fold Change	Peptide	Phosphosite
Significantly Hyper-phosphorylated	MAPK3	mitogen-activated protein kinase 3	0.000559435	2.047200064	RIADPEHDHTGFLTEYVATRWYRAPEIMLNS	Y204
	PGAM1	phosphoglycerate mutase 1	0.014520552	2.018688828	MWLPVVRTWRLNERHYGGLTGLNKAETAAKH	Y92
	ATP8B1	ATPase phospholipid transporting 8B1	0.004799647	1.971187413	VSTRRSAYAFSHQRGYADLISSGRSIRKKRS	Y1217
	MAPK1	mitogen-activated protein kinase 1	0.011164164	1.93104769	RVADPDHDHTGFLTEYVATRWYRAPEIMLNS	Y187
	PTPN11	protein tyrosine phosphatase non-receptor type 11	0.027141565	1.898836623	RNGAVTHIKIQNTGDYYDLYGGEKFATLAEL	Y62
	CLDN3	claudin 3	0.001731505	1.841117183	SCPPREKKYTATKVVYSAPRSTGPGASLGTG	Y198
	MAPK14	mitogen-activated protein kinase 14	0.017363163	1.784491807	LDFGLARHTDDEMTGYVATRWYRAPEIMLNW	Y182
	ALDOA	aldolase, fructose-bisphosphate A	0.014855488	1.76308238	PEILPDGDHDLKRCQYVTEKVLAAVYKALSD	Y204
	SERINC5	serine incorporator 5	0.019522417	1.729444275	LTSTTRSSSDALQGRYAAPELEIARCCFCFS	Y345
	MGP	matrix Gla protein	0.002399721	1.57676244	ELNREACDDYRLCERYAMVYGYNAAYNRYFR	Y82
Significantly Hypo-phosphorylated	CASKIN2	CASK interacting protein 2	0.007122306	-1.67290809	RLLLEGGVDVNIRNTYNQTALDIVNQFTTSQ	Y253
	ITSN2	intersectin 2	0.059437881	-1.82222321	IIPGSEVKREEPEALYAAVNKKPTSAAYSVG	Y968
	PKP4	plakophilin 4	0.005105368	-2.07293536	STDYSTQYGLKSTTNYVDFYSTKRPSYRAEQ	Y1168
	PARD3	par-3 family cell polarity regulator	0.002749129	-2.10762893	AKTREFRERQARERDYAEIQDFHRTFGCDDE	Y1080

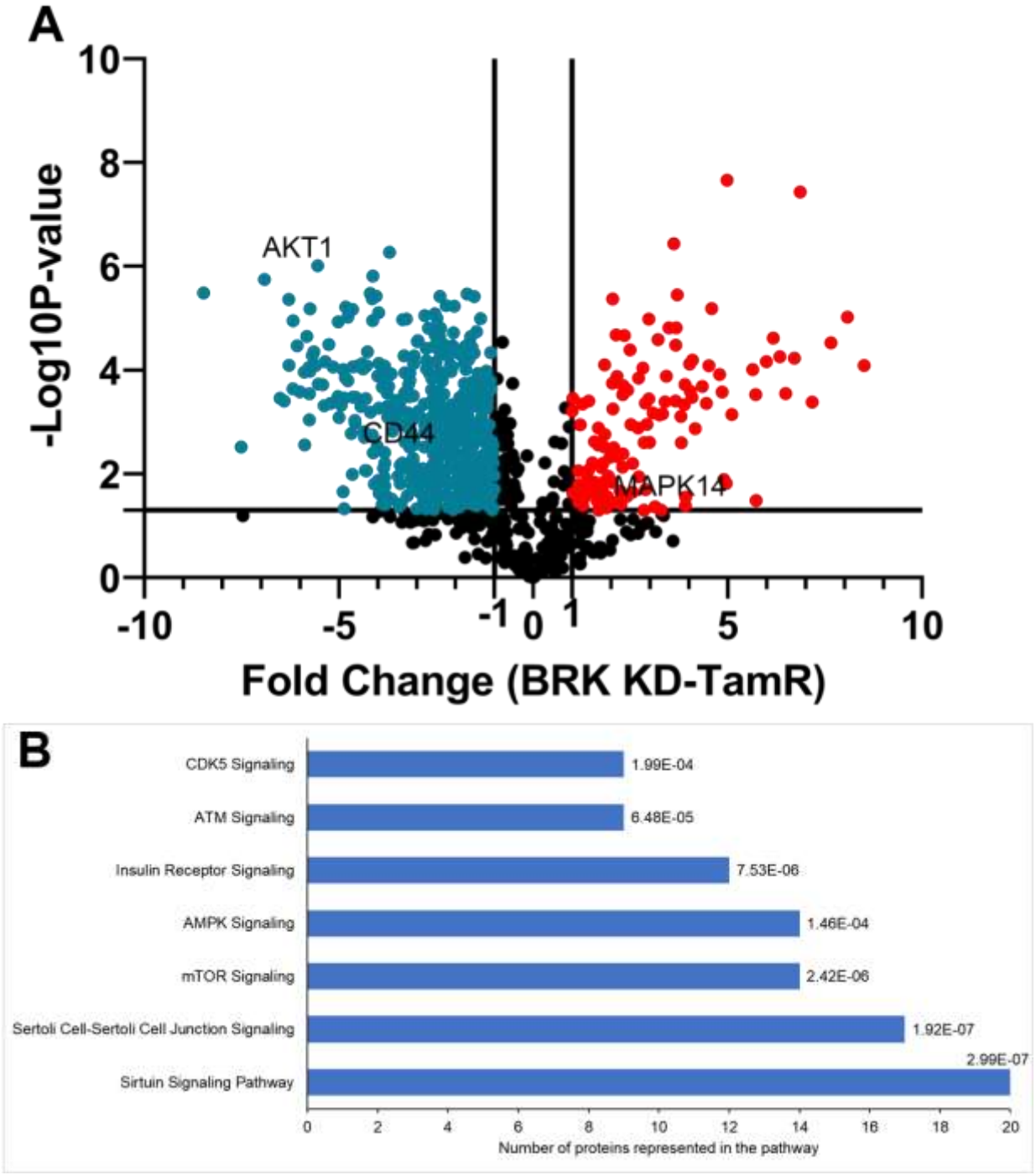

Figure 4.19. Fold-change and pathway analyses of phosphoproteomics data comparing the phosphopeptides quantified in TamR BRK KD cells vs their TamR counterpart. **A)** Volcano plot depicting differentially hyper and hypophosphorylated peptides in TamR BRK KD vs TamR cells ($p<0.05$, n=3). **B)** Top signaling pathways overrepresented in pathway enrichment analysis of the hyper and hypophosphorylated peptides represented in **A)**.

4.7.4 Total proteomics analysis combined with phosphotyrosine proteomics analysis workflow

Total proteomics analysis was also conducted to identify the effect of BRK knockdown on protein expression. Additionally, total proteomics analysis allows us to combine phosphoproteomics analysis with total peptide abundance to yield the relative phosphorylation of a given site as a function of total protein analyzed through MS (Fig. 4.20). Cell lysates generated previously (section 4.7.1) were used for total proteomics analysis, with 1 mg starting material per cell line. The workflow for sample preparation remained the same as before (section 4.7.1) with respect to reduction, alkylation, and digestion of the proteins in the lysates to the peptides required for MS analysis.

Overall, 3966 proteins were analyzed for significantly up and downregulated proteins in TamR vs Parental and TamR BRK KD vs TamR cells (Figs 4.21 and 4.22). Significant changes (denoted by the black curves in Figs 4.21a and 4.22b) were determined using the program Perseus by setting a p value of 0.05 with significant fold changes being set by Perseus' normalization algorithm (Tyanova and Cox, 2018).

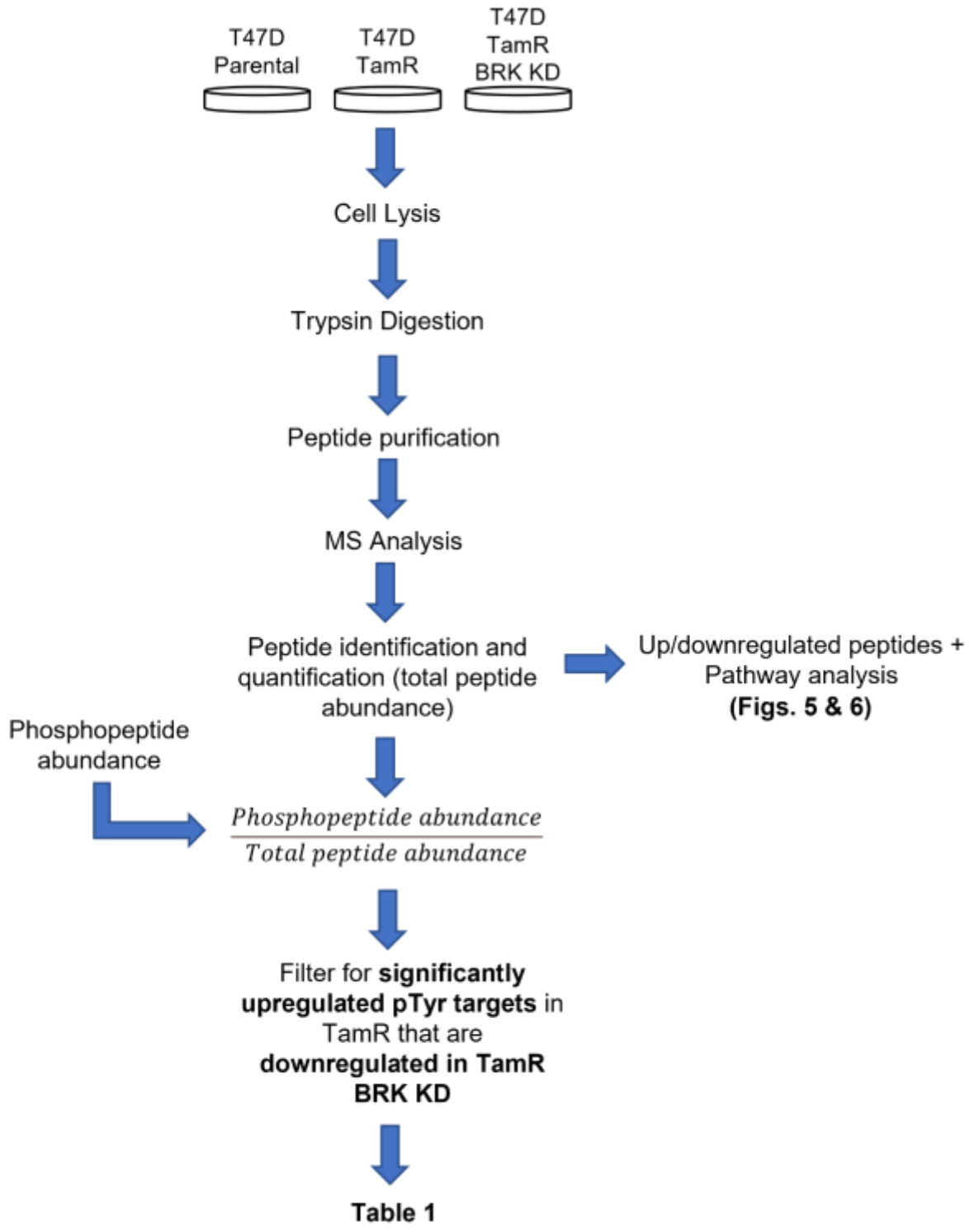

Figure 4.20. Workflow of label-free quantitative proteomics analysis, including the combining of proteomics and phosphoproteomics analyses to yield relative phosphorylation analysis downstream.

4.7.5 Identification of differentially expressed proteins in TamR vs Parental T47D cells

Changes in total protein expression can drive the development and maintenance of Tamoxifen resistance, therefore the analysis of differentially expressed proteins in TamR would elucidate pathways and regulatory mechanisms that are dysregulated when resistance is developed (Rani *et al.*, 2019).

Of the numerous proteins identified as significantly up-regulated in TamR vs parental T47D cells, 23 proteins were found to be involved in PDGFR (Platelet-derived growth factor receptor)-beta signaling (Fig. 4.21B). A recent publication revealed that the inhibition of PDGFR signaling resensitized TamR breast cancer cells to the drug, displaying the importance of the pathway to Tamoxifen resistance (Kim *et al.*, 2021). The proteins identified as a part of this pathway in this dataset include GRB2 (Growth factor receptor-bound protein 2), an adaptor protein involved in EGFR signaling which itself drives Tamoxifen resistance (Rani *et al.*, 2019). A second protein, BCAR1 (breast cancer antiestrogen resistance 1), was upregulated in TamR cells, which corroborates previous experimental findings (Kumbrink and Kirsch, 2012). Finally, increased expression of ABL1 was found in this dataset and the tyrosine kinase is involved in the enhancement of resistance to Tamoxifen (Zhao *et al.*, 2010).

Interestingly, the pathway involving the targets of c-myc transcriptional activation was also enriched in TamR cells compared to parental cells (Fig. 4.21B). The involvement of this pathway in the upregulation of proteins in TamR is consistent with c-myc's contributions to Tamoxifen resistance (Chen *et al.*, 2020). Additionally, the representation of c-myc targets in upregulated TamR pathways is consistent with the possible IRS1-directed increase in c-myc transcription shown in the results detailed in section 4.6.7. Of the c-myc targets enriched in this pathway, the overexpression of TP53 has been previously associated with conferring Tamoxifen resistance, albeit this is only prevalent in cases where TP53 is mutated (Grote *et al.*, 2021).

Overall, these findings indicate the importance of both c-myc transcriptional activation and PDGFR to Tamoxifen resistance. PDGFR is an alternative growth factor receptor pathway that drives Tamoxifen resistance as it has not been targeted using therapies (Kim *et al.*, 2021). Our results indicate that targeting it may be effective in combating TamR breast tumours.

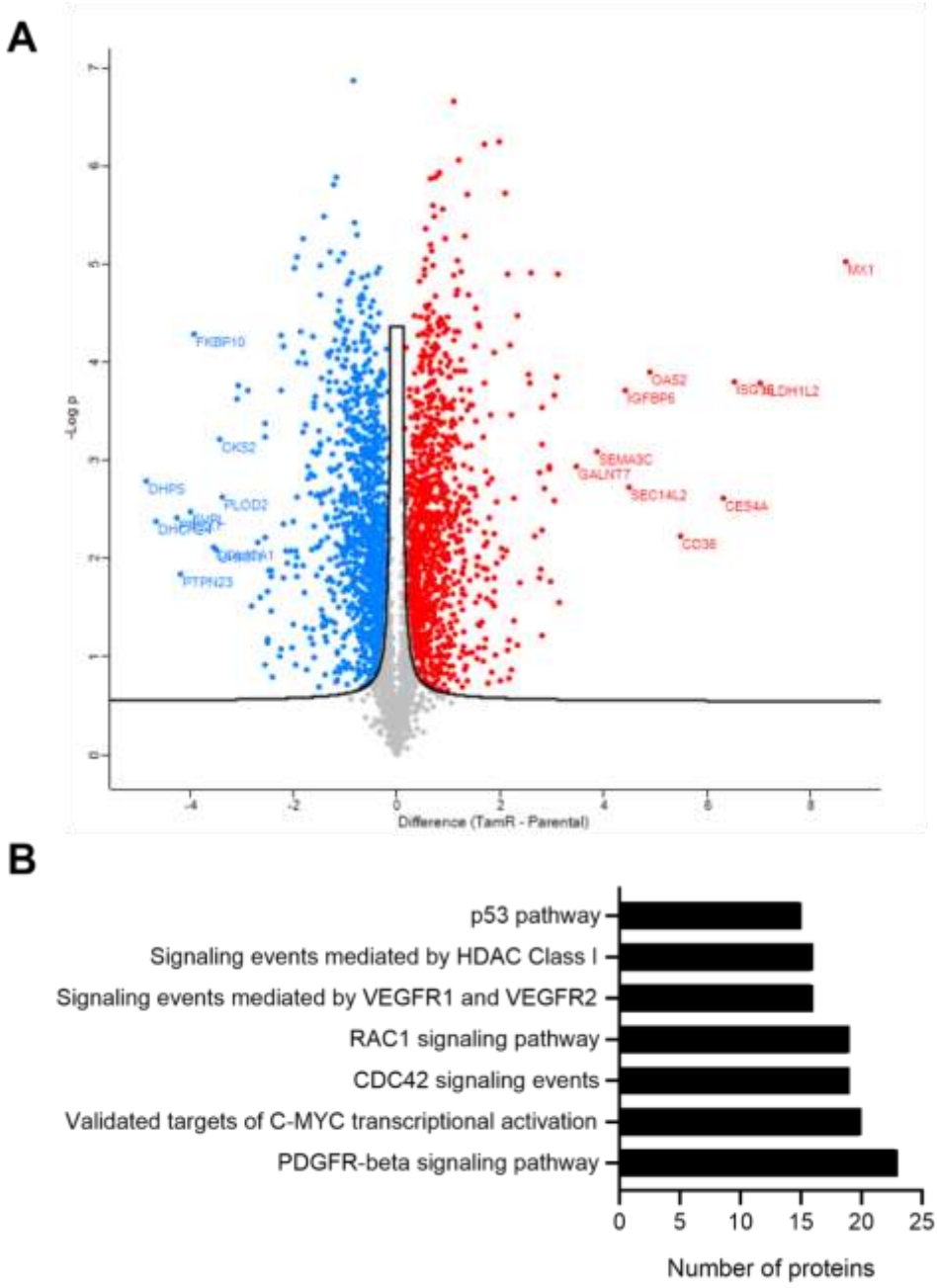

Figure 4.21. Fold-change and pathway analyses of T47D TamR vs Parental proteomics data. **A)** Volcano plot is depicted with the fold change of each protein versus the negative log of p value which was calculated through a student's t-test (n=3, $p < 0.05$). Labeled data points are top 10 up/downregulated proteins in TamR vs Parental. Data points above the black curves are determined as significant. Curve limits are determined through statistical analysis using Perseus software. **B)** Top signaling pathways identified from pathway enrichment analysis of the upregulated proteins in the T47D TamR cells.

4.7.6 Identification of differentially expressed proteins when BRK is knocked down in TamR T47D cells

BRK knockdown may drive protein downregulation downstream of its kinase activity, which in turn may resensitize TamR cell lines to the therapy. To investigate this, downregulated proteins identified in the comparison between T47D TamR BRK KD and T47D TamR cell lines were analyzed for pathways overrepresented.

PDGFR-beta signaling was found to be downregulated overall because of BRK knockdown. A total of 17 proteins associated with this pathway were identified in our dataset (Fig. 4.22B). In fact, the 3 targets described in the previous section, BCAR1, GRB2 and ABL1 were all reduced in expression when BRK was knocked down in TamR. The association between BRK and the PDGFR pathway, including its association with the 3 proteins mentioned above, has not been characterized. However, I can hypothesize that because BRK is involved in the activation of EGFR and prevention of its degradation and turnover, BRK knockdown would increase EGFR turnover and GRB2 downregulation, as it is an EGFR adaptor protein (Li *et al.*, 2012). Thus, BRK may contribute to Tamoxifen resistance by either directly or indirectly affecting the expression of proteins involved in PDGFR signaling, thereby bypassing Tamoxifen's effects through growth factor signaling.

Validated targets of c-myc transcriptional activation were also overrepresented in the pathway analysis (Fig. 4.22B). The downregulation of this pathway is consistent with the reduction of c-myc transcription with both BRK knockdown and inhibition in an IRS1-mediated manner. Since overexpression of TP53, a target of c-myc transcription activation, has been shown to confer resistance, it is reasonable to assume that the reduction in TP53 levels may contribute to the restoration of Tamoxifen sensitivity (Grote *et al.*, 2021).

Our results imply that BRK contributes to tamoxifen resistance by regulating PDGFR signaling as well as c-myc transcriptional activation, possibly through its action on IRS1. It follows, therefore, that BRK inhibition could be a powerful tool to combat Tamoxifen resistance as the potential therapy could affect various important signaling pathways.

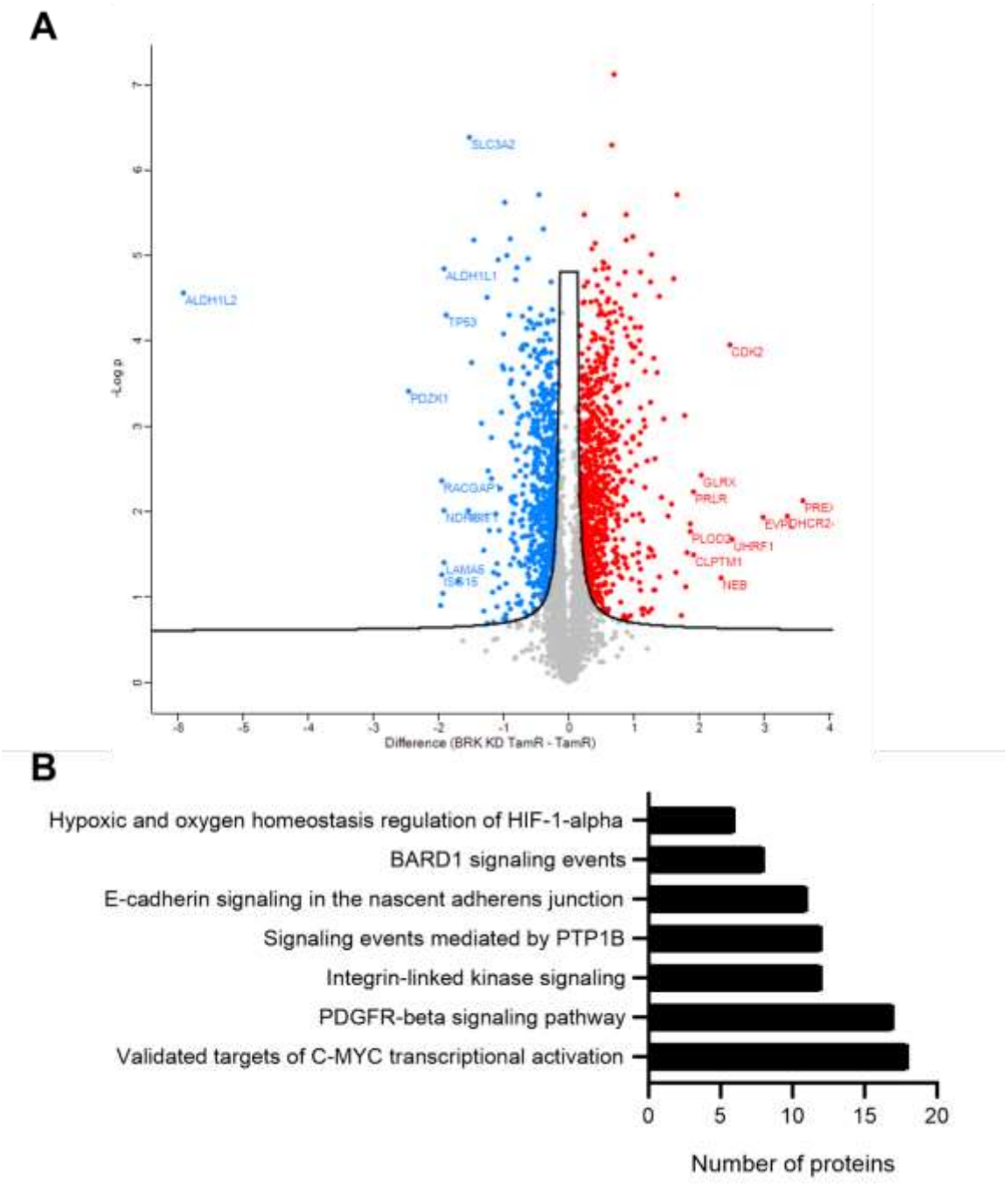

Figure 4.22. Fold-change and pathway analyses of T47D TamR BRK KD vs TamR proteomics data. **A)** Volcano plot is depicted with the fold change of each protein versus the negative log of p value which was calculated through a student's t-test (n=3, $p < 0.05$). Labeled data points are top 10 up/downregulated proteins in TamR BRK KD vs TamR. Data points above the black curves are determined as significant. Curve limits are determined through statistical analysis using Perseus software. **B)** Top signaling pathways identified from pathway enrichment analysis of the downregulated proteins in the T47D TamR cells.

4.7.7 Analysis of phosphopeptide vs total peptide abundance using phosphoproteomics and proteomics data (phospho/total analysis)

When investigating differential phosphorylation of proteins, it is important to take total protein expression into account as it affects the relative activity of a given kinase or protein in general (Singh *et al.*, 2017). For example, it is possible for a phosphosite to appear hypophosphorylated simply because of low protein expression which reduces the number of peptides of that protein that may enter MS analysis. This may not be captured in phosphoproteomics analysis without concurrent proteomics analysis. Therefore, after having narrowed down and determined potential BRK specific, differentially regulated pTyr targets through phosphoproteomics analysis, it was important to combine this with the total proteomics analysis obtained at the same time. The proteins identified through the above analysis were matched with their corresponding phosphopeptides in the phosphoproteomics analysis conducted previously, with a focus on pTyr phosphopeptides as modification in these sites may be a direct result of BRK activity. Matched phospho and total peptide pairs of intensities (measure of peptide abundance) were then divided to yield phospho over total intensity in all 3 cell lines (Parental, TamR and TamR BRK KD). A log2 function was applied to all intensities and then comparisons were made between TamR vs Parental and TamR BRK KD vs TamR by subtracting log2 (phospho/total intensity) of the conditions being compared (summarized in Fig. 4.20).

4.7.8 Relative activity analysis reveals possible BRK targets affected by TamR and BRK knockdown in TamR

Of the 118 pTyr peptides identified, 42 were matched with their corresponding total protein abundances. Of these, I sought to specifically find targets that were significantly hyperphosphorylated in TamR and significantly hypophosphorylated when BRK was knocked down in TamR as this trend would be an indication of BRK's possible action on the target at the pTyr phosphosite in question. A total of 3 such candidates were found (Table 4.5).

CDK1 (Cyclin-Dependent Kinase 1) was found to be hyperphosphorylated at its Y15 phosphosite in TamR (1.5820 fold-change, $p<0.05$) while these sites were hypophosphorylated when BRK was knocked down (-1.5729 fold-change, $p<0.05$). This is interesting as the phosphoproteomics

analysis alone indicated that Y15 was hypophosphorylated in TamR. However, the proteomics analysis revealed that the observation of hypophosphorylation was a result of reduced overall CDK1 expression in TamR. This observation highlights the importance of considering total protein levels when interpreting phosphorylation data. While these tyrosine sites are inhibitory, their phosphorylation has been shown to result in the induction of cell growth and tumourigenesis recently, though this effect may be highly context-dependent and therefore bears further investigation in the TamR context (Wang *et al.*, 2015).

Delta catenin-1 was identified as hypophosphorylated at the uncharacterized Y904 site when BRK was knocked down while being hyperphosphorylated in TamR. The protein may be significant in promoting breast cancer malignancy as described previously (Zhang *et al.*, 2015). In a phosphoproteomics analysis of Src substrates in mammary epithelial cells stimulated with Colony Stimulating Factor (CSF), the Y904 site was reported as being a potential Src substrate (Knowlton *et al.*, 2010). As Src and BRK do share similarities in substrates and targets, it is possible that BRK regulates the phosphorylation of the Y904 site on delta canenin-1 which may be important to the maintenance of Tamoxifen resistance.

Finally, both GSK3-alpha (Glycogen synthase kinase-3) was found to be hypophosphorylated at its active site Y279, when BRK was knocked down in TamR cells. The hyperphosphorylation of the site has been shown to induce cell growth and overall, GSK3 expression has been associated with conferral of drug resistance, making it an excellent candidate for investigation on its interaction with BRK in TamR (Duda *et al.*, 2020). Furthermore, GSK3 is linked to insulin receptor signaling through IRS1-PI3K-AKT signaling (Duda *et al.*, 2020). It should be noted, however, that traditionally, AKT activation results in GSK3 inhibition while other studies have shown that GSK3 has both tumour promoter and tumour suppressor activity in breast cancer (Duda *et al.*, 2020). Like CDK1 phosphorylation, if BRK does interact with GSK3, the effect of the interaction will likely be highly context dependent and will require extensive characterization.

Table 4.5. Significantly hyper/hypophosphorylated phosphopeptides were matched with their corresponding total peptide abundances.

Targets that are affected by BRK KD in TamR (hyperphosphorylated in TamR, hypophosphorylated in TamR BRK KD)								
Protein Name	Description	Phosphosite(s) identified	Effect of site on modified protein	Effect of site on biological process	Adjusted Fold Change (TamR BRK KD vs TamR)	p-value (TamR BRK KD vs TamR)	Adjusted Fold change(TamR vs Parental)	p-value (TamR vs Parental)
CDK1	Cyclin-dependent kinase 1	Y15	Inhibition	Cell growth induced	-1.5729	0.0021	1.5820	0.0029
CTNND1	Catenin delta-1	Y904	Uncharacterized		-1.0684	0.0083	0.6786	0.0455
GSK3A	Glycogen synthase kinase-3 alpha	Y279	Activation	Cell growth induced	-1.9163	0.0074	2.5140	0.0037

Following this match, relative phosphorylation was calculated by dividing phosphopeptide abundance with total peptide abundance. Finally, relative fold change between the respective cell lines was calculated ($p<0.05$, $n=3$). Targets were only chosen if they were hyperphosphorylated in TamR and hypophosphorylated when BRK was knocked down in TamR. "Effect of the site on protein function" (activation/inhibition) and "Effect of site on biological process" were obtained through the PhosphospitePlus database (https://www.phosphosite.org/homeAction.action).

4.8 Validation of BRK-specific targets in TamR

4.8.1 BRK knockdown reduces CDK1 Y15 and δ-catenin Y904 phosphorylation

Having identified potential targets of BRK phosphorylation in Tamoxifen resistant T47D cells, validation became necessary to ensure that these phosphorylation changes were reproducible *in vitro*. Therefore, western blotting analysis was conducted using phospho-specific antibodies against CDK1 Y15, delta catenin-1 Y904 and glycogen synthase kinase-3 alpha Y279.

The results in Fig. 4.23A show that the phosphorylation of CDK1 at Y15 is reduced in TamR and is further reduced when BRK is knocked down. However, CDK1 protein levels are themselves reduced in TamR, thereby accounting for the reduction of CDK1 Y15 levels. This reduction in total CDK1 levels in TamR is sustained when BRK is knocked down, implying that BRK knockdown does not necessarily affect total CDK1 levels but may play a role in reducing CDK1 Y15 phosphorylation (Fig. 4.23A). The magnitude of these changes, when quantified, agree with the phospho over total protein calculations inferred from the MS analyses (Fig. 4.23B).

Similarly, delta catenin-1 Y904 follows the trend of being hyperphosphorylated in TamR while being hypophosphorylated when BRK is knocked down in TamR cells (Fig. 4.23A). Interestingly,

the magnitude of the differential phosphorylation observed in delta catenin-1 was significantly higher than that observed in the phospho/total proteomics analyses (Fig. 4.23B). This may be a result of the loss of delta catenin-1 peptides during MS sample preparation.

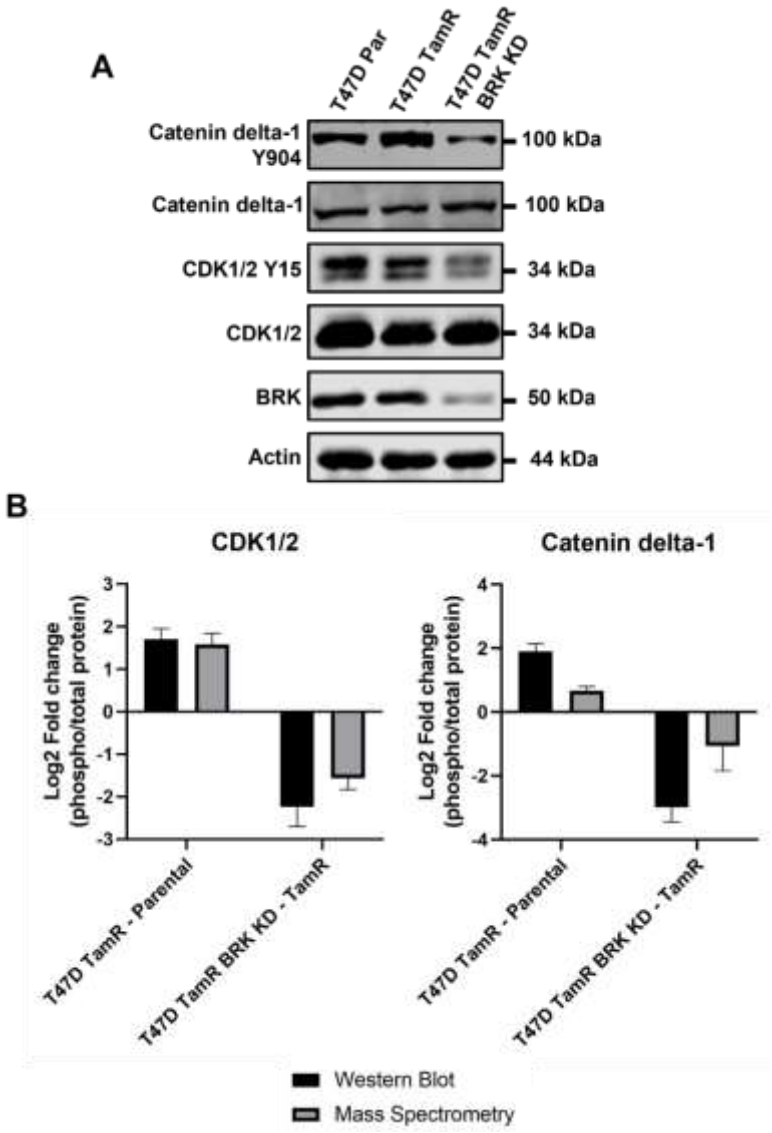

Figure 4.23. Validation of CDK1 and catenin delta-1 as targets affected by BRK knockdown in TamR. **A)** Western blot analysis of CDK1 phosphorylation at the Y15 site and total CDK1/2, catenin delta-1 and phosphocatenin delta-1 at Y904 reveals hypophosphorylation of these proteins when BRK is knocked down in T47D TamR cells. **B)** Quantification of the Western blots in a. Both phospho and total protein levels were normalized to actin to control for differences in loading. Relative phosphorylation levels were then calculated by dividing phosphoprotein abundance with total protein abundance (n=3). Western blot quantifications were compared with quantified phosphopeptide/total peptide values obtained through mass spectrometry (n=3).

Having validated that BRK knockdown did indeed result in the observed hyper and hypophosphorylation of the targets tested, I next queried whether there was a direct interaction between BRK and either CDK1 or delta catenin-1 by conducting immunoprecipitation of BRK and detecting the presence or absence of these potential interactors. These findings indicate that while BRK does influence CDK1 and delta catenin-1 phosphorylation, it may not directly interact with these proteins and may require intermediary factors to mediate this intereaction.

GSK3-alpha could not be detected in these cell lines and has therefore been excluded from investigation. This may be due to primary antibody deficiencies or due to the context specific nature of GSK3-alpha activity.

4.9 Model of the proposed mechanism of action of BRK in Tamoxifen resistant breast cancer through IGFR/Insulin receptor signaling

To summarize the findings of the present work, the ability of BRK to perform multiple functions within the insulin/IGFR signaling pathway can be considered as the pathway can help connect the diverse actions of BRK discovered through these results. To aid the construction of a model that could consolidate the results in this thesis, the protein-protein interaction database STRING-DB (www.string-db.org) was queried with the targets of BRK found in the results described so far (Szklarczyk *et al.*, 2020). Namely, BRK, delta catenin-1, CDK1, STAT3 and IRS1 were entered into the database to generate a possible interaction network. The network of potential interactions thus obtained was combined with experimental data from this work to generate the provisional model for the action of BRK in Tamoxifen resistance through the IGF1R/insulin receptor signaling pathway (Fig. 4.24). BRK drives Tamoxifen resistance by regulating intermediaries downstream of growth factor receptor activation, thereby bypassing Tamoxifen's growth inhibitory effects by mediating estrogen-independent signaling. Amongst these intermediaries are 1) IRS1, through which BRK can indirectly regulate cyclin D1 expression which itself regulates cell division and proliferation, 2) STAT3, through which BRK regulates CDK1 and therefore the cell cycle, allowing TamR cells to circumvent the growth arrest caused by Tamoxifen 3) AKT, through which BRK can potentially regulate delta catenin-1 through E-cadherin regulation which has been shown to drive epithelial to mesenchymal transition and may drive chemoresistance or TamR in this case (Soto *et al.*, 2008).

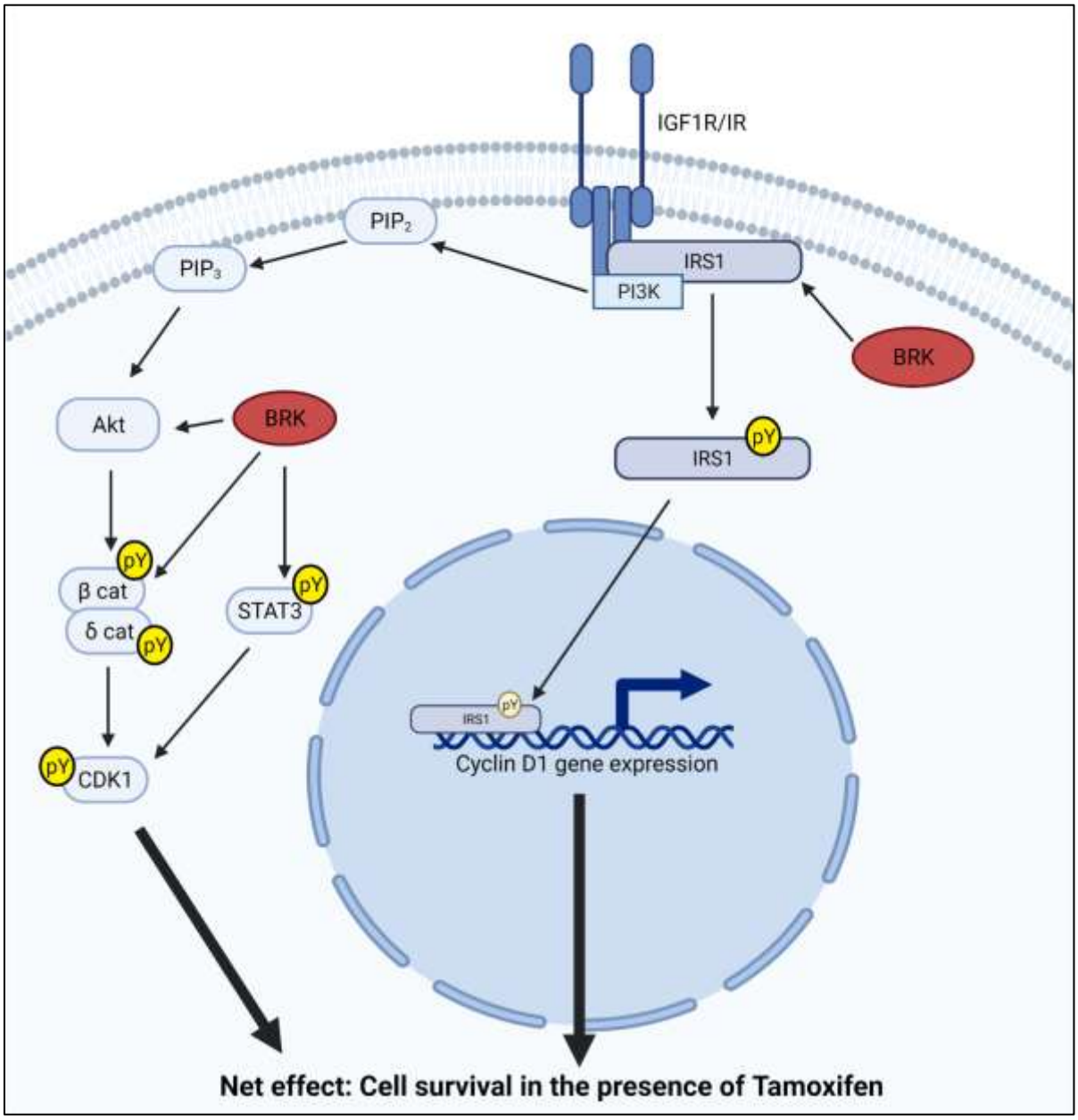

Figure 4.24. Potential model for the mechanism of action of BRK in TamR through its regulation of the IGFR/insulin signaling pathway and signaling intermediaries downstream.

5.0 GENERAL DISCUSSION

5.1 Conclusions

Tamoxifen resistance in breast cancer cases can be driven by estrogen-independent signaling mechanisms, mediated by growth factor receptor signaling stimulated by growth factors ((Rani *et al.*, 2019). Targeting receptor tyrosine kinases, such as IGFR, EGFR and HER2 that regulate this process has not yielded successful clinical results in terms of restoring Tamoxifen sensitivity in these tumours (Hanker *et al.*, 2020). As a non-receptor tyrosine kinase, BRK acts as an intermediary between growth factor receptor activation and the activation of downstream signaling effector proteins such as AKT, MAP kinases such as ERK1/2, and regulators of gene transcription such as STAT3 (Ang *et al.*, 2021). Therefore, it is reasonable that BRK would play a role in conferring drug resistance against Tamoxifen by regulating growth factor signaling, particularly through the insulin or IGFR signaling pathways (which share many effectors and intermediaries) which was elucidated in this work.

I conducted phosphoproteomics analysis comparing MCF7 Parental vs TamR cells and T47D TamR vs T47D TamR BRK KD cells to find differentially phosphorylated targets in TamR and the effect of BRK KD on these targets. Through this analysis, I found that IRS1 S1101, an inhibitory phosphosite, was hypophosphorylated in MCF7 TamR cells but hyperphosphorylated in T47D TamR BRK KD cells. I corroborated these findings in the T47D cells and quantitatively compared the differences in the expression of IRS1 S1101 between the two experiments (mass spectrometry and western blot). IRS1 S1101 was indeed hypophosphorylated in T47D TamR cells vs Parental and hyperphosphorylated in TamR BRK KD cells vs TamR cells. The S1101 site has previously been associated with downregulation of insulin receptor signaling (Li *et al.*, 2004). The inhibition of the protein by phosphorylation at this site after BRK knockdown suggests the inhibition of IGF1R and insulin receptor signaling pathways, both of which have previously been implicated in tamoxifen-resistance and anti-ER therapy resistance in general (Mills *et al.*, 2018).

Taken together with the co-immunoprecipitation of BRK and IRS1, these results lead to the hypothesis that BRK regulates tamoxifen resistance through its interaction with IRS1 and, by extension, its effect on IGF1R and insulin receptor signaling. Additionally, BRK may play a role

in the stimulation of cell proliferation by IRS1, through PI3K and MAPK signaling in TamR cells and the reduction in cell proliferation upon BRK knockdown and inhibition may be partially due to the subsequent inhibition of IRS1 functioning. The inhibition of BRK using Tilfrinib did result in the inhibition of IRS1 through the hyperphosphorylation of the S1101 site, supporting the suggestion that BRK activity was necessary for the disinhibition of IRS1 but not for direct interaction with the protein as BRK-IRS1 coimmunoprecipitation was unaffected. This may be explained by the necessity of the SH2 and SH3 domains of BRK for direct interaction with its target and because Tilfrinib targets the kinase domain and not these domains, direct interaction between BRK and IRS1 is not affected by BRK inhibition. Additionally, BRK knockdown also affected the Y896 site on IRS1, which is involved in the increased activity of IRS1 as well as Grb2 binding (Knowlden *et al.*, 2008). As per the model proposed in Fig. 4.24, I hypothesize that BRK directly phosphorylates and activates IRS1 at this site. The site was discovered to be important not only to the conferral of resistance against the anti-EGFR therapy Gelfitinib, but also to the IGF1R-driven conferral of TamR (Knowlden *et al.*, 2008). The phosphorylation of Y896 also drives MAPK signaling, which further validates the model described in Fig. 4.24 wherein BRK's primary function in TamR is to drive signaling cascades downstream of the IGFR/IR (Knowlden *et al.*, 2008).

RTPCR analyses showed that the stimulation of T47D parental cells with insulin (8 µg/mL) was sufficient to induce cyclin D1 and c-myc gene transcription. These genes were chosen as functional readouts of IRS1-mediated gene regulation based on a previous literature (Dearth *et al.*, 2006; Lai *et al.*, 2001; Mawson *et al.*, 2005). Additionally, these genes are important in the regulation of cell proliferation in tamoxifen-resistant cells as cyclin D1 was found to be necessary for TamR cell proliferation and increased expression of c-myc was demonstrated to play a role in cell proliferation (Chen *et al.*, 2020; Kilker and Planas-Silva, 2006). Having established that insulin-mediated stimulation of IRS1 increased cyclin D1 and c-myc transcription, I then assessed the effect of BRK knockdown and inhibition on the mRNA levels of these genes. Both cyclin D1 and c-myc mRNA expression was reduced both when BRK was knocked down and when BRK was inhibited by Tilfrinib. Following the principle that c-myc and cyclin D1 gene transcription functions as a readout of IRS1 activity, the result lends further support to the hypothesis that BRK-IRS1 interaction leads to increased cell proliferation in TamR cells through IRS1-mediated cyclin

D1 gene transcription, among other pathways. Furthermore, ChIP qPCR analysis revealed that IRS1 did indeed localize to the promoter region of cyclin D1, though I was not able to find IRS1 at the promoter site of c-myc. The lack of IRS1 localization to the c-myc promoter region after BRK knockdown and inhibition in T47D TamR cells may indicate an alternative regulatory mechanism for c-myc expression which is independent of BRK-IRS1 interaction. Notably, however, c-myc mRNA was found to be significantly increased in T47D TamR vs T47D Parental cells. This result corroborates previous studies that have indicated that c-myc expression is important to TamR (Chen *et al.*, 2020). Assaying c-myc protein expression in these cell lines may further elucidate these trends.

The identification of STY phosphosites in T47D Parental, TamR and TamR BRK KD cells through high throughput phosphoproteomics analysis revealed key pathways and potential substrates involved in Tamoxifen resistance and affected by BRK knockdown. By combining TiO_2 enrichment of pSTY sites with pY-specific enrichment, I was able to find 118 pY phosphosites and 3739 pST sites across the 3 cell lines and their biological replicates (n=3). By contrast, the TiO_2 enrichment approach alone did not yield any pY peptide enrichment. One of the crucial tyrosine phosphosites identified was that of the p38MAPK Y182 site. p38MAPK was found to be hypophosphorylated in TamR vs Parental cells and hyperphosphorylated when BRK was knocked down in TamR cells. Functionally, Ito and colleagues have shown that the hyperphosphorylation of this site upon BRK knockdown was crucial for BRK-mediated apoptosis in both MCF7 and T47D TamR cells in the presence of Tamoxifen (Ito *et al.*, 2017). While it has been hypothesized that p38 MAPK is a BRK substrate, the mechanisms by which BRK downregulation leads to p38 MAPK activation through increased Y182 phosphorylation remain unclear (Ito *et al.*, 2017; Ostrander *et al.*, 2007). Another substrate of BRK, AKT1 was found to be differentially phosphorylated at the S124 residue in the phosphoproteomics data. AKT1 was found to be hyperphosphorylated in TamR vs Parental cells while being hypophosphorylated when BRK was knocked down in TamR cells. The S124 phosphosite is associated with the induction of enzymatic activity (Bellacosa *et al.*, 1998). Functionally, the activation of AKT1 by BRK has been associated with prevention of anoikis in colon cancer cells and increase in cell proliferation as well as tumour growth (Riggio *et al.*, 2017; Zheng *et al.*, 2013). Taken together, the data suggests that BRK, through its regulation of AKT1, confers increased cell proliferation and prevents cell death in

TamR cells and that the knockdown of BRK abrogates these functions, resulting in resensitization of these cells to Tamoxifen.

By supplementing phosphoproteomics data with total proteomics analysis, I was able to determine the relative phosphorylation of potential BRK targets in TamR cells. Targets that were hyperphosphorylated on tyrosine residues in TamR but hypophosphorylated when BRK was knocked down were the focus of further analyses as these would be the most likely to be targeted by BRK's function as a tyrosine kinase. Three targets were thus identified, CDK1 Y15, delta catenin-1 Y904 and GSK3-alpha Y279.

CDK1 Y15 is a widely characterized site that is important to the functioning of CDK1 in cell cycle regulation as it is a kinase-inhibitory site (Malumbres, 2014). The phosphorylation of this site prevents cell cycle progression from the G2 to M phase by abrogating CDK1 recognition of its substrates, preventing their phosphorylation (Malumbres, 2014). Interestingly, increase in CDK1 Y15 phosphorylation has been shown to, 1) prevent Taxol-induced apoptosis in triple negative breast cancer cells, 2) contribute to drug resistance in osteosarcoma cell lines, and 3) contribute to to aggressive skin tumour development (Hu *et al.*, 2022; Tan *et al.*, 2002; Wang *et al.*, 2015). Therefore, it is possible that the inhibition of CDK1 through the phosphorylation of Y15 contributes to increased tumour growth and drug resistance.

The findings in this present thesis validate that CDK1 Y15 is indeed hyperphosphorylated in TamR cells and hypophosphorylated when BRK is knocked down (Figs. 4.23 and Table 4.5). The hyperphosphorylation of the inhibitory tyrosine in Tamoxifen resistant cells may contribute to the increased growth rate of these cells in the presence of Tamoxifen (Fig. 4.2 and 4.3). The knockdown of BRK in TamR cells reduces the phosphorylation of this site, thereby contributing to the relatively reduced growth in these cells in the presence of Tamoxifen. It is reasonable to conclude that CDK1 Y15 contributes to Tamoxifen resistance possibly by preventing apoptosis induced by the cytostatic effects of Tamoxifen. By combining phospho and total proteomics data, I accounted for changes in CDK1 total protein expression (CDK1 levels were reduced in TamR) and determined CDK1 relative kinase activity in TamR and TamR BRK KD models. In fact, considering the studies that have identified the inhibition of CDK1 as an important factor in

escaping apoptosis and inducing drug resistance, the reducing in total CDK1 protein levels in TamR may be vital to its mechanism of action in Tamoxifen resistance.

Having established that CDK1 Y15 phosphorylation is affected by BRK knockdown in TamR cells, I inquired whether BRK directly interacts with CDK1 and thereby drives phosphorylation of CDK1 at this site. While coimmunoprecipitation results showed no interaction between BRK and CDK1, it may be possible that an intermediary is required for the interaction between the two kinases. By entering these proteins into the protein-protein interaction database String-DB, I can speculate the possible intermediary for this interaction. According to String-DB, it is possible that BRK interacts with CDK1 through STAT3 (Fig. 4.24). STAT3 is a well characterized BRK substrate, which lends credence to this possibility (Liu *et al.*, 2006). Our results have also shown that BRK knockdown affects STAT3 activation through the hypophosphorylation of its Y702 site. Therefore it may be reasonable to hypothesize that BRK indirectly regulates CDK1 Y15 phosphorylation through its interaction with STAT3 and STAT3's interaction with CDK1 (Shi *et al.*, 2006).

By using phospho/total proteomics analysis, I also identified delta catenin-1 Y904 as a differentially phosphorylated site in TamR and when BRK is knocked down in TamR (Table 4.5 and Fig. 4.23). While the site has frequently been identified in other high throughput phosphoproteomics analyses, its importance to delta catenin-1 functioning has not been biochemically characterized (Knowlton *et al.*, 2010; Sharma *et al.*, 2014). Knowlton and colleagues determined that the site may be involved in the stabilization of E-cadherin and that phosphorylation of the site by SRC leads to reduced cell-cell adhesion in breast epithelial cells (Knowlton *et al.*, 2010). Their findings, taken together with the results presented in Table 4.5 and Fig. 4.23, present the possibility that Y904 phosphorylation of delta catenin-1 results in the dysregulation of E-cadherin which can then increase proliferation in TamR cells through the activation of MAP kinase signaling. Interestingly, as BRK is related to SRC, it may recognize the Y904 site on delta catenin-1 as well and may regulated its phosphorylation. However, I was not able to find a direct interaction between BRK and delta catenin-1 through immunoprecipitation analysis. The reduction of Y904 phosphorylation on delta catenin-1 still indicates a role for BRK in the regulation of the protein in TamR cells. By querying String-DB, a possible interaction

between AKT and delta catenin emerged. Upon further analysis, it is possible that this interaction may be a result of AKT regulation of β-catenin, another cell adhesion protein which controls cell proliferation and interacts directly with BRK (Palka-Hamblin *et al.*, 2010). β-catenin has also been implicated in driving Tamoxifen resistance as a study inhibiting its activity showed resensitization of TamR cells to the drug (Won *et al.*, 2016). It is therefore possible that the interaction between BRK and delta catenin-1 requires the intermediary β-catenin and through this, BRK controls Tamoxifen resistance in breast cancer cells. A recent study showed that the blockage of β-catenin/CDK1 signaling restored drug sensitivity in hepatocellular carcinoma xenografts that were resistant to the therapy sorafenib (Wu et al., 2018). Therefore, I can model a possible interaction between BRK, β-catenin, delta-catenin-1 and CDK1 which can contribute to drug resistance (Fig. 5.1). I can hypothesize that BRK contributes to Tamoxifen resistance by regulating the β-catenin, delta-catenin-1 pathway which itself plays a role in regulating CDK1 activity, thereby conferring cell survival in the presence of Tamoxifen (Fig. 5.1).

Finally, pathway analyses revealed the overrepresentation of IGF-1 and Insulin receptor signaling in both TamR vs Parental as well as TamR BRK KD vs TamR comparisons. This is congruent with the pathway analysis conducted in MCF7 Parental vs TamR and T47D TamR vs TamR BRK KD cells previously where these signaling pathways were also enriched. In finding these pathways in both datasets, I can be confident in continuing the investigation of the interaction of BRK and IRS1 and their role in Tamoxifen resistance as IRS1 is a crucial mediator of both IGF1 and Insulin receptor signaling (Rabiee et al., 2018).

As stated above, one of the most crucial ways in which breast tumours become resistant to Tamoxifen is through the activation of estrogen-independent growth factor signaling (Rani *et al.*, 2019). Through the results described in this thesis, it is clear that BRK contributes to TamR by regulating various downstream effectors such as CDK1, delta catenin-1, STAT3, p38 and IRS1 in growth factor signaling pathways, particularly the IGFR/Insulin receptor signaling pathways. Therefore, by targeting BRK, one can simultaneously combat several effector proteins whose regulation is often shared between various growth factor receptor signaling pathways. This effectively abrogates one of the major mechanisms driving Tamoxifen resistant breast cancer and therefore makes BRK a viable target for combatting TamR.

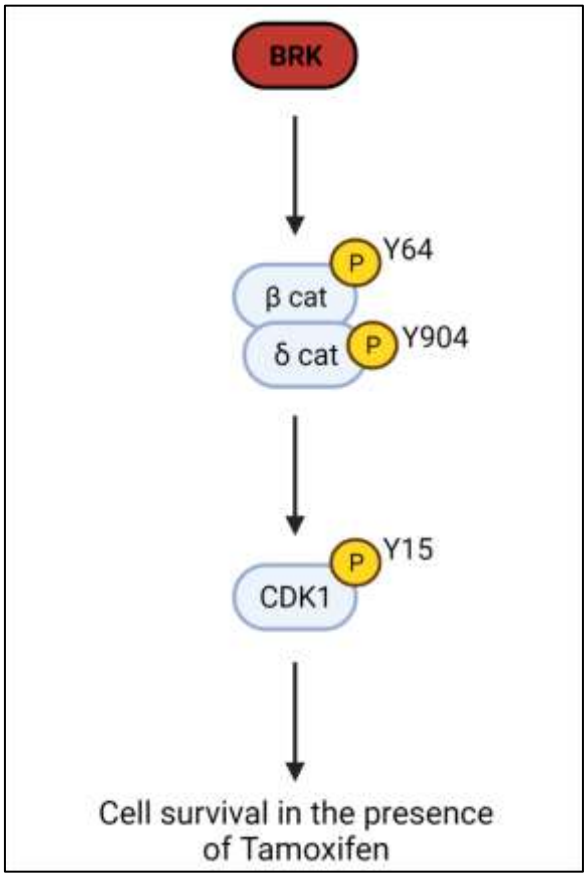

Figure 5.1. Model of BRK's mode of action in regulating Tamoxifen resistance by possibly controlling β catenin-delta catenin-CDK1 signaling.

5.2 Future directions

5.2.1 Characterizing the effects of BRK inhibition and knockdown on TamR *in vivo*

While the present work has characterized the effects of both BRK knockdown and inhibition *in vitro*, using TamR cell lines, it is important to extend this work to characterize how these conditions can affect TamR mouse xenografts *in vivo*. *In vivo* characterization of the BRK inhibitor use in this context would increase the clinical significance of these results while also serving as an effective pre-clinical analysis for the use of Tilfrinib. Additionally, it would be prudent to repeat phosphoproteomics and total proteomics analyses on these mouse xenografts to determine if the changes seen *in vitro* can be replicated *in vivo* while primarily using Tilfrinib as a BRK inhibitor. Patient-derived xenografts (PDX) are increasingly being used as *in vivo* models of cancer and have been used previously to study Tamoxifen resistance (Simões *et al.*, 2015). Therefore, a TamR PDX

mouse models can be developed to study the effects of BRK inhibition and would serve as an excellent pre-clinical evaluation for the effectiveness of Tilfrinib in the treatment of TamR.

5.2.2 Phospho and total proteomics analysis of Tamoxifen resistant patient tumours

In addition to developing TamR PDX mouse models, patient derived, TamR tumours can also be used for high throughput analyses of changes in protein expression and phosphorylation status of kinases. It has been established that there are multiple key differences in significantly altered kinases and genes in cancer cell lines and how these observations are different when translated to analyses of cancer tissue (Ertel *et al.*, 2006). Therefore, it is important to determine if the changes observed at the cell line level (in T47D and MCF7 TamR cells) are also observed at a tumour level (in patient derived TamR tumours). By extension, to determine the role of BRK in driving TamR, patient-derived cell lines can be grown and depleted of BRK protein levels or of its kinase activity before MS analysis for phospho and total proteomics analysis.

5.2.3 Characterizing the functional relationship between BRK, CDK1 and delta catenin-1

While I characterized the effect of BRK knockdown on CDK1 Y15 phosphorylation and delta catenin-1 Y904 phosphorylation levels, the functional effect and biological significance of these changes bares investigation. It would be interesting to investigate if the effect of BRK on these sites is direct or whether BRK acts through intermediaries. The Y904 site on delta catenin-1 has not been functionally characterized (Hong et al., 2016). It is possible that BRK recognizes delta catenin-1 as a substrate and phosphorylates it directly at the site. This can be studied by using *in vitro* kinase assays, generating site-directed mutations at Y904 of delta catenin-1 and looking for BRK binding at the site. Additionally, using CRISPR-directed knock-in, the point mutation at the Y904 site can be introduced in TamR cells to investigate the effect of abrogation of this phosphosite on drug resistance. This approach is suggested as an inhibitor that targets delta-catenin-1 has not been developed yet. If the abrogation of the Y904 site influences Tamoxifen resistance, it may then lead to inhibitors against delta catenin-1 as a target to combat drug resistance. In contrast, the Y15 site on CDK1 has been well characterized as inhibitory to its kinase activity, thereby causing cell cycle arrest before mitosis (Johnson *et al.*, 2010). Interestingly, CDK1 inhibition has been shown to reverse 5-fluorouracil resistance in therapy-refractive

colorectal cancer cells (Zhu et al., 2020). However, CDK1 inhibition through Y15 hyperphosphorylation by HER2 in triple negative breast cancer cells has been shown to induce Taxol resistance (Tan *et al.*, 2002). Y15 phosphorylation by HER2 indicates the site's importance to drug resistance and cancer cell proliferation overall as HER2 plays a role in both processes (Rani *et al.*, 2019). The role of BRK in the regulation of this site is undescribed currently. As stated in the model in Fig. 5.1, BRK may act on CDK1 through the β catenin-delta catenin-1 complex as BRK has been known to interact with β catenin directly. It is also possible that BRK may regulate CDK1 Y15 phosphorylation through its phosphorylation of HER2 which then phosphorylates CDK1 at the site and thereby contributes to its hyperphosphorylation in TamR. To elucidate the relationship between BRK, CDK1 and delta catenin-1, it is important to first identify if BRK directly interacts with CDK1 at its Y15 site or if it acts on the site through the catenin family proteins. Additionally, it is worth investigating how the phosphorylation of this site, which is normally associated with inactive CDK1 and cell cycle arrest, could result in Tamoxifen resistance. It is possible that the phosphorylation of the site allows for TamR cells to escape Tamoxifen-induced cell death and use alternative mechanisms for survival and growth (Tan *et al.*, 2002). Therefore, a mechanistic understanding of how this site drives TamR may lead to a better understanding of how CDK1 inhibitors may be used against TamR.

5.2.4 Investigation of alternative targets in Tamoxifen resistance

BRK is only one tyrosine kinase that is regulating signaling events in TamR. It would be interesting to investigate other signaling changes and the kinases that drive them, as an extension of the phosphorylation changes observed in the datasets described in Tables 4.1 and 4.3. For example, ILF3 (Interleukin enhancer-binding factor 3) is frequently overexpressed in colorectal cancer cells and has been found to promote breast tumour growth (Hu et al., 2013; Li et al., 2020). The S860 site on this protein was hyperphosphorylated in MCF7 TamR cells vs MCF7 Parental cells (Table 4.1). The characterization of this site and its importance to TamR would be a novel discovery. Similarly, HSPB1 (Heat shock protein beta 1) was found to be hyperphosphorylated in T47D TamR cells at its Y82 site. The site was unaffected when BRK was knocked down in these cells but its importance to TamR can still be investigated. HSPB1 activity is induced by phosphorylation of this site and this increase in activity is associated with the survival of pancreatic cancer cells in

response to genotoxic stress (Grierson et al., 2021). It is possible that the site is involved in the conferral of Tamoxifen resistance through its involvement in the stress response signaling pathway. Inhibitors that target HSPB1, such as RP101 and Quercetin, are commercially available and can therefore be used to investigate the involvement of the protein and its activation site in Tamoxifen resistance. While these are 2 examples, there are various sites listed in Tables 4.1 and 4.3 that can be analyzed for their potential role in Tamoxifen resistance.

Similarly, alternative targets from Tables 4.4 can be investigated to query the role of BRK in TamR cells. For this thesis, I narrowed down BRK-specific hits by only looking at pY phosphosites that were differentially phosphorylated in TamR, how they were affected when BRK was knocked down and if their total peptide abundances were discovered through proteomics. However, there are sites that may still be affected by BRK (listed in Table 4.4) but were discarded due to their total peptides not being found through proteomics. For example, PKP4 (plakophilin 4) was hypophosphorylated at its Y1168 site when BRK was knocked down in TamR cells but was filtered out as its total peptide abundance was not found through proteomics. PKP4 belongs to the plakophilin family of proteins which are involved in cell-cell adhesion (Neuber et al., 2010). PKP4 phosphorylation at the Y1168 site does not currently have a known kinase, according to the database Phosphosite.org. BRK may recognize this site and phosphorylate it, thereby playing a role in Tamoxifen resistance. Such a novel site would be ideal for future analysis.

6.0 REFERENCES

Acconcia, F., Manavathi, B., Mascarenhas, J., Talukder, A.H., Mills, G., and Kumar, R. (2006). An inherent role of integrin-linked kinase-estrogen receptor alpha interaction in cell migration. Cancer Res *66*, 11030-11038. 10.1158/0008-5472.Can-06-2676.

Aka, J.A., and Lin, S.X. (2012). Comparison of functional proteomic analyses of human breast cancer cell lines T47D and MCF7. PLoS One *7*, e31532. 10.1371/journal.pone.0031532.

Anderson, T.M.R., Ma, S.H., Kerkvliet, C.P., Peng, Y., Helle, T.M., Krutilina, R.I., Raj, G.V., Cidlowski, J.A., Ostrander, J.H., Schwertfeger, K.L., et al. (2018). Taxol Induces Brk-dependent Prosurvival Phenotypes in TNBC Cells through an AhR/GR/HIF-driven Signaling Axis. Molecular Cancer Research *16*, 1761-1772. 10.1158/1541-7786.Mcr-18-0410.

Ang, H.L., Yuan, Y., Lai, X., Tan, T.Z., Wang, L., Huang, B.B., Pandey, V., Huang, R.Y., Lobie, P.E., Goh, B.C., et al. (2021). Putting the BRK on breast cancer: From molecular target to therapeutics. Theranostics *11*, 1115-1128. 10.7150/thno.49716.

Ardito, F., Giuliani, M., Perrone, D., Troiano, G., and Lo Muzio, L. (2017). The crucial role of protein phosphorylation in cell signaling and its use as targeted therapy (Review). Int J Mol Med *40*, 271-280. 10.3892/ijmm.2017.3036.

Ariazi, E.A., Brailoiu, E., Yerrum, S., Shupp, H.A., Slifker, M.J., Cunliffe, H.E., Black, M.A., Donato, A.L., Arterburn, J.B., Oprea, T.I., et al. (2010). The G protein-coupled receptor GPR30 inhibits proliferation of estrogen receptor-positive breast cancer cells. Cancer Res *70*, 1184-1194. 10.1158/0008-5472.Can-09-3068.

Asghar Butt, S., Søgaard, L.V., Ardenkjaer-Larsen, J.H., Lauritzen, M.H., Engelholm, L.H., Paulson, O.B., Mirza, O., Holck, S., Magnusson, P., and Åkeson, P. (2015). Monitoring mammary tumor progression and effect of tamoxifen treatment in MMTV-PymT using MRI and magnetic resonance spectroscopy with hyperpolarized [1-13C]pyruvate. Magn Reson Med *73*, 51-58. 10.1002/mrm.25095.

Aubele, M., Vidojkovic, S., Braselmann, H., Ritterswurden, D., Auer, G., Atkinson, M.J., Tapio, S., Hofler, H., Rauser, S., and Bartlett, J.M. (2009). Overexpression of PTK6 (breast tumor kinase) protein--a prognostic factor for long-term breast cancer survival--is not due to gene amplification. Virchows Arch *455*, 117-123. 10.1007/s00428-009-0809-8.

Aubele, M., Walch, A.K., Ludyga, N., Braselmann, H., Atkinson, M.J., Luber, B., Auer, G., Tapio, S., Cooke, T., and Bartlett, J.M. (2008). Prognostic value of protein tyrosine kinase 6 (PTK6) for long-term survival of breast cancer patients. Br J Cancer *99*, 1089-1095. 6604660 [pii]

10.1038/sj.bjc.6604660.

Augusto, T.V., Correia-da-Silva, G., Rodrigues, C.M.P., Teixeira, N., and Amaral, C. (2018). Acquired resistance to aromatase inhibitors: where we stand! Endocrine-related cancer *25*, R283-R301. 10.1530/erc-17-0425.

Azuma, K., Urano, T., Horie-Inoue, K., Hayashi, S., Sakai, R., Ouchi, Y., and Inoue, S. (2009). Association of estrogen receptor alpha and histone deacetylase 6 causes rapid deacetylation of tubulin in breast cancer cells. Cancer Res *69*, 2935-2940. 10.1158/0008-5472.Can-08-3458.

Batth, T.S., Papetti, M., Pfeiffer, A., Tollenaere, M.A.X., Francavilla, C., and Olsen, J.V. (2018). Large-Scale Phosphoproteomics Reveals Shp-2 Phosphatase-Dependent Regulators of Pdgf Receptor Signaling. Cell Rep *22*, 2784-2796. 10.1016/j.celrep.2018.02.038.

Becker, M.A., Ibrahim, Y.H., Cui, X., Lee, A.V., and Yee, D. (2011). The IGF pathway regulates ERα through a S6K1-dependent mechanism in breast cancer cells. Mol Endocrinol *25*, 516-528. 10.1210/me.2010-0373.

Belachew, E.B., and Sewasew, D.T. (2021). Molecular Mechanisms of Endocrine Resistance in Estrogen-Receptor-Positive Breast Cancer. Frontiers in Endocrinology *12*. 10.3389/fendo.2021.599586.

Bellacosa, A., Chan, T.O., Ahmed, N.N., Datta, K., Malstrom, S., Stokoe, D., McCormick, F., Feng, J., and Tsichlis, P. (1998). Akt activation by growth factors is a multiple-step process: the role of the PH domain. Oncogene *17*, 313-325. 10.1038/sj.onc.1201947.

Bhatnagar, A.S. (2007). The discovery and mechanism of action of letrozole. Breast Cancer Res Tr *105*, 7-17. 10.1007/s10549-007-9696-3.

Bhullar, K.S., Lagarón, N.O., McGowan, E.M., Parmar, I., Jha, A., Hubbard, B.P., and Rupasinghe, H.P.V. (2018). Kinase-targeted cancer therapies: progress, challenges and future directions. Mol Cancer *17*, 48. 10.1186/s12943-018-0804-2.

Boer, K. (2017). Fulvestrant in advanced breast cancer: evidence to date and place in therapy. Ther Adv Med Oncol *9*, 465-479. 10.1177/1758834017711097.

Bourdeau, V.r., Deschênes, J., Métivier, R.l., Nagai, Y., Nguyen, D., Bretschneider, N., Gannon, F., White, J.H., and Mader, S. (2004). Genome-Wide Identification of High-Affinity Estrogen Response Elements in Human and Mouse. Mol Endocrinol *18*, 1411-1427. 10.1210/me.2003-0441.

Bourton, E., Hussain, H., Plowman, P., Harvey, A., and Parris, C. (2015). Radiosensitivity of human breast cancer cell lines expressing the breast tumor kinase (Brk).

Brauer, P.M., and Tyner, A.L. (2009). RAKing in AKT: a tumor suppressor function for the intracellular tyrosine kinase FRK. Cell Cycle *8*, 2728-2732. 9389 [pii].

Breuer, K., Foroushani, A.K., Laird, M.R., Chen, C., Sribnaia, A., Lo, R., Winsor, G.L., Hancock, R.E.W., Brinkman, F.S.L., and Lynn, D.J. (2012). InnateDB: systems biology of innate immunity and beyond—recent updates and continuing curation. Nucleic Acids Research *41*, D1228-D1233. 10.1093/nar/gks1147.

Broselid, S., Cheng, B., Sjöström, M., Lövgren, K., Klug-De Santiago, H.L., Belting, M., Jirström, K., Malmström, P., Olde, B., Bendahl, P.O., et al. (2013). G protein-coupled estrogen receptor is

apoptotic and correlates with increased distant disease-free survival of estrogen receptor-positive breast cancer patients. Clin Cancer Res *19*, 1681-1692. 10.1158/1078-0432.Ccr-12-2376.

Butti, R., Das, S., Gunasekaran, V.P., Yadav, A.S., Kumar, D., and Kundu, G.C. (2018). Receptor tyrosine kinases (RTKs) in breast cancer: signaling, therapeutic implications and challenges. Mol Cancer *17*, 34. 10.1186/s12943-018-0797-x.

Castro, N.E., and Lange, C.A. (2010). Breast tumor kinase and extracellular signal-regulated kinase 5 mediate Met receptor signaling to cell migration in breast cancer cells. Breast Cancer Res *12*, R60. 10.1186/bcr2622.

Chakraborty, G., Jain, S., and Kundu, G.C. (2008). Osteopontin promotes vascular endothelial growth factor-dependent breast tumor growth and angiogenesis via autocrine and paracrine mechanisms. Cancer Res *68*, 152-161. 68/1/152 [pii]

10.1158/0008-5472.CAN-07-2126.

Chang, M. (2012). Tamoxifen resistance in breast cancer. Biomol Ther (Seoul) *20*, 256-267. 10.4062/biomolther.2012.20.3.256.

Chen, H.Y., Shen, C.H., Tsai, Y.T., Lin, F.C., Huang, Y.P., and Chen, R.H. (2004). Brk activates rac1 and promotes cell migration and invasion by phosphorylating paxillin. Mol. Cell. Biol. *24*, 10558-10572.

Chen, R., Guo, S., Yang, C., Sun, L., Zong, B., Li, K., Liu, L., Tu, G., Liu, M., and Liu, S. (2020). Although c-MYC contributes to tamoxifen resistance, it improves cisplatin sensitivity in ER-positive breast cancer. Int J Oncol *56*, 932-944. 10.3892/ijo.2020.4987.

Cheng, R., Qi, L., Kong, X., Wang, Z., Fang, Y., and Wang, J. (2020). Identification of the Significant Genes Regulated by Estrogen Receptor in Estrogen Receptor-Positive Breast Cancer and Their Expression Pattern Changes When Tamoxifen or Fulvestrant Resistance Occurs. Frontiers in Genetics *11*. 10.3389/fgene.2020.538734.

Coldman, A., Phillips, N., Wilson, C., Decker, K., Chiarelli, A.M., Brisson, J., Zhang, B., Payne, J., Doyle, G., and Ahmad, R. (2014). Pan-Canadian study of mammography screening and mortality from breast cancer. J Natl Cancer Inst *106*. 10.1093/jnci/dju261.

Cox, J., and Mann, M. (2008). MaxQuant enables high peptide identification rates, individualized p.p.b.-range mass accuracies and proteome-wide protein quantification. Nat Biotechnol *26*, 1367-1372. 10.1038/nbt.1511.

Cox, J., Neuhauser, N., Michalski, A., Scheltema, R.A., Olsen, J.V., and Mann, M. (2011). Andromeda: a peptide search engine integrated into the MaxQuant environment. J Proteome Res *10*, 1794-1805. 10.1021/pr101065j.

Creighton, C.J., Massarweh, S., Huang, S., Tsimelzon, A., Hilsenbeck, S.G., Osborne, C.K., Shou, J., Malorni, L., and Schiff, R. (2008). Development of Resistance to Targeted Therapies Transforms the Clinically Associated Molecular Profile Subtype of Breast Tumor Xenografts. Cancer Research *68*, 7493-7501. 10.1158/0008-5472.Can-08-1404.

Dai, X., Li, T., Bai, Z., Yang, Y., Liu, X., Zhan, J., and Shi, B. (2015). Breast cancer intrinsic subtype classification, clinical use and future trends. Am J Cancer Res *5*, 2929-2943.

Daniel, A.R., Hagan, C.R., and Lange, C.A. (2011). Progesterone receptor action: defining a role in breast cancer. Expert Rev Endocrinol Metab *6*, 359-369. 10.1586/eem.11.25.

Davies, C., Godwin, J., Gray, R., Clarke, M., Cutter, D., Darby, S., McGale, P., Pan, H.C., Taylor, C., Wang, Y.C., et al. (2011). Relevance of breast cancer hormone receptors and other factors to the efficacy of adjuvant tamoxifen: patient-level meta-analysis of randomised trials. Lancet *378*, 771-784. 10.1016/S0140-6736(11)60993-8.

Davies, G.F., Berg, A., Postnikoff, S.D.L., Wilson, H.L., Arnason, T.G., Kusalik, A., and Harkness, T.A.A. (2014). TFPI1 Mediates Resistance to Doxorubicin in Breast Cancer Cells by Inducing a Hypoxic-Like Response. Plos One *9*. ARTN e84611

10.1371/journal.pone.0084611.

Davis, J.M., Navolanic, P.M., Weinstein-Oppenheimer, C.R., Steelman, L.S., Hu, W., Konopleva, M., Blagosklonny, M.V., and McCubrey, J.A. (2003). Raf-1 and Bcl-2 Induce Distinct and Common Pathways That Contribute to Breast Cancer Drug Resistance1. Clinical Cancer Research *9*, 1161-1170.

De Francesco, E.M., Pellegrino, M., Santolla, M.F., Lappano, R., Ricchio, E., Abonante, S., and Maggiolini, M. (2014). GPER mediates activation of HIF1α/VEGF signaling by estrogens. Cancer Res *74*, 4053-4064. 10.1158/0008-5472.Can-13-3590.

Dearth, R.K., Cui, X., Kim, H.J., Kuiatse, I., Lawrence, N.A., Zhang, X., Divisova, J., Britton, O.L., Mohsin, S., Allred, D.C., et al. (2006). Mammary tumorigenesis and metastasis caused by overexpression of insulin receptor substrate 1 (IRS-1) or IRS-2. Mol Cell Biol *26*, 9302-9314. 10.1128/mcb.00260-06.

Deeks, E.D., and Scott, L.J. (2009). Exemestane. Drugs *69*, 889-918. 10.2165/00003495-200969070-00007.

Dhillon, A.S., Hagan, S., Rath, O., and Kolch, W. (2007). MAP kinase signalling pathways in cancer. Oncogene *26*, 3279-3290. 10.1038/sj.onc.1210421.

Du, Z., and Lovly, C.M. (2018). Mechanisms of receptor tyrosine kinase activation in cancer. Mol Cancer *17*, 58. 10.1186/s12943-018-0782-4.

Duda, P., Akula, S.M., Abrams, S.L., Steelman, L.S., Martelli, A.M., Cocco, L., Ratti, S., Candido, S., Libra, M., Montalto, G., et al. (2020). Targeting GSK3 and Associated Signaling Pathways Involved in Cancer. Cells *9*. 10.3390/cells9051110.

Dwyer, A.R., Kerkvliet, C.J.P., Krutilina, R., Playa, H., Park, D., Thomas, W., Smeester, B., Seagroves, T.N., and Lange, C.A. (2020). SAT-133 Breast Tumor Kinase (Brk/PTK6) Mediates

Triple Negative Breast Cancer Cell Migration and Taxol Resistance via SH2 Domain-Dependent Activation of RhoA and AhR. Journal of the Endocrine Society *4*. 10.1210/jendso/bvaa046.1750.

Ertel, A., Verghese, A., Byers, S.W., Ochs, M., and Tozeren, A. (2006). Pathway-specific differences between tumor cell lines and normal and tumor tissue cells. Mol Cancer *5*, 55. 10.1186/1476-4598-5-55.

Fagan, D.H., Uselman, R.R., Sachdev, D., and Yee, D. (2012). Expression of type I insulin-like growth factor receptor (IGF1R) in tamoxifen-resistant cells: Implications for cotargeting of IGF1R and estrogen receptor (ER) in breast cancer. Journal of Clinical Oncology *30*, e13590-e13590. 10.1200/jco.2012.30.15_suppl.e13590.

Fan, G., Aleem, S., Yang, M., Miller, W.T., and Tonks, N.K. (2015). Protein-tyrosine Phosphatase and Kinase Specificity in Regulation of SRC and Breast Tumor Kinase. J Biol Chem *290*, 15934-15947. 10.1074/jbc.M115.651703.

Fan, G., Lin, G., Lucito, R., and Tonks, N.K. (2013). Protein-tyrosine phosphatase 1B antagonized signaling by insulin-like growth factor-1 receptor and kinase BRK/PTK6 in ovarian cancer cells. J Biol Chem *288*, 24923-24934. 10.1074/jbc.M113.482737.

Fan, J., Yin, W.-J., Lu, J.-S., Wang, L., Wu, J., Wu, F.-Y., Di, G.-H., Shen, Z.-Z., and Shao, Z.-M. (2008). ERα negative breast cancer cells restore response to endocrine therapy by combination treatment with both HDAC inhibitor and DNMT inhibitor. J Cancer Res Clin Oncol *134*, 883-890. 10.1007/s00432-008-0354-x.

Fernando, R.I., and Wimalasena, J. (2004). Estradiol abrogates apoptosis in breast cancer cells through inactivation of BAD: Ras-dependent nongenomic pathways requiring signaling through ERK and Akt. Mol Biol Cell *15*, 3266-3284. 10.1091/mbc.e03-11-0823.

Filardo, E.J., Quinn, J.A., Bland, K.I., and Frackelton, A.R., Jr. (2000). Estrogen-Induced Activation of Erk-1 and Erk-2 Requires the G Protein-Coupled Receptor Homolog, GPR30, and

Occurs via Trans-Activation of the Epidermal Growth Factor Receptor through Release of HB-EGF. Mol Endocrinol *14*, 1649-1660. 10.1210/mend.14.10.0532.

Frogne, T., Jepsen, J.S., Larsen, S.S., Fog, C.K., Brockdorff, B.L., and Lykkesfeldt, A.E. (2005). Antiestrogen-resistant human breast cancer cells require activated protein kinase B/Akt for growth. Endocr Relat Cancer *12*, 599-614. 10.1677/erc.1.00946.

Fuentes, N., and Silveyra, P. (2019). Estrogen receptor signaling mechanisms. Adv Protein Chem Struct Biol *116*, 135-170. 10.1016/bs.apcsb.2019.01.001.

Fuqua, S.A.W., Wiltschke, C., Zhang, Q.X., Borg, A.k., Castles, C.G., Friedrichs, W.E., Hopp, T., Hilsenbeck, S., Mohsin, S., O'Connell, P., and Allred, D.C. (2000). A Hypersensitive Estrogen Receptor-α Mutation in Premalignant Breast Lesions1. Cancer Research *60*, 4026-4029.

Furman, C., Hao, M.-H., Prajapati, S., Reynolds, D., Rimkunas, V., Zheng, G.Z., Zhu, P., and Korpal, M. (2019). Estrogen Receptor Covalent Antagonists: The Best Is Yet to Come. Cancer Research *79*, 1740-1745. 10.1158/0008-5472.Can-18-3634.

Gao, Y., Cimica, V., and Reich, N.C. (2012). Suppressor of cytokine signaling 3 inhibits breast tumor kinase activation of STAT3. J Biol Chem *287*, 20904-20912. 10.1074/jbc.M111.334144.

Garcia, R., Bowman, T.L., Niu, G., Yu, H., Minton, S., Muro-Cacho, C.A., Cox, C.E., Falcone, R., Fairclough, R., Parsons, S., et al. (2001). Constitutive activation of Stat3 by the Src and JAK tyrosine kinases participates in growth regulation of human breast carcinoma cells. Oncogene *20*, 2499-2513. 10.1038/sj.onc.1204349.

Gartner, E. (2017). Lapatinib and Tamoxifen in Treating Patients With Locally Advanced or Metastatic Breast Cancer That Did Not Respond to Previous Tamoxifen. https://ClinicalTrials.gov/show/NCT00118157.

Gerritsen, J.S., and White, F.M. (2021). Phosphoproteomics: a valuable tool for uncovering molecular signaling in cancer cells. Expert Rev Proteomic *18*, 661-674. 10.1080/14789450.2021.1976152.

Ghosh, D., Lo, J., Morton, D., Valette, D., Xi, J., Griswold, J., Hubbell, S., Egbuta, C., Jiang, W., An, J., and Davies, H.M. (2012). Novel aromatase inhibitors by structure-guided design. J Med Chem *55*, 8464-8476. 10.1021/jm300930n.

Gocek, E., Moulas, A.N., and Studzinski, G.P. (2014). Non-receptor protein tyrosine kinases signaling pathways in normal and cancer cells. Critical Reviews in Clinical Laboratory Sciences *51*, 125-137. 10.3109/10408363.2013.874403.

Goel, R.K., and Lukong, K.E. (2015). Tracing the footprints of the breast cancer oncogene BRK - Past till present. Biochim Biophys Acta *1856*, 39-54. 10.1016/j.bbcan.2015.05.001.

Goel, R.K., and Lukong, K.E. (2016). Understanding the cellular roles of Fyn-related kinase (FRK): implications in cancer biology. Cancer Metastasis Rev *35*, 179-199. 10.1007/s10555-016-9623-3.

Graves, P.R., and Haystead, T.A. (2002). Molecular biologist's guide to proteomics. Microbiol Mol Biol Rev *66*, 39-63; table of contents. 10.1128/mmbr.66.1.39-63.2002.

Grierson, P.M., Dodhiawala, P.B., Cheng, Y., Chen, T.H., Khawar, I.A., Wei, Q., Zhang, D., Li, L., Herndon, J., Monahan, J.B., et al. (2021). The MK2/Hsp27 axis is a major survival mechanism for pancreatic ductal adenocarcinoma under genotoxic stress. Sci Transl Med *13*, eabb5445. 10.1126/scitranslmed.abb5445.

Grote, I., Bartels, S., Kandt, L., Bollmann, L., Christgen, H., Gronewold, M., Raap, M., Lehmann, U., Gluz, O., Nitz, U., et al. (2021). TP53 mutations are associated with primary endocrine resistance in luminal early breast cancer. Cancer Medicine *10*, 8581-8594. https://doi.org/10.1002/cam4.4376.

Guney Eskiler, G., Cecener, G., Tunca, B., and Egeli, U. (2016). An in vitro model for the development of acquired tamoxifen resistance. Cell Biol Toxicol. 10.1007/s10565-016-9355-8.

Gutierrez, M.C., Detre, S., Johnston, S., Mohsin, S.K., Shou, J., Allred, D.C., Schiff, R., Osborne, C.K., and Dowsett, M. (2005). Molecular Changes in Tamoxifen-Resistant Breast Cancer: Relationship Between Estrogen Receptor, HER-2, and p38 Mitogen-Activated Protein Kinase. Journal of Clinical Oncology *23*, 2469-2476. 10.1200/JCO.2005.01.172.

Guvakova, M.A., and Surmacz, E. (1997). Tamoxifen Interferes with the Insulin-like Growth Factor I Receptor (IGF-IR) Signaling Pathway in Breast Cancer Cells1. Cancer Research *57*, 2606-2610.

Haeyul, L., Mirang, K., Kyoung-Hwa, L., Kyung-Nam, K., and Seung-Taek, L. (1998). Exon-Intron Structure of the Human PTK6 Gene Demonstrates That PTK6 Constitutes a Distinct Family of Non-Receptor Tyrosine Kinase. Molecules & Cells (Springer Science & Business Media B.V.) *8*, 401-407.

Hanahan, D., and Weinberg, R.A. (2011). Hallmarks of cancer: the next generation. Cell *144*, 646-674. 10.1016/j.cell.2011.02.013.

Hanker, A.B., Sudhan, D.R., and Arteaga, C.L. (2020). Overcoming Endocrine Resistance in Breast Cancer. Cancer Cell *37*, 496-513. https://doi.org/10.1016/j.ccell.2020.03.009.

Harbeck, N., Penault-Llorca, F., Cortes, J., Gnant, M., Houssami, N., Poortmans, P., Ruddy, K., Tsang, J., and Cardoso, F. (2019). Breast cancer. Nature Reviews Disease Primers *5*, 66. 10.1038/s41572-019-0111-2.

Hartkopf, A.D., Grischke, E.M., and Brucker, S.Y. (2020). Endocrine-Resistant Breast Cancer: Mechanisms and Treatment. Breast Care *15*, 347-354. 10.1159/000508675.

He, M., Jin, Q., Chen, C., Liu, Y., Ye, X., Jiang, Y., Ji, F., Qian, H., Gan, D., Yue, S., et al. (2019). The miR-186-3p/EREG axis orchestrates tamoxifen resistance and aerobic glycolysis in breast cancer cells. Oncogene *38*, 5551-5565. 10.1038/s41388-019-0817-3.

Helsens, K., Martens, L., Vandekerckhove, J., and Gevaert, K. (2007). MascotDatfile: An open-source library to fully parse and analyse MASCOT MS/MS search results. Proteomics *7*, 364-366. https://doi.org/10.1002/pmic.200600682.

Hiscox, S., Baruha, B., Smith, C., Bellerby, R., Goddard, L., Jordan, N., Poghosyan, Z., Nicholson, R.I., Barrett-Lee, P., and Gee, J. (2012). Overexpression of CD44 accompanies acquired tamoxifen resistance in MCF7 cells and augments their sensitivity to the stromal factors, heregulin and hyaluronan. BMC Cancer *12*, 458. 10.1186/1471-2407-12-458.

Hong, J.Y., Oh, I.H., and McCrea, P.D. (2016). Phosphorylation and isoform use in p120-catenin during development and tumorigenesis. Biochim Biophys Acta *1863*, 102-114. 10.1016/j.bbamcr.2015.10.008.

Hsu, J.L., and Hung, M.C. (2016). The role of HER2, EGFR, and other receptor tyrosine kinases in breast cancer. Cancer Metastasis Rev *35*, 575-588. 10.1007/s10555-016-9649-6.

Hsu, L.H., Chu, N.M., Lin, Y.F., and Kao, S.H. (2019). G-Protein Coupled Estrogen Receptor in Breast Cancer. Int J Mol Sci *20*. 10.3390/ijms20020306.

Hu, Q., Lu, Y.Y., Noh, H., Hong, S., Dong, Z., Ding, H.F., Su, S.B., and Huang, S. (2013). Interleukin enhancer-binding factor 3 promotes breast tumor progression by regulating sustained urokinase-type plasminogen activator expression. Oncogene *32*, 3933-3943. 10.1038/onc.2012.414.

Hu, Z., Li, L., Lan, W., Wei, X., Wen, X., Wu, P., Zhang, X., Xi, X., Li, Y., Wu, L., et al. (2022). Enrichment of Wee1/CDC2 and NF-κB Signaling Pathway Constituents Mutually Contributes to CDDP Resistance in Human Osteosarcoma. Cancer Res Treat *54*, 277-293. 10.4143/crt.2021.320.

Ikeda, O., Sekine, Y., Mizushima, A., Nakasuji, M., Miyasaka, Y., Yamamoto, C., Muromoto, R., Nanbo, A., Oritani, K., Yoshimura, A., and Matsuda, T. (2010). Interactions of STAP-2 with Brk and STAT3 participate in cell growth of human breast cancer cells. J Biol Chem *285*, 38093-38103. M110.162388 [pii]

10.1074/jbc.M110.162388.

Irie, H.Y., Shrestha, Y., Selfors, L.M., Frye, F., Iida, N., Wang, Z., Zou, L., Yao, J., Lu, Y., Epstein, C.B., et al. (2010). PTK6 regulates IGF-1-induced anchorage-independent survival. PLoS One *5*, e11729. 10.1371/journal.pone.0011729.

Irwin, M.E., Bohin, N., and Boerner, J.L. (2011). Src family kinases mediate epidermal growth factor receptor signaling from lipid rafts in breast cancer cells. Cancer Biol Ther *12*, 718-726. 10.4161/cbt.12.8.16907.

Ito, K., Park, S.H., Katsyv, I., Zhang, W., De Angelis, C., Schiff, R., and Irie, H.Y. (2017). PTK6 regulates growth and survival of endocrine therapy-resistant ER+ breast cancer cells. NPJ Breast Cancer *3*, 45. 10.1038/s41523-017-0047-1.

Jehmlich, N., Golatowski, C., Murr, A., Salazar, G., Dhople, V.M., Hammer, E., and Völker, U. (2014). Comparative evaluation of peptide desalting methods for salivary proteome analysis. Clinica Chimica Acta *434*, 16-20. https://doi.org/10.1016/j.cca.2014.04.003.

Jeselsohn, R., Yelensky, R., Buchwalter, G., Frampton, G., Meric-Bernstam, F., Gonzalez-Angulo, A.M., Ferrer-Lozano, J., Perez-Fidalgo, J.A., Cristofanilli, M., Gómez, H., et al. (2014). Emergence of Constitutively Active Estrogen Receptor-α Mutations in Pretreated Advanced Estrogen Receptor–Positive Breast Cancer. Clinical Cancer Research *20*, 1757-1767. 10.1158/1078-0432.Ccr-13-2332.

Jiagge, E., Jibril, A.S., Chitale, D., Bensenhaver, J.M., Awuah, B., Hoenerhoff, M., Adjei, E., Bekele, M., Abebe, E., Nathanson, S.D., et al. (2016). Comparative Analysis of Breast Cancer Phenotypes in African American, White American, and West Versus East African patients:

Correlation Between African Ancestry and Triple-Negative Breast Cancer. Ann Surg Oncol *23*, 3843-3849. 10.1245/s10434-016-5420-z.

Jiang, J., Gui, F., He, Z., Li, L., Li, Y., Li, S., Wu, X., Deng, Z., Sun, X., Huang, X., et al. (2017). Targeting BRK-Positive Breast Cancers with Small-Molecule Kinase Inhibitors. Cancer Res *77*, 175-186. 10.1158/0008-5472.CAN-16-1038.

Jiang, Q., Zhang, X., Dai, X., Han, S., Wu, X., Wang, L., Wei, W., Zhang, N., Xie, W., and Guo, J. (2022). S6K1-mediated phosphorylation of PDK1 impairs AKT kinase activity and oncogenic functions. Nature Communications *13*, 1548. 10.1038/s41467-022-28910-8.

Johnson, K.S., Conant, E.F., and Soo, M.S. (2020). Molecular Subtypes of Breast Cancer: A Review for Breast Radiologists. Journal of Breast Imaging *3*, 12-24. 10.1093/jbi/wbaa110.

Johnson, N., Bentley, J., Wang, L.Z., Newell, D.R., Robson, C.N., Shapiro, G.I., and Curtin, N.J. (2010). Pre-clinical evaluation of cyclin-dependent kinase 2 and 1 inhibition in anti-estrogen-sensitive and resistant breast cancer cells. British Journal of Cancer *102*, 342-350. 10.1038/sj.bjc.6605479.

Johnston, S.R.D., Saccani-Jotti, G., Smith, I.E., Salter, J., Newby, J., Coppen, M., Ebbs, S.R., and Dowsett, M. (1995). Changes in Estrogen Receptor, Progesterone Receptor, and pS2 Expression in Tamoxifen-resistant Human Breast Cancer1. Cancer Research *55*, 3331-3338.

Jordan, N.J., Gee, J.M.W., Barrow, D., Wakeling, A.E., and Nicholson, R.I. (2004). Increased Constitutive Activity of PKB/Akt in Tamoxifen Resistant Breast Cancer MCF-7 Cells. Breast Cancer Res Tr *87*, 167-180. 10.1023/B:BREA.0000041623.21338.47.

Jordan, V.C. (2006). Tamoxifen (ICI46,474) as a targeted therapy to treat and prevent breast cancer. British Journal of Pharmacology *147*, S269-S276. https://doi.org/10.1038/sj.bjp.0706399.

Kamalati, T., Jolin, H.E., Fry, M.J., and Crompton, M.R. (2000a). Expression of the BRK tyrosine kinase in mammary epithelial cells enhances the coupling of EGF signalling to PI 3-kinase and Akt, via erbB3 phosphorylation. Oncogene *19*, 5471-5476. 10.1038/sj.onc.1203931.

Kamalati, T., Jolin, H.E., Fry, M.J., and Crompton, M.R. (2000b). Expression of the BRK tyrosine kinase in mammary epithelian cells enhances the coupling of EGF signalling to PI 3-kinase and Akt, via erbB3 phosphorylation. Oncogene *19*, 5471-5476.

Kamalati, T., Jolin, H.E., Mitchell, P.J., Barker, K.T., Jackson, L.E., Dean, C.J., Page, M.J., Gusterson, B.A., and Crompton, M.R. (1996). Brk, a breast tumor-derived non-receptor protein-tyrosine kinase, sensitizes mammary epithelial cells to epidermal growth factor. J Biol Chem *271*, 30956-30963.

Kanshin, E., Michnick, S., and Thibault, P. (2012). Sample preparation and analytical strategies for large-scale phosphoproteomics experiments. Semin Cell Dev Biol *23*, 843-853. 10.1016/j.semcdb.2012.05.005.

Keydar, I., Chen, L., Karby, S., Weiss, F.R., Delarea, J., Radu, M., Chaitcik, S., and Brenner, H.J. (1979). Establishment and characterization of a cell line of human breast carcinoma origin. European Journal of Cancer (1965) *15*, 659-670. https://doi.org/10.1016/0014-2964(79)90139-7.

Kilker, R.L., and Planas-Silva, M.D. (2006). Cyclin D1 is necessary for tamoxifen-induced cell cycle progression in human breast cancer cells. Cancer Res *66*, 11478-11484. 10.1158/0008-5472.Can-06-1755.

Kim, H., and Lee, S.T. (2005). An intramolecular interaction between SH2-kinase linker and kinase domain is essential for the catalytic activity of protein-tyrosine kinase-6. J Biol Chem *280*, 28973-28980.

Kim, S., You, D., Jeong, Y., Yoon, S.Y., Kim, S.A., and Lee, J.E. (2021). Inhibition of platelet-derived growth factor receptor synergistically increases the pharmacological effect of

tamoxifen in estrogen receptor α positive breast cancer. Oncol Lett *21*, 294. 10.3892/ol.2021.12555.

Kirkegaard, T., Witton, C.J., McGlynn, L.M., Tovey, S.M., Dunne, B., Lyon, A., and Bartlett, J.M. (2005). AKT activation predicts outcome in breast cancer patients treated with tamoxifen. J Pathol *207*, 139-146. https://doi.org/10.1002/path.1829.

Knowlden, J.M., Jones, H.E., Barrow, D., Gee, J.M.W., Nicholson, R.I., and Hutcheson, I.R. (2008). Insulin receptor substrate-1 involvement in epidermal growth factor receptor and insulin-like growth factor receptor signalling: implication for Gefitinib ('Iressa') response and resistance. Breast Cancer Res Tr *111*, 79-91. 10.1007/s10549-007-9763-9.

Knowlton, M.L., Selfors, L.M., Wrobel, C.N., Gu, T.L., Ballif, B.A., Gygi, S.P., Polakiewicz, R., and Brugge, J.S. (2010). Profiling Y561-dependent and -independent substrates of CSF-1R in epithelial cells. PLoS One *5*, e13587. 10.1371/journal.pone.0013587.

Krisnamurti, D.G.B., Louisa, M., Anggraeni, E., and Wanandi, S.I. (2016). Drug Efflux Transporters Are Overexpressed in Short-Term Tamoxifen-Induced MCF7 Breast Cancer Cells. Advances in Pharmacological Sciences *2016*, 6702424. 10.1155/2016/6702424.

Kumbrink, J., and Kirsch, K.H. (2012). Regulation of p130(Cas)/BCAR1 expression in tamoxifen-sensitive and tamoxifen-resistant breast cancer cells by EGR1 and NAB2. Neoplasia *14*, 108-120. 10.1593/neo.111760.

Lai, A., Sarcevic, B., Prall, O.W., and Sutherland, R.L. (2001). Insulin/insulin-like growth factor-I and estrogen cooperate to stimulate cyclin E-Cdk2 activation and cell Cycle progression in MCF-7 breast cancer cells through differential regulation of cyclin E and p21(WAF1/Cip1). J Biol Chem *276*, 25823-25833. 10.1074/jbc.M100925200.

Law, J.H., Habibi, G., Hu, K., Masoudi, H., Wang, M.Y.C., Stratford, A.L., Park, E., Gee, J.M.W., Finlay, P., Jones, H.E., et al. (2008). Phosphorylated Insulin-Like Growth Factor-I/Insulin

Receptor Is Present in All Breast Cancer Subtypes and Is Related to Poor Survival. Cancer Research *68*, 10238-10246. 10.1158/0008-5472.Can-08-2755.

Le Dily, F., and Beato, M. (2018). Signaling by Steroid Hormones in the 3D Nuclear Space. International Journal of Molecular Sciences *19*, 306.

Le Romancer, M., Treilleux, I., Leconte, N., Robin-Lespinasse, Y., Sentis, S., Bouchekioua-Bouzaghou, K., Goddard, S., Gobert-Gosse, S., and Corbo, L. (2008). Regulation of estrogen rapid signaling through arginine methylation by PRMT1. Mol Cell *31*, 212-221.

Leary, A.F., Drury, S., Detre, S., Pancholi, S., Lykkesfeldt, A.E., Martin, L.-A., Dowsett, M., and Johnston, S.R.D. (2010). Lapatinib Restores Hormone Sensitivity with Differential Effects on Estrogen Receptor Signaling in Cell Models of Human Epidermal Growth Factor Receptor 2–Negative Breast Cancer with Acquired Endocrine Resistance. Clinical Cancer Research *16*, 1486-1497. 10.1158/1078-0432.Ccr-09-1764.

Lee, A.V., Oesterreich, S., and Davidson, N.E. (2015). MCF-7 cells--changing the course of breast cancer research and care for 45 years. J Natl Cancer Inst *107*. 10.1093/jnci/djv073.

Lee, Y.R., Park, J., Yu, H.N., Kim, J.S., Youn, H.J., and Jung, S.H. (2005). Up-regulation of PI3K/Akt signaling by 17beta-estradiol through activation of estrogen receptor-alpha, but not estrogen receptor-beta, and stimulates cell growth in breast cancer cells. Biochem Biophys Res Commun *336*, 1221-1226. 10.1016/j.bbrc.2005.08.256.

Levin, E.R. (2009). Membrane oestrogen receptor alpha signalling to cell functions. J Physiol *587*, 5019-5023. 10.1113/jphysiol.2009.177097.

Li, K., Wu, J.-l., Qin, B., Fan, Z., Tang, Q., Lu, W., Zhang, H., Xing, F., Meng, M., Zou, S., et al. (2020). ILF3 is a substrate of SPOP for regulating serine biosynthesis in colorectal cancer. Cell Research *30*, 163-178. 10.1038/s41422-019-0257-1.

Li, W., Shi, X., Xu, Y., Wan, J., Wei, S., and Zhu, R. (2017). Tamoxifen promotes apoptosis and inhibits invasion in estrogen-positive breast cancer MCF-7 cells. Mol Med Rep *16*, 478-484. 10.3892/mmr.2017.6603.

Li, X., Lu, Y., Liang, K., Hsu, J.M., Albarracin, C., Mills, G.B., Hung, M.C., and Fan, Z. (2012). Brk/PTK6 sustains activated EGFR signaling through inhibiting EGFR degradation and transactivating EGFR. Oncogene. 10.1038/onc.2011.608

onc2011608 [pii].

Li, Y., Soos, T.J., Li, X., Wu, J., Degennaro, M., Sun, X., Littman, D.R., Birnbaum, M.J., and Polakiewicz, R.D. (2004). Protein kinase C Theta inhibits insulin signaling by phosphorylating IRS1 at Ser(1101). J Biol Chem *279*, 45304-45307. 10.1074/jbc.C400186200.

Liu, L., Gao, Y., Qiu, H., Miller, W.T., Poli, V., and Reich, N.C. (2006). Identification of STAT3 as a specific substrate of breast tumor kinase. Oncogene *25*, 4904-4912. 1209501 [pii]

10.1038/sj.onc.1209501.

Lofgren, K.A., Ostrander, J.H., Housa, D., Hubbard, G.K., Locatelli, A., Bliss, R.L., Schwertfeger, K.L., and Lange, C.A. (2011). Mammary gland specific expression of Brk/PTK6 promotes delayed involution and tumor formation associated with activation of p38 MAPK. Breast Cancer Res *13*, R89. bcr2946 [pii]

10.1186/bcr2946.

Long, X., and Nephew, K.P. (2006). Fulvestrant (ICI 182,780)-dependent Interacting Proteins Mediate Immobilization and Degradation of Estrogen Receptor-α*. J Biol Chem *281*, 9607-9615. https://doi.org/10.1074/jbc.M510809200.

López-Colomé, A.M., Lee-Rivera, I., Benavides-Hidalgo, R., and López, E. (2017). Paxillin: a crossroad in pathological cell migration. Journal of Hematology & Oncology *10*, 50. 10.1186/s13045-017-0418-y.

Lu, Y., Yu, Q., Liu, J.H., Zhang, J., Wang, H., Koul, D., McMurray, J.S., Fang, X., Yung, W.K.A., Siminovitch, K.A., and Mills, G.B. (2003). Src Family Protein-tyrosine Kinases Alter the Function of PTEN to Regulate Phosphatidylinositol 3-Kinase/AKT Cascades*. J Biol Chem *278*, 40057-40066. https://doi.org/10.1074/jbc.M303621200.

Ludyga, N., Anastasov, N., Gonzalez-Vasconcellos, I., Ram, M., Hofler, H., and Aubele, M. (2011). Impact of protein tyrosine kinase 6 (PTK6) on human epidermal growth factor receptor (HER) signalling in breast cancer. Mol Biosyst. 10.1039/c0mb00286k.

Ludyga, N., Anastasov, N., Rosemann, M., Seiler, J., Lohmann, N., Braselmann, H., Mengele, K., Schmitt, M., Hofler, H., and Aubele, M. (2013). Effects of simultaneous knockdown of HER2 and PTK6 on malignancy and tumor progression in human breast cancer cells. Mol Cancer Res *11*, 381-392. 10.1158/1541-7786.MCR-12-0378.

Lukong, K.E., Larocque, D., Tyner, A.L., and Richard, S. (2005). Tyrosine phosphorylation of sam68 by breast tumor kinase regulates intranuclear localization and cell cycle progression. J Biol Chem *280*, 38639-38647.

Lumachi, F., Santeufemia, D.A., and Basso, S.M. (2015). Current medical treatment of estrogen receptor-positive breast cancer. World J Biol Chem *6*, 231-239. 10.4331/wjbc.v6.i3.231.

Maennling, A.E., Tur, M.K., Niebert, M., Klockenbring, T., Zeppernick, F., Gattenlöhner, S., Meinhold-Heerlein, I., and Hussain, A.F. (2019). Molecular Targeting Therapy against EGFR Family in Breast Cancer: Progress and Future Potentials. Cancers (Basel) *11*. 10.3390/cancers11121826.

Mahmoud, K.A., Krug, M., Wersig, T., Slynko, I., Schachtele, C., Totzke, F., Sippl, W., and Hilgeroth, A. (2014). Discovery of 4-anilino alpha-carbolines as novel Brk inhibitors. Bioorg Med Chem Lett *24*, 1948-1951. 10.1016/j.bmcl.2014.03.002.

Malumbres, M. (2014). Cyclin-dependent kinases. Genome Biology *15*, 122. 10.1186/gb4184.

Manavathi, B., Dey, O., Gajulapalli, V.N.R., Bhatia, R.S., Bugide, S., and Kumar, R. (2013). Derailed estrogen signaling and breast cancer: an authentic couple. Endocrine reviews *34*, 1-32. 10.1210/er.2011-1057.

Mardilovich, K., Pankratz, S.L., and Shaw, L.M. (2009). Expression and function of the insulin receptor substrate proteins in cancer. Cell Communication and Signaling *7*, 14. 10.1186/1478-811X-7-14.

Marson, L.P., Kurian, K.M., Miller, W.R., and Dixon, J.M. (2001). The effect of tamoxifen on breast tumour vascularity. Breast Cancer Res Tr *66*, 9-15. 10.1023/A:1010672605265.

Martellucci, S., Clementi, L., Sabetta, S., Mattei, V., Botta, L., and Angelucci, A. (2020). Src Family Kinases as Therapeutic Targets in Advanced Solid Tumors: What We Have Learned so Far. Cancers (Basel) *12*. 10.3390/cancers12061448.

Massarweh, S., Osborne, C.K., Creighton, C.J., Qin, L., Tsimelzon, A., Huang, S., Weiss, H., Rimawi, M., and Schiff, R. (2008). Tamoxifen resistance in breast tumors is driven by growth factor receptor signaling with repression of classic estrogen receptor genomic function. Cancer research *68*, 826-833. 10.1158/0008-5472.CAN-07-2707.

Mawson, A., Lai, A., Carroll, J.S., Sergio, C.M., Mitchell, C.J., and Sarcevic, B. (2005). Estrogen and insulin/IGF-1 cooperatively stimulate cell cycle progression in MCF-7 breast cancer cells through differential regulation of c-Myc and cyclin D1. Mol Cell Endocrinol *229*, 161-173. 10.1016/j.mce.2004.08.002.

Merenbakh-Lamin, K., Ben-Baruch, N., Yeheskel, A., Dvir, A., Soussan-Gutman, L., Jeselsohn, R., Yelensky, R., Brown, M., Miller, V.A., Sarid, D., et al. (2013). D538G Mutation in Estrogen Receptor-α: A Novel Mechanism for Acquired Endocrine Resistance in Breast Cancer. Cancer Research *73*, 6856-6864. 10.1158/0008-5472.Can-13-1197.

Miah, S., Banks, C.A.S., Ogunbolude, Y., Bagu, E.T., Berg, J.M., Saraf, A., Tettey, T.T., Hattem, G., Dayebgadoh, G., Kempf, C.G., et al. (2019). BRK phosphorylates SMAD4 for proteasomal degradation and inhibits tumor suppressor FRK to control SNAIL, SLUG, and metastatic potential. Sci Adv *5*, eaaw3113. 10.1126/sciadv.aaw3113.

Milani, M., Jha, G., and Potter, D.A. (2009). Anastrozole Use in Early Stage Breast Cancer of Post-Menopausal Women. Clin Med Ther *1*, 141-156. 10.4137/cmt.s9.

Mills, J.N., Rutkovsky, A.C., and Giordano, A. (2018). Mechanisms of resistance in estrogen receptor positive breast cancer: overcoming resistance to tamoxifen/aromatase inhibitors. Current Opinion in Pharmacology *41*, 59-65. https://doi.org/10.1016/j.coph.2018.04.009.

Mitchell, P.J., Barker, K.T., Martindale, J.E., Kamalati, T., Lowe, P.N., Page, M.J., Gusterson, B.A., and Crompton, M.R. (1994). Cloning and characterization of cDNAs encoding a novel non-receptor tyrosine kinase, brk, expressed in human breast tumours. Oncogene *9*, 2383-2390.

Mitchell, P.J., Sara, E.A., and Crompton, M.R. (2000). A novel adaptor-like protein which is a substrate for the non-receptor tyrosine kinase, BRK. Oncogene *19*, 4273-4282.

Moerkens, M., Zhang, Y., Wester, L., van de Water, B., and Meerman, J.H.N. (2014). Epidermal growth factor receptor signalling in human breast cancer cells operates parallel to estrogen receptor α signalling and results in tamoxifen insensitive proliferation. BMC Cancer *14*, 283. 10.1186/1471-2407-14-283.

Moody, S.E., Schinzel, A.C., Singh, S., Izzo, F., Strickland, M.R., Luo, L., Thomas, S.R., Boehm, J.S., Kim, S.Y., Wang, Z.C., and Hahn, W.C. (2015). PRKACA mediates resistance to HER2-targeted therapy in breast cancer cells and restores anti-apoptotic signaling. Oncogene *34*, 2061-2071. 10.1038/onc.2014.153.

Morelli, C., Garofalo, C., Sisci, D., del Rincon, S., Cascio, S., Tu, X., Vecchione, A., Sauter, E.R., Miller, W.H., Jr., and Surmacz, E. (2004). Nuclear insulin receptor substrate 1 interacts with estrogen receptor alpha at ERE promoters. Oncogene *23*, 7517-7526. 10.1038/sj.onc.1208014.

Moriai, R., Tsuji, N., Moriai, M., Kobayashi, D., and Watanabe, N. (2009). Survivin plays as a resistant factor against tamoxifen-induced apoptosis in human breast cancer cells. Breast Cancer Res Tr *117*, 261-271. 10.1007/s10549-008-0164-5.

Müller, T., and Winter, D. (2017). Systematic Evaluation of Protein Reduction and Alkylation Reveals Massive Unspecific Side Effects by Iodine-containing Reagents. Mol Cell Proteomics *16*, 1173-1187. 10.1074/mcp.M116.064048.

Munster, P.N., Thurn, K.T., Thomas, S., Raha, P., Lacevic, M., Miller, A., Melisko, M., Ismail-Khan, R., Rugo, H., Moasser, M., and Minton, S.E. (2011). A phase II study of the histone deacetylase inhibitor vorinostat combined with tamoxifen for the treatment of patients with hormone therapy-resistant breast cancer. British Journal of Cancer *104*, 1828-1835. 10.1038/bjc.2011.156.

Nagao, H., Cai, W., Albrechtsen, N.J.W., Steger, M., Batista, T.M., Pan, H., Dreyfuss, J.M., Mann, M., and Kahn, C.R. (2021). Distinct signaling by insulin and IGF-1 receptors and their extra- and intracellular domains. Proceedings of the National Academy of Sciences *118*, e2019474118. doi:10.1073/pnas.2019474118.

Nathan, M.R., and Schmid, P. (2017). A Review of Fulvestrant in Breast Cancer. Oncol Ther *5*, 17-29. 10.1007/s40487-017-0046-2.

Nayar, U., Cohen, O., Kapstad, C., Cuoco, M.S., Waks, A.G., Wander, S.A., Painter, C., Freeman, S., Persky, N.S., Marini, L., et al. (2019). Acquired HER2 mutations in ER+ metastatic breast cancer confer resistance to estrogen receptor–directed therapies. Nature Genetics *51*, 207-216. 10.1038/s41588-018-0287-5.

Neuber, S., Mühmer, M., Wratten, D., Koch, P.J., Moll, R., and Schmidt, A. (2010). The desmosomal plaque proteins of the plakophilin family. Dermatol Res Pract *2010*, 101452. 10.1155/2010/101452.

O'Lone, R., Frith, M.C., Karlsson, E.K., and Hansen, U. (2004). Genomic targets of nuclear estrogen receptors. Mol Endocrinol *18*, 1859-1875. 10.1210/me.2003-0044.

Oelze, M., Mahmoud, K.A., Sippl, W., Wersig, T., Hilgeroth, A., and Ritter, C.A. (2015). Novel 4-anilino-alpha-carboline derivatives induce cell death in nonadhesive breast cancer cells through inhibition of Brk activity. Int J Clin Pharmacol Ther *53*, 1052-1055. 10.5414/CPXCES14EA07.

Osborne, C.K., Neven, P., Dirix, L.Y., Mackey, J.R., Robert, J., Underhill, C., Schiff, R., Gutierrez, C., Migliaccio, I., Anagnostou, V.K., et al. (2011). Gefitinib or Placebo in Combination with Tamoxifen in Patients with Hormone Receptor–Positive Metastatic Breast Cancer: A Randomized Phase II Study. Clinical Cancer Research *17*, 1147-1159. 10.1158/1078-0432.Ccr-10-1869.

Ostrander, J.H., Daniel, A.R., Lofgren, K., Kleer, C.G., and Lange, C.A. (2007). Breast tumor kinase (protein tyrosine kinase 6) regulates heregulin-induced activation of ERK5 and p38 MAP kinases in breast cancer cells. Cancer Res *67*, 4199-4209. 67/9/4199 [pii]

10.1158/0008-5472.CAN-06-3409.

Ottaviano, Y.L., Issa, J.-P., Parl, F.F., Smith, H.S., Baylin, S.B., and Davidson, N.E. (1994). Methylation of the Estrogen Receptor Gene CpG Island Marks Loss of Estrogen Receptor Expression in Human Breast Cancer Cells1. Cancer Research *54*, 2552-2555.

Palka-Hamblin, H.L., Gierut, J.J., Bie, W., Brauer, P.M., Zheng, Y., Asara, J.M., and Tyner, A.L. (2010). Identification of beta-catenin as a target of the intracellular tyrosine kinase PTK6. J Cell Sci *123*, 236-245. jcs.053264 [pii]

10.1242/jcs.053264.

Park, S.H., Lee, K.H., Kim, H., and Lee, S.T. (1997). Assignment of the human PTK6 gene encoding a non-receptor protein tyrosine kinase to 20q13.3 by fluorescence in situ hybridization. Cytogenet Cell Genet *77*, 271-272.

Peck, D., and Isacke, C.M. (1998). Hyaluronan-dependent cell migration can be blocked by a CD44 cytoplasmic domain peptide containing a phosphoserine at position 325. J Cell Sci *111 (Pt 11)*, 1595-1601.

Peng, M., Ball-Kell, S.M., and Tyner, A.L. (2015). Protein tyrosine kinase 6 promotes ERBB2-induced mammary gland tumorigenesis in the mouse. Cell Death Dis *6*, e1848. 10.1038/cddis.2015.210.

Peng, M., Emmadi, R., Wang, Z., Wiley, E.L., Gann, P.H., Khan, S.A., Banerji, N., McDonald, W., Asztalos, S., Pham, T.N., et al. (2014). PTK6/BRK is expressed in the normal mammary gland and activated at the plasma membrane in breast tumors. Oncotarget *5*, 6038-6048.

Pérez-Tenorio, G., Berglund, F., Esguerra Merca, A., Nordenskjöld, B., Rutqvist, L.E., Skoog, L., and Stål, O. (2006). Cytoplasmic p21WAF1/CIP1 correlates with Akt activation and poorresponse to tamoxifen in breast cancer. Int J Oncol *28*, 1031-1042. 10.3892/ijo.28.5.1031.

Pernas, S., and Tolaney, S.M. (2019). HER2-positive breast cancer: new therapeutic frontiers and overcoming resistance. Ther Adv Med Oncol *11*, 1758835919833519. 10.1177/1758835919833519.

Perou, C.M., Sorlie, T., Eisen, M.B., van de Rijn, M., Jeffrey, S.S., Rees, C.A., Pollack, J.R., Ross, D.T., Johnsen, H., Akslen, L.A., et al. (2000). Molecular portraits of human breast tumours. Nature *406*, 747-752. 10.1038/35021093.

Pires, I.M., Blokland, N.J., Broos, A.W., Poujade, F.A., Senra, J.M., Eccles, S.A., Span, P.N., Harvey, A.J., and Hammond, E.M. (2014). HIF-1α-independent hypoxia-induced rapid PTK6

stabilization is associated with increased motility and invasion. Cancer Biol Ther *15*, 1350-1357. 10.4161/cbt.29822.

Powell, E., and Xu, W. (2008). Intermolecular interactions identify ligand-selective activity of estrogen receptor α/β dimers. Proceedings of the National Academy of Sciences *105*, 19012-19017. doi:10.1073/pnas.0807274105.

Puppe, J., Seifert, T., Eichler, C., Pilch, H., Mallmann, P., and Malter, W. (2020). Genomic Signatures in Luminal Breast Cancer. Breast Care *15*, 355-365. 10.1159/000509846.

Qiu, H., and Miller, W.T. (2002). Regulation of the nonreceptor tyrosine kinase Brk by autophosphorylation and by autoinhibition. J Biol Chem *277*, 34634-34641. 10.1074/jbc.M203877200

M203877200 [pii].

Qiu, H., Zappacosta, F., Su, W., Annan, R.S., and Miller, W.T. (2005). Interaction between Brk kinase and insulin receptor substrate-4. Oncogene *24*, 5656-5664.

Quirke, V.M. (2017). Tamoxifen from Failed Contraceptive Pill to Best-Selling Breast Cancer Medicine: A Case-Study in Pharmaceutical Innovation. Frontiers in Pharmacology *8*. 10.3389/fphar.2017.00620.

Rabiee, A., Kruger, M., Ardenkjaer-Larsen, J., Kahn, C.R., and Emanuelli, B. (2018). Distinct signalling properties of insulin receptor substrate (IRS)-1 and IRS-2 in mediating insulin/IGF-1 action. Cell Signal *47*, 1-15. 10.1016/j.cellsig.2018.03.003.

Radivojac, P., Baenziger, P.H., Kann, M.G., Mort, M.E., Hahn, M.W., and Mooney, S.D. (2008). Gain and loss of phosphorylation sites in human cancer. Bioinformatics *24*, i241-i247. 10.1093/bioinformatics/btn267.

Rani, A., Stebbing, J., Giamas, G., and Murphy, J. (2019). Endocrine Resistance in Hormone Receptor Positive Breast Cancer–From Mechanism to Therapy. Frontiers in Endocrinology *10*. 10.3389/fendo.2019.00245.

Regan Anderson, T.M., Ma, S.H., Raj, G.V., Cidlowski, J.A., Helle, T.M., Knutson, T.P., Krutilina, R.I., Seagroves, T.N., and Lange, C.A. (2016). Breast Tumor Kinase (Brk/PTK6) Is Induced by HIF, Glucocorticoid Receptor, and PELP1-Mediated Stress Signaling in Triple-Negative Breast Cancer. Cancer Res *76*, 1653-1663. 10.1158/0008-5472.CAN-15-2510.

Regan Anderson, T.M., Peacock, D.L., Daniel, A.R., Hubbard, G.K., Lofgren, K.A., Girard, B.J., Schorg, A., Hoogewijs, D., Wenger, R.H., Seagroves, T.N., and Lange, C.A. (2013). Breast tumor kinase (Brk/PTK6) is a mediator of hypoxia-associated breast cancer progression. Cancer Res *73*, 5810-5820. 10.1158/0008-5472.CAN-13-0523.

Revankar, C.M., Cimino, D.F., Sklar, L.A., Arterburn, J.B., and Prossnitz, E.R. (2005). A Transmembrane Intracellular Estrogen Receptor Mediates Rapid Cell Signaling. Science *307*, 1625-1630. doi:10.1126/science.1106943.

Riggio, M., Perrone, M.C., Polo, M.L., Rodriguez, M.J., May, M., Abba, M., Lanari, C., and Novaro, V. (2017). AKT1 and AKT2 isoforms play distinct roles during breast cancer progression through the regulation of specific downstream proteins. Sci Rep-Uk *7*, 44244. 10.1038/srep44244.

Robertson, J.F.R., Bondarenko, I.M., Trishkina, E., Dvorkin, M., Panasci, L., Manikhas, A., Shparyk, Y., Cardona-Huerta, S., Cheung, K.L., Philco-Salas, M.J., et al. (2016). Fulvestrant 500 mg versus anastrozole 1 mg for hormone receptor-positive advanced breast cancer (FALCON): an international, randomised, double-blind, phase 3 trial. Lancet *388*, 2997-3005. 10.1016/s0140-6736(16)32389-3.

Robinson, D.R., Wu, Y.M., and Lin, S.F. (2000). The protein tyrosine kinase family of the human genome. Oncogene *19*, 5548-5557.

Rostoker, R., Abelson, S., Bitton-Worms, K., Genkin, I., Ben-Shmuel, S., Dakwar, M., Orr, Z.S., Caspi, A., Tzukerman, M., and LeRoith, D. (2015). Highly specific role of the insulin receptor in breast cancer progression. Endocr Relat Cancer *22*, 145-157. 10.1530/erc-14-0490.

Rouhimoghadam, M., Safarian, S., Carroll, J.S., Sheibani, N., and Bidkhori, G. (2018). Tamoxifen-Induced Apoptosis of MCF-7 Cells via GPR30/PI3K/MAPKs Interactions: Verification by ODE Modeling and RNA Sequencing. Front Physiol *9*. 10.3389/fphys.2018.00907.

Rush, J., Moritz, A., Lee, K.A., Guo, A., Goss, V.L., Spek, E.J., Zhang, H., Zha, X.-M., Polakiewicz, R.D., and Comb, M.J. (2005). Immunoaffinity profiling of tyrosine phosphorylation in cancer cells. Nat Biotechnol *23*, 94-101. 10.1038/nbt1046.

Savage, S.R., and Zhang, B. (2020). Using phosphoproteomics data to understand cellular signaling: a comprehensive guide to bioinformatics resources. Clinical Proteomics *17*, 27. 10.1186/s12014-020-09290-x.

Searle, B.C. (2010). Scaffold: A bioinformatic tool for validating MS/MS-based proteomic studies. Proteomics *10*, 1265-1269. https://doi.org/10.1002/pmic.200900437.

Semenza, G.L. (2012). Hypoxia-inducible factors: mediators of cancer progression and targets for cancer therapy. Trends Pharmacol Sci *33*, 207-214. 10.1016/j.tips.2012.01.005.

Sharma, K., D'Souza, R.C., Tyanova, S., Schaab, C., Wisniewski, J.R., Cox, J., and Mann, M. (2014). Ultradeep human phosphoproteome reveals a distinct regulatory nature of Tyr and Ser/Thr-based signaling. Cell Rep *8*, 1583-1594. 10.1016/j.celrep.2014.07.036.

Shen, C.H., Chen, H.Y., Lin, M.S., Li, F.Y., Chang, C.C., Kuo, M.L., Settleman, J., and Chen, R.H. (2008). Breast tumor kinase phosphorylates p190RhoGAP to regulate rho and ras and promote breast carcinoma growth, migration, and invasion. Cancer Res *68*, 7779-7787.

Shi, X., Zhang, H., Paddon, H., Lee, G., Cao, X., and Pelech, S. (2006). Phosphorylation of STAT3 Serine-727 by Cyclin-Dependent Kinase 1 Is Critical for Nocodazole-Induced Mitotic Arrest. Biochemistry *45*, 5857-5867. 10.1021/bi052490j.

Shiau, A.K., Barstad, D., Loria, P.M., Cheng, L., Kushner, P.J., Agard, D.A., and Greene, G.L. (1998). The Structural Basis of Estrogen Receptor/Coactivator Recognition and the Antagonism of This Interaction by Tamoxifen. Cell *95*, 927-937. 10.1016/S0092-8674(00)81717-1.

Shou, J., Massarweh, S., Osborne, C.K., Wakeling, A.E., Ali, S., Weiss, H., and Schiff, R. (2004). Mechanisms of tamoxifen resistance: increased estrogen receptor-HER2/neu cross-talk in ER/HER2-positive breast cancer. J Natl Cancer Inst *96*, 926-935. 10.1093/jnci/djh166.

Simões, B.M., O'Brien, C.S., Eyre, R., Silva, A., Yu, L., Sarmiento-Castro, A., Alférez, D.G., Spence, K., Santiago-Gómez, A., Chemi, F., et al. (2015). Anti-estrogen Resistance in Human Breast Tumors Is Driven by JAG1-NOTCH4-Dependent Cancer Stem Cell Activity. Cell Rep *12*, 1968-1977. 10.1016/j.celrep.2015.08.050.

Singh, V., Ram, M., Kumar, R., Prasad, R., Roy, B.K., and Singh, K.K. (2017). Phosphorylation: Implications in Cancer. Protein J *36*, 1-6. 10.1007/s10930-017-9696-z.

Sinha, A., and Mann, M. (2020). A beginner's guide to mass spectrometry–based proteomics. The Biochemist *42*, 64-69. 10.1042/bio20200057.

Sisci, D., Morelli, C., Cascio, S., Lanzino, M., Garofalo, C., Reiss, K., Garcia, M., Russo, A., Andò, S., and Surmacz, E. (2007). The estrogen receptor alpha:insulin receptor substrate 1 complex in breast cancer: structure-function relationships. Ann Oncol *18 Suppl 6*, vi81-85. 10.1093/annonc/mdm232.

Song, R.X., Barnes, C.J., Zhang, Z., Bao, Y., Kumar, R., and Santen, R.J. (2004). The role of Shc and insulin-like growth factor 1 receptor in mediating the translocation of estrogen receptor alpha to the plasma membrane. Proc Natl Acad Sci U S A *101*, 2076-2081. 10.1073/pnas.0308334100.

Sorlie, T. (2007). Molecular classification of breast tumors: toward improved diagnostics and treatments. Methods Mol Biol *360*, 91-114. 10.1385/1-59745-165-7:91.

Soto, E., Yanagisawa, M., Marlow, L.A., Copland, J.A., Perez, E.A., and Anastasiadis, P.Z. (2008). p120 catenin induces opposing effects on tumor cell growth depending on E-cadherin expression. J Cell Biol *183*, 737-749. 10.1083/jcb.200805113.

Stokes, M.P., Farnsworth, C.L., Moritz, A., Silva, J.C., Jia, X., Lee, K.A., Guo, A., Polakiewicz, R.D., and Comb, M.J. (2012). PTMScan direct: identification and quantification of peptides from critical signaling proteins by immunoaffinity enrichment coupled with LC-MS/MS. Mol Cell Proteomics *11*, 187-201. 10.1074/mcp.M111.015883.

Sun, J., Nawaz, Z., and Slingerland, J.M. (2007). Long-Range Activation of GREB1 by Estrogen Receptor via Three Distal Consensus Estrogen-Responsive Elements in Breast Cancer Cells. Mol Endocrinol *21*, 2651-2662. 10.1210/me.2007-0082.

Sung, H., Ferlay, J., Siegel, R.L., Laversanne, M., Soerjomataram, I., Jemal, A., and Bray, F. (2021). Global Cancer Statistics 2020: GLOBOCAN Estimates of Incidence and Mortality Worldwide for 36 Cancers in 185 Countries. CA: A Cancer Journal for Clinicians *71*, 209-249. https://doi.org/10.3322/caac.21660.

Szklarczyk, D., Gable, A.L., Nastou, K.C., Lyon, D., Kirsch, R., Pyysalo, S., Doncheva, N.T., Legeay, M., Fang, T., Bork, P., et al. (2020). The STRING database in 2021: customizable protein–protein networks, and functional characterization of user-uploaded gene/measurement sets. Nucleic Acids Research *49*, D605-D612. 10.1093/nar/gkaa1074.

Tabár, L., Dean, P.B., Chen, T.H., Yen, A.M., Chen, S.L., Fann, J.C., Chiu, S.Y., Ku, M.M., Wu, W.Y., Hsu, C.Y., et al. (2019). The incidence of fatal breast cancer measures the increased effectiveness of therapy in women participating in mammography screening. Cancer *125*, 515-523. 10.1002/cncr.31840.

Takeshita, T., Yamamoto, Y., Yamamoto-Ibusuki, M., Inao, T., Sueta, A., Fujiwara, S., Omoto, Y., and Iwase, H. (2016). Clinical significance of monitoring ESR1 mutations in circulating cell-free DNA in estrogen receptor positive breast cancer patients. Oncotarget *7*, 32504-32518. 10.18632/oncotarget.8839.

Tan, M., Jing, T., Lan, K.-H., Neal, C.L., Li, P., Lee, S., Fang, D., Nagata, Y., Liu, J., Arlinghaus, R., et al. (2002). Phosphorylation on Tyrosine-15 of p34Cdc2 by ErbB2 Inhibits p34Cdc2 Activation and Is Involved in Resistance to Taxol-Induced Apoptosis. Molecular cell *9*, 993-1004. https://doi.org/10.1016/S1097-2765(02)00510-5.

Templeton, A.J., Diez-Gonzalez, L., Ace, O., Vera-Badillo, F., Šeruga, B., Jordán, J., Amir, E., Pandiella, A., and Ocaña, A. (2014). Prognostic relevance of receptor tyrosine kinase expression in breast cancer: A meta-analysis. Cancer Treatment Reviews *40*, 1048-1055. https://doi.org/10.1016/j.ctrv.2014.08.003.

Toy, W., Shen, Y., Won, H., Green, B., Sakr, R.A., Will, M., Li, Z., Gala, K., Fanning, S., King, T.A., et al. (2013). ESR1 ligand-binding domain mutations in hormone-resistant breast cancer. Nature Genetics *45*, 1439-1445. 10.1038/ng.2822.

Turdo, A., D'Accardo, C., Glaviano, A., Porcelli, G., Colarossi, C., Colarossi, L., Mare, M., Faldetta, N., Modica, C., Pistone, G., et al. (2021). Targeting Phosphatases and Kinases: How to Checkmate Cancer. Frontiers in Cell and Developmental Biology *9*. 10.3389/fcell.2021.690306.

Tyanova, S., and Cox, J. (2018). Perseus: A Bioinformatics Platform for Integrative Analysis of Proteomics Data in Cancer Research. In Cancer Systems Biology: Methods and Protocols, L. von Stechow, ed. (Springer New York), pp. 133-148. 10.1007/978-1-4939-7493-1_7.

Ugolkov, A., Gaisina, I., Zhang, J.S., Billadeau, D.D., White, K., Kozikowski, A., Jain, S., Cristofanilli, M., Giles, F., O'Halloran, T., et al. (2016). GSK-3 inhibition overcomes chemoresistance in human breast cancer. Cancer Lett *380*, 384-392. 10.1016/j.canlet.2016.07.006.

Urban, J. (2022). A review on recent trends in the phosphoproteomics workflow. From sample preparation to data analysis. Analytica Chimica Acta *1199*, 338857. https://doi.org/10.1016/j.aca.2021.338857.

Vaziri-Gohar, A., Zheng, Y., and Houston, K.D. (2017). IGF-1 Receptor Modulates FoxO1-Mediated Tamoxifen Response in Breast Cancer Cells. Molecular Cancer Research *15*, 489-497. 10.1158/1541-7786.Mcr-16-0176.

Vlastaridis, P., Kyriakidou, P., Chaliotis, A., Van de Peer, Y., Oliver, S.G., and Amoutzias, G.D. (2017). Estimating the total number of phosphoproteins and phosphorylation sites in eukaryotic proteomes. Gigascience *6*, 1-11. 10.1093/gigascience/giw015.

Vuong, D., Simpson, P.T., Green, B., Cummings, M.C., and Lakhani, S.R. (2014). Molecular classification of breast cancer. Virchows Arch *465*, 1-14. 10.1007/s00428-014-1593-7.

Wang, Z., Slipicevic, A., Førsund, M., Trope, C.G., Nesland, J.M., and Holm, R. (2015). Expression of CDK1(Tyr15), pCDK1(Thr161), Cyclin B1 (total) and pCyclin B1(Ser126) in vulvar squamous cell carcinoma and their relations with clinicopatological features and prognosis. PLoS One *10*, e0121398. 10.1371/journal.pone.0121398.

Weaver, A.M., and Silva, C.M. (2007). Signal transducer and activator of transcription 5b: a new target of breast tumor kinase/protein tyrosine kinase 6. Breat Cancer Res *9*, R79.

Won, H.S., Lee, K.M., Oh, J.E., Nam, E.M., and Lee, K.E. (2016). Inhibition of β-Catenin to Overcome Endocrine Resistance in Tamoxifen-Resistant Breast Cancer Cell Line. PLoS One *11*, e0155983. 10.1371/journal.pone.0155983.

Wu, A., Chen, J., and Baserga, R. (2008). Nuclear insulin receptor substrate-1 activates promoters of cell cycle progression genes. Oncogene *27*, 397-403. 10.1038/sj.onc.1210636.

Wu, C.X., Wang, X.Q., Chok, S.H., Man, K., Tsang, S.H.Y., Chan, A.C.Y., Ma, K.W., Xia, W., and Cheung, T.T. (2018). Blocking CDK1/PDK1/β-Catenin signaling by CDK1 inhibitor RO3306

increased the efficacy of sorafenib treatment by targeting cancer stem cells in a preclinical model of hepatocellular carcinoma. Theranostics *8*, 3737-3750. 10.7150/thno.25487.

Xiang, B., Chatti, K., Qiu, H., Lakshmi, B., Krasnitz, A., Hicks, J., Yu, M., Miller, W.T., and Muthuswamy, S.K. (2008). Brk is coamplified with ErbB2 to promote proliferation in breast cancer. Proc Natl Acad Sci U S A. *105*, 12463-12468.

Yang, X., Phillips, D.L., Ferguson, A.T., Nelson, W.G., Herman, J.G., and Davidson, N.E. (2001). Synergistic Activation of Functional Estrogen Receptor (ER)-α by DNA Methyltransferase and Histone Deacetylase Inhibition in Human ER-α-negative Breast Cancer Cells1. Cancer Research *61*, 7025-7029.

Yaşar, P., Ayaz, G., User, S.D., Güpür, G., and Muyan, M. (2016). Molecular mechanism of estrogen-estrogen receptor signaling. Reprod Med Biol *16*, 4-20. 10.1002/rmb2.12006.

Yeh, W.L., Shioda, K., Coser, K.R., Rivizzigno, D., McSweeney, K.R., and Shioda, T. (2013). Fulvestrant-induced cell death and proteasomal degradation of estrogen receptor α protein in MCF-7 cells require the CSK c-Src tyrosine kinase. PLoS One *8*, e60889. 10.1371/journal.pone.0060889.

Yim, E.K., Peng, G., Dai, H., Hu, R., Li, K., Lu, Y., Mills, G.B., Meric-Bernstam, F., Hennessy, B.T., Craven, R.J., and Lin, S.Y. (2009). Rak functions as a tumor suppressor by regulating PTEN protein stability and function. Cancer Cell *15*, 304-314. S1535-6108(09)00043-9 [pii]

10.1016/j.ccr.2009.02.012.

Zekas, E., and Prossnitz, E.R. (2015). Estrogen-mediated inactivation of FOXO3a by the G protein-coupled estrogen receptor GPER. BMC Cancer *15*, 702. 10.1186/s12885-015-1699-6.

Zhang, D., Zhang, J.Y., and Wang, E.H. (2015). δ-catenin promotes the malignant phenotype in breast cancer. Tumour Biol *36*, 569-575. 10.1007/s13277-014-2680-8.

Zhang, P., Ostrander, J.H., Faivre, E.J., Olsen, A., Fitzsimmons, D., and Lange, C.A. (2005). Regulated association of protein kinase B/Akt with breast tumor kinase. J Biol Chem *280*, 1982-1991. M412038200 [pii]

10.1074/jbc.M412038200.

Zhang, Y., Wester, L., He, J., Geiger, T., Moerkens, M., Siddappa, R., Helmijr, J.A., Timmermans, M.M., Look, M.P., van Deurzen, C.H.M., et al. (2018). IGF1R signaling drives antiestrogen resistance through PAK2/PIX activation in luminal breast cancer. Oncogene *37*, 1869-1884. 10.1038/s41388-017-0027-9.

Zhao, H., Ou-Yang, F., Chen, I.F., Hou, M.-F., Yuan, S.-S.F., Chang, H.-L., Lee, Y.-C., Plattner, R., Waltz, S.E., Ho, S.-M., et al. (2010). Enhanced resistance to tamoxifen by the c-ABL proto-oncogene in breast cancer. Neoplasia (New York, N.Y.) *12*, 214-223. 10.1593/neo.91576.

Zheng, Y., Gierut, J., Wang, Z., Miao, J., Asara, J.M., and Tyner, A.L. (2013). Protein tyrosine kinase 6 protects cells from anoikis by directly phosphorylating focal adhesion kinase and activating AKT. Oncogene *32*, 4304-4312. 10.1038/onc.2012.427.

Zheng, Y., Peng, M., Wang, Z., Asara, J.M., and Tyner, A.L. (2010). Protein tyrosine kinase 6 directly phosphorylates AKT and promotes AKT activation in response to epidermal growth factor. Mol Cell Biol *30*, 4280-4292. MCB.00024-10 [pii]

10.1128/MCB.00024-10.

Zheng, Y., Sowers, J.Y., and Houston, K.D. (2020). IGFBP-1 Expression Promotes Tamoxifen Resistance in Breast Cancer Cells via Erk Pathway Activation. Frontiers in Endocrinology *11*. 10.3389/fendo.2020.00233.

Zhou, J., Yi, Q., and Tang, L. (2019). The roles of nuclear focal adhesion kinase (FAK) on Cancer: a focused review. Journal of Experimental & Clinical Cancer Research *38*, 250. 10.1186/s13046-019-1265-1.

Zhu, C., Qi, X., Chen, Y., Sun, B., Dai, Y., and Gu, Y. (2011). PI3K/Akt and MAPK/ERK1/2 signaling pathways are involved in IGF-1-induced VEGF-C upregulation in breast cancer. J Cancer Res Clin Oncol *137*, 1587-1594. 10.1007/s00432-011-1049-2.

Zhu, Y., Li, K., Zhang, J., Wang, L., Sheng, L., and Yan, L. (2020). Inhibition of CDK1 Reverses the Resistance of 5-Fu in Colorectal Cancer. Cancer Manag Res *12*, 11271-11283. 10.2147/cmar.S255895.